12-2013

Sympathetic Nerve Modulation of Joint Pathology in Adjuvant-Induced Arthritis

Carlo Anthony Wood

LOMA LINDA UNIVERSITY
School of Medicine
in conjunction with the
Faculty of Graduate Studies

———————————————

Sympathetic Nerve Modulation of Joint Pathology in Adjuvant-
Induced Arthritis

by

Carlo Anthony Wood

———————————————

A Dissertation submitted in partial satisfaction
of the requirements for the degree of
Doctor of Philosophy in Anatomy

———————————————

December 2013

Each person whose signature appears below certifies that this dissertation in his/her opinion is adequate, in scope and quality, as a dissertation for the degree of Doctor of Philophy.

_____ , Chairperson
Denise Bellinger, Associate Professor of Anatomy

_____
Raymond Hall, Associate Professor of Physiology, Pharmacology and Cell Physiology

_____
Paul McMillan, Professor of Anatomy, Histology, Bone Cell Biology, Quantitative Morphology, and Image Analysis

_____
Jon Wergedal, Research Professor in the Department of Medicine

_____
Ken Wright, Assistant Professor of Anatomy, Gross Anatomy, Bone Cell Biology, Apoptosis, and Histomorphometry

ACKNOWLEDGMENTS

CONTENT

FIGURES

ABBREVIATIONS

AA   adjuvant-induced arthritis

ANOVA   analysis of variance

AR   adrenergic receptor(s)

BMD   bone mineral density

CFA   Complete Freund's adjuvant

CGRP   calcitonin gene related peptide

CIA   collagen induced arthritis

CNS   central nervous system

COMP   cartilage oligometric matrix protein

COX   cyclooxygenase

CRH   corticotrophin releasing hormone

CT   computed tomography

Dbh   dopamine beta-hydroxylase

DMARDs   disease modifying antirheumatic drugs

DRG   dorsal root ganglion

GM-CSF   granulocyte-monocyte colony stimulating factor

H&E   hematoxylin and eosin

HLA   human leukocyte antigen

HPA   hypothalamic-pituitary-adrenal axis

IFN   interferon

IL   interleukin

M-CSF   macrophage colony stimulating factor

MIF	macrophage migration inhibitory factor
MIP-1α	macrophage inflammatory protein
MMP	matrix metaloproteinases
NE	norepinephrine
NGF	nerve growth factor
NMU	neuromedian U
NPY	neuropeptide Y
NSAIDs	nonsteroidal anti-inflammatory drugs
OCIF	osteoclast inhibitory factor
ODF	osteoclast differentiation factor
OPG	osteoprotegerine
PAD	peptidylarginine deiminase
PDGF	platelet-derived growth factor
PG	prostaglandins
PIA	pristane-induced arthritis
PKA	protein kinase A
PPAR	peroxisome proliferator activated receptors
PTH	parathyroid hormone
RA	rheumatoid arthritis
RANK	receptor-activator of nuclear kappa β
SNS	sympathetic nervous system
SP	substance P
TH	tyrosine hydroxylase

TNF-α   tumor necrosis factor alpha

TRAP   tartrate-resistant acid phosphatase

VEGF   vascular endothelial growth factor

VIP   vasoactive intestinal polypeptide

ABSTRACT OF THE DISSERATION

Sympathetic Nerve Modulation of Joint Pathology in Adjuvant-
Induced Arthritis

by

Carlo Anthony Wood

Doctor of Philosophy, Graduate Program in Anatomy
Loma Linda University, December 2013
Denise L. Bellinger, Chairperson

Background: There is increasing data suggesting a net increase in sympathetic tone plays an important role in rheumatoid arthritis. Several studies have reported altered distribution and density of autonomic nerves in patients with rheumatoid arthritis and animal models for the disease. This provides anatomical evidence that supports a neurally-mediated drive in inflammation and joint destruction.

Methods: Adult rats were injected with complete Freund's adjuvant. At 12 days post immunization, animals were randomly placed into a drug treatment group (SH1293, which interacts with α- and β_2-ARs), an adjuvant arthritic group, or a control group. These animals were sacrificed at 14, 21, 28 and 126 days. The ankles were then evaluated for changes in lymphocytes, bone area, osteoclasts, cartilage, pannus, sympathetic nerves, and bone volume.

Results: At 21 days, the drug treated group showed a significant improvement in lymphocytes, cartilage and bone volume. There was also a decrease in pannus and preservation of sympathetic nerves that was not significant. At 28 days, the drug treated group did not appear to show any significance, however, there was still an improvement in lymphocytes, pannus, and sympathetic nerves. The cartilage and bone volume became

significantly less. Investigation of bone area and osteoclasts revealed 2 distinct groups.

Some responded favorably to the drug while some responded less favorably. At both 21

and 28 days the high responding SH1293 rats showed a significant improvement in bone

area and osteoclasts. There appears to be significant correlations between the variables and

a strong general trend of joint preservation with the drug's usage. At 126 days there were

continued remodeling changes noted.

Conclusion: Blocking increased sympathetic activity does alter bone metabolism in

adjuvant-induced arthritic rats. These effects seem to be mediated by reduced

norepinephrine interaction with adrenergic receptors peripherally.

CHAPTER ONE

INTRODUCTION

What is Rheumatoid Arthritis (RA)?

Disease Characteristics

RA is a chronic, systemic inflammatory disease that may affect many tissues and

organs, but principally targets the synovial joints producing an inflammatory synovitis

that often progresses to destruction of the articular cartilage and ankylosis of the joints.

RA nearly always affects multiple joints (polyarthritis), most commonly the small joints

of the hands, feet and cervical spine, but larger joints like the shoulder and knee can also

be involved. RA can cause diffuse inflammation in the lungs, pericardium, pleura, and

sclera, as well as nodular lesions, commonly under the skin; the latter sign is associated

with a poor prognosis. The natural course of RA is almost invariably one of persistent

symptoms, waxing and waning in intensity, and a progressive deterioration of joint

structures leading to deformations and disability.

Epidemiology

The prevalence of the disease ranges from 0.24% to 1.0% of the world's

population (Imboden, 2009), or approximately 3 cases per 10,000 per annum.   The onset

of RA is rare under age 15, and then the incidence rises with age until the age of 80. It

most often occurs between the ages of 40 and 50 for women and somewhat later in men

(Alamanos et al, 2008). Women are afflicted with RA 3 to 5 times as often as men. It is

4 times more common in smokers than nonsmokers. Patients with arthritis and rheumatism have the highest percentage of disability in the United States at 17%, larger than spine problems (13%), heart disease (10%) or respiratory disease (7%) (Klippel, 2001). Disability results from pain, joint deformity, and substantial loss of functioning and mobility.

Diagnosis

RA is diagnosed mainly on symptoms and signs, and with blood tests, particularly for rheumatoid factor (RF) and X-rays. However, bone erosion in RA can be analyzed clinically a few different ways. This is important because taking into account only one piece of evidence may lead to the wrong hypothesis and therefore incorrect diagnosis and treatment. It is much more effective to build a case with multiple pieces of evidence before coming to a conclusion. Forty percent bone loss is needed before osteoporosis can be detected by X-ray. Ultrasound, bone density tests and MRI are more sensitive methods of imaging the joints, and have demonstrated that joint damage occurs much earlier in the disease than previously thought, leading to earlier treatment with anti-rheumatic drugs in order to treat before the damage occurs.

Treatment of RA

There is no known cure for RA, but many different treatments are used to alleviate current symptoms and/or to modify the disease process (i.e., prevent future destruction of the joints). Drugs are used to control symptoms of the disease (e.g., analgesics like acetaminophen and aspirin to relieve pain and reduce inflammation) (DiPaola, 2008). Nonsteroidal anti-inflammatory drugs (NSAIDs) like diclofenac,

ibuprofen, indomethacin, ketoprofen, meloxicam, and naproxen can be used to treat the

symptoms of inflammation, but do not alter the course of the disease. Treatment with

cyclooxygenase (COX)-II inhibitors like celecoxib, narcotic/analgesics (e.g.,

propxyphen), oral corticosteroids (e.g., methylprednisolone) or injectable corticosteroids,

also suppress inflammation in severe organ disease or life threatening disease.

Treatments that modify the disease progression are called disease-modifying

antirheumatic drugs (DMARDs) and include auranofin, cyclosporine gold salts, and

hydroxychloroquine, which slow progression of joint damage, as well as, decreases pain

and swelling. These drugs are given in conjunction with drugs that treat the symptoms of

the disease. Earlier treatment with DMARDs is beneficial, in that they may interrupt

positive feedback loops established by the abnormal immune response, which improves

the outcome from RA for years afterward.

More recently, biological agents produced through genetic engineering have been

used to treat moderate to severe RA. These include tumor necrosis factor (TNF) blockers

like adalimumab, infliximab, and etanercept, interleukin (IL)-1 inhibitors like anakinra

(IL-1 receptor antagonist or IL-1ra), monoclonal antibodies against B cells, like

rituximab, T cell costimulation blockers, like abatacept, and IL-6 blockers, like

tocilizumab. These agents suppress inflammation and retard or block joint destruction in

RA (Di Paola, 2008).

Adalimumab, etanercept, and anakinra, block IL-1 activity and prevent bone

erosion by interacting with receptor activator of nuclear factor kappa-β (RANK) ligand

(RANKL) which reduces the signs and symptoms of RA (Schett, 2006). Similarly, drugs

that block TNF-α effectively target bone erosion and seem to halt progression of

radiologically detected damage, reduce pain and improve mobility. These may be the best drugs on the market at this time.

Because the immune system is regulated by the brain, drugs targeting the nervous system are also effective. Beta-blockers have been shown to have a favorable outcome in animal models, increasing bone mineral density and lowering fracture risk. $\beta2$-adrenergic agonists demonstrate different effects on RA disease severity depending on the time at which they are administered in relation to the disease stage. When terbutaline, a β-adrenergic receptor agonist, is given to rats during the antigen processing stage, there is exacerbation of the disease. In contrast, when given at the time point of disease onset (day 14) into the chronic inflammatory phase, there are marked dorsoplantar foot width and X-ray analysis improvements (Lubahn et al, 2004). When the β-adrenergic receptor antagonist, propranolol is administered 2 days before immunization through 28 days, it also reduces disease severity (Levine et al, 1988). It is thought that blocking the beta receptor should shift the immune response to the arthritogenic antigen towards a cell-mediated response, presumably a beneficial way for the processing of the arthritogenic antigen. Blocking the β-adrenergic receptor stimulation during disease development inhibits the expression of α 1-adrenergic receptors on monocytes and macrophages, since chronic β-adrenergic receptor stimulation has previously been demonstrated to induce α 1-adrenergic receptor expression on these cells. This would be expected to reduce proinflammatory cytokine production stimulated by norepinepherine (NE) or epinephrine binding to α 1-adrenergic receptors and thus decrease disease severity in this phase (Lorton et al, 2003). The effects on humans are still unclear and more research is needed before beta-blockers can be considered as a good option in low bone mass diseases

(Elefteriou, 2008). One of the aims of this study is to examine the effect of an adrenergic drug, SH1293, on disease progression in an animal model of RA.

Prognosis

The course of RA varies greatly, with some individuals having mild short-term symptoms, but in most cases, the disease is progressive for life. Approximately 20-30% of RA patients will have subcutaneous nodules (rheumatoid nodules). Activities of daily living are impaired in most individuals. After 5 years, about 33% are not able to work, and after 10 years, about half have substantial functional disability. Poor prognostic factors include persistent synovitis, early erosive disease, extra-articular findings (i.e., subcutaneous rheumatoid nodules), positive serum RF, poor functional status, socioeconomic factors, elevated acute phase response (erythrocyte sedimentation rate (ESR), C-reactive protein (CRP), and increased clinical severity. Most sources cite a lifespan reduction of 5 to 10 years in individuals with RA. Many factors are associated with the higher mortality, including: (1) young age of onset; (2) long disease duration; (3) comorbidity with other health problems; (4) severe manifestation of RA; (5) high amount of joint damage; and (6) involvement of organs other than the joints.

Pathogenesis – Antigen Induction and Infectious Triggers

For a long time, certain infections have been suspected to be a trigger for RA, via autoimmune mechanisms. Antibodies directed against specific epitopes of the pathogen were believed to cross-react with self protein and display molecular mimicry. Infectious organisms suspected of triggering RA include *Mycoplasma*, *Erysipelothrix*, parvovirus B19 and rubella, but these associations have never been supported in epidemiological

studies. Epidemiological studies have confirmed a potential association between RA and two herpes virus infections: Epstein-Barr virus (EBV) and Human Herpes Virus 6 (HHV-6) (Imboden, 2009). Individuals with RA are more likely to exhibit an abnormal immune response to EBV (Klippel, 2001). The allele HLA-DRB1*0404 is associated with low frequencies of T cells specific for EBV glycoprotein 110 and predisposes one to RA (Lorton et al, 2003).

There is little evidence to support a particular antigen in the development of RA. Similarly, there is no clear data that physical and emotional effects, stress and improper diet could be a trigger for the disease. The many negative findings suggest that either the trigger varies, or that it might be a chance event inherent with the immune response (Lorton et al, 2008). Recently, citrullinated protein antigens have been proposed as a trigger for RA (Imboden, 2009). Citrullination of proteins is a posttranslational modification in which peptidylarginine residues are converted to peptidylcitrulline by peptidylarginine deaminases (PADs). PAD activity requires high concentrations of calcium, for instance calcium that occurs extracellularly or in apoptotic cells. The physiologic role of citrullination is uncertain. However, ciltrullinated proteins are found in sites of inflammation, including RA joints (Imboden, 2009). Citrullinated proteins found in RA joints include fibrin and vimentin (Imboden, 2009). Citrullinated proteins are not specific to RA and have been found in other forms of arthritis (Imboden, 2009).

Antibodies to citrullinated protein antigens are detected in about 70% of RA patients (Imboden, 2009). Autoantibodies recognize citrulline in the context of neighboring amino acids. These antibodies can appear years prior to the onset of articular symptoms. Little is know of the evolution of the antibody response to

6

citrullinated protein antigens during this preclinical phase. Citrullination of certain peptides increases their affinity for shared-epitope-expressing HLA-DR molecules and facilitates their presentation to T cells (Imboden, 2009).

Circulating antibodies to type II collagen found in articular cartilage are common in patients with RA, and B cells producing antibodies to type II cartilage are present in RA synovium (Imboden, 2009). However, anti-type II collagen antibodies never precede the clinical onset of RA. They usually appear after damage to articular cartilage.

Key factors related to the pathogenesis include: (1) a genetic link with HLA-DR4 (most specifically HLA-DR4 – DR0401 and 0404) and related allotypes of major histocompatibilty (MHC) Class II, and with the T cell-associated protein, protein tyrosine phosphatase, non-receptor type 22 (PTPN22); (2) a dramatic response in many cases to blocking the activity of TNF-α and depletion of B lymphocytes, without a comparable response to T cell depletion; (3) a more or less random pattern of whether and when predisposed individuals are affected; (4) the presence of autoantibodies to IgG Fc RF; (5) antibodies to citrullinated peptides (Imboden, 2009); and (6) a link with cigarette smoking that appears to be causal and related to its ability to promote the formation of citrullinated proteins. Both B and T cells are essential to the disease, but neither cell appears to be necessary at the site of inflammation, favoring immune complexes (based on antibody synthesized elsewhere) as the initiators of joint inflammation. These data suggest that RA involves abnormal B cell-T cell interaction, with antigen presentation by B cells to T cells via HLA-DR eliciting T cell help and consequent production of RF and citrullinated peptides. Inflammation is driven either by B or T cell products, which stimulates the release of TNF and other cytokines.

If TNF release is stimulated by B cell products (i.e., RF or antibodies to citrullinated peptides as immune complexes) through immunoglobulin Fc receptor activation, then RA could be considered as a form of Type III hypersensitivity. Alternatively, if TNF release is stimulated by T cell products (i.e., IL-17), then it may be similar to type IV hypersensitivity. The study of the relative roles of immune complexes and T cell products in inflammation in RA have been studied and debated for 30 years, but these issues have not been resolved. It is clear that both B and T cells are essential to the disease, but there is good evidence that neither cell is necessary at the site of inflammation, which favors immune complexes, based on antibody synthesis elsewhere, as the initiators, even if they are not the sole perpetuators of inflammation.

Collective data suggests that the locally relevant cells are plasma cells, which derive from B cells. Their secreted products, RF and antibodies to citrullinated peptides, appear to activate macrophages through Fc receptors, and perhaps complement binding, which can contribute to inflammation of the synovium via edema, vasodilation, and infiltration of T cells (CD4 cells as nodular aggregates and CD8 cells as diffuse infiltrates). Additionally, synovial macrophages and dendritic cells function as antigen-presenting cells by expressing MHC class II molecules, leading to an established local immune reaction in the tissue. The disease progresses in concert with the formation of granulation tissue at the edges of the synovial lining, stimulating pannus formation, extensive angiogenesis and production of enzymes that cause tissue damage. Modern pharmacological treatments of RA target the mediators of these processes. Once the inflammatory reaction is established, the synovium thickens, the cartilage and the underlying bone begins to disintegrate, destroying the joint over time.

Pathophysiology –Abnormal T Cell Response

The pathophysiology of RA is not entirely clear, but the factors that allow an abnormal immune response, once RA is initiated and develops into a permanent, chronic disease, are becoming more clearly understood. Several genes have been liked to increases in local synovial and systemic levels of proinflammatory cytokines. The genetic association with HLA-DR4 and newly discovered associations with several additional genes (Imboden, 2009) implicate altered thresholds in the regulation of the adaptive immune response. HLA-DRB1, PTPN22 and STAT4 all contribute to T cell function. These genes play a role in thymic selection of T cells, the presentation of peptide antigens to mature T cells, thresholds for T cell activation, or differentiation into T-helper (Th)1 and Th17 cells (Imboden, 2009).

The HLA locus accounts for 30-50% of overall genetic susceptibility (Imboden, 2009), with the strongest correlation occurring with the HLA-DRB1 allele. PTPN22 gene apparently is related to diminished T cell receptor signaling and susceptibility to RA (Imboden, 2009). Additionally, the signal transducer and activator of transcription 4 (STAT4) gene, which is expressed by lymphoid and myeloid tissues plays a critical role in IL-12-, IL-23-, interferon (IFN)-α- and IFN-β-mediated IFN-γ production, IL-12-mediated development of a Th1 response, and IL-23-mediated survival and expansion of proinflammatory Th17 cells and their production of IL-17 (Imboden, 2009). The locus, 6q23, and TNF receptor-associated factor 1 (TRAF1), limits inflammation mediated by TNF-α (Imboden, 2009) and negatively regulates TNF-α and T cell receptor- mediated signals mediated through TNF receptors and through the T cell receptor.

Cellular and Molecular Mechanisms in Bone Remodeling

Normal Structure of Bones/Joint of the Hind Limb

The ankle joint is made up of 3 bones: the tibia, fibula and talus. In the rat, the tibia and fibula are fused together distally forming one long bone which is located superior to the talus. The talus rests on the calcaneus and anteriorly, these two tarsal bones articulate with other tarsal bones. The tarsal bones articulate with the metatarsals, which in turn articulate with the phalanges. My region of interest will be limited to the tibia/fibula, at the point where the two bones coalesce, and the talus. This is otherwise known as the talocrural joint. The tibia/fibula is a long and hollow bone with cortical bone surrounding a medulary canal. Located within the medulary canal is bone marrow. Near the end of the bone, the canal diminishes and trabecular bone takes its place. The thick cortical bone is tapered into a thinner layer of cortical bone. The distal end of the tibia/fibula is covered with articular cartilage. The superior surface of the talus is also covered with articular cartilage and is mostly made up of trabecular bone.

Normal Bone Remodeling

Bone remodeling is a controlled turnover of the load-bearing extracellular matrix portion of the skeleton that involves cyclic bone resorption and formation. In this cycle, the surface of inactive bone is covered with bone lining cells thought to be of the osteoblast lineage. In inactive areas they are more squamous and in active areas demonstrate a more columnar appearance. These cells give rise to osteoblast precursors in response to systemic and local signals (Skerry 1995, Togari 2002). However, resorption is the first step in this process.

Osteoclast precursors in the marrow are recruited and attracted to the site to be

eroded (Skerry 1995, Szekanecz 2007). These cells differentiate and at the same time

become activated multinucleated osteoclasts. Active resorption will occur when the

osteoclasts bind to the bone surface via integrins. The osteoclasts secrete proteases and

hydrogen ions to remove mineral and collagen (Skerry 1995, Takeuchi 2000).

Resorption occurs until the osteoclasts are signaled to stop. This process involves

elevation of extracellular calcium concentration, growth factors released from the bone

matrix, or osteocyte signals (Skerry 1995).

A reversal phase occurs when the osteoclasts release themselves from the bone

surface (Skerry 1995). A few mononuclear phagocytes remain and are thought to

possibly be involved in recruitment of new osteoblast precursors (Skerry 1995).

Resorption is then followed by coupled formation in which mature osteoblasts lay down

unmineralized bone, also called osteoid, in the resorbed area made by the osteoclast.

Osteoid mineralization occurs from the existing bone surface so the integrity of the bone

remains. The surface then becomes quiet again as the bone lining cells repopulate the

area (Skerry 1995).

In order for bone to be remodeled, osteoclasts must perform two functions. The

first function is to remove hydroxyapatite mineral from bone and second is to degrade

collagenous and non-collagenous proteins (Klippel 2001, Skerry 1995). The binding of

the osteoclast to the bone involves sealing with contractile proteins and allows the cell to

maintain a specific environment in the resorption space (Klippel 2001, Skerry 1995).

The acidic environment of the resorption space results from the secretion of hydrogen

ions which is then transported across the ruffled border by a proton pump, an effect

mediated by carbonic anhydrase (Skerry 1995). Enzymes, like cathepsin, are secreted into the resorption space by exocytosis, where they degrade the matrix proteins (Klippel 1995, Skerry 2001, Skerry 1995).

Hormones Affecting Bone Remodeling

Remodeling is influenced by a number of factors found in the circulation. These include, but are not limited to, prostaglandin E_2, calcitonin, 1,25 dihydroxyvitamin D, parathyroid hormone (PTH), and estrogen. Lining cells express specific receptors for these blood-borne mediators. Prostaglandins (PGs) are one of the regulators included in local bone remodeling, particularly PGE_2. At different concentrations, PGs will either stimulate bone formation or cause remodeling (Skerry and Gowen, 1995). PGs share synergistic and antagonistic actions with many cytokines. IL-1 and TNF act as synergists to induce PGE_2 release from osteoblast like cells; however, IL-1 and TNF induced osteoblast proliferation is inhibited by PGs (Skerry and Gowen, 1995).

After binding to its surface receptors on osteoblasts, PTH stimulates bone resorption and controls calcium homeostasis by recruiting and activating osteoclast precursor cells, and promoting their access to the bone surface. Constant administration of PTH causes resorption, whereas intermittent administration of the same total amount of PTH enhances formation (Skerry and Gowen, 1995).

Steroid hormones like 1,25 dihydroxyvitamin D and estrogen act on intracellular receptors. 1,25 dihydroxyvitamin D stimulates lining cell production of cytokines, which activate osteoclasts. Estrogen depletion causes proliferation of osteoclasts, and therefore has a high impact on bone remodeling (Skerry and Gowen, 1995). Calcitonin inhibits resorption when it binds to osteoclasts via specific cell surface receptors. This causes

retraction of cytoplasmic extensions, decreased motility, and possibly detachment from the bone surface (Skerry and Gowen, 1995).

Involvement of Cytokines in Normal Regulation of Bone and in RA

A large number of T cells reside in the inflamed RA synovial tissue (DiPaola and Cuzzocrea, 2008; Imboden, 2009; Klippel, 2001). However, it has been difficult to define the role of the T cell in propagation of the articular inflammation. There has been renewed interest in the proinflammatory role of the Th17 pathway, since the Th1-mediated path has not been convincingly involved in the pathophysiology of RA (Imboden, 2009).

Th17 differentiation is initiated by IL-6 acting in concert with transforming growth factor beta (TGF-β), and enhanced by TNF-α and IL-1β (Imboden, 2009). IL-17 is found in inflamed RA joints and can cause monocytes, macrophages, fibroblasts, osteoclasts, and chondrocytes (Imboden, 2009) to induce the release of many molecules involved in joint destruction, including proinflammatory cytokines (IL-1β, IL-6, and TNF-α), COX-2, PGE_2, and matrix metalloproteinases (MMP). IL-17 also upregulates RANKL on chondrocytes and osteoblasts, which promotes osteoclast development (Imboden, 2009), and subsequent joint destruction and bone resorption in RA. IL-17 has been identified in the synovial fluid of RA patients, but not in osteoarthritis, a non-inflammatory degenerative disease that destroys the joint as a result of wear and tear (Imboden, 2009).

Treg cells, a unique population of $CD4^+CD25^+$ T cells that require transcription factor FoxP3 (Imboden, 2009) for their development, are present in the arthritic joint and are abnormal in RA. These cells suppress CD4 and CD8 T cell responses through cell-

cell contact and play an essential role in maintaining peripheral tolerance to self. Defective Treg cell production of TNF-α and IFN-γ results in persistent synovial inflammation (Imboden, 2009).

A number of cells are responsible for secreting cytokines, chemokines, growth factors, proteases and other mediators (Miller et al, 2000; Nissalo et al, 2002; Skerry and Gowen, 1995). One of the main cell types are the macrophages, which differentiate from monocytes. Both of these cells are crucial in the development and sustainability of inflammation, leukocyte adhesion and migration, matrix degradation and angiogenesis (Klippel, 2001; Owan and Ibaraki, 1994; Poole et al, 1995; Poole, 2001; Szekanecz and Koch, 2007). The cytokine, macrophage migration-inhibitory factor (MIF), is involved in macrophage activation and cytokine production. Macrophages secrete a host of products including cytokines, growth factors, polypeptide hormones, complement components, proteolytic enzymes, enzyme inhibitors, soluble cell adhesion molecules, extracellular matrix components, binding proteins, cyclooxygenase products, and nitrogen intermediates (Owan and Ibaraki, 1994; Szekanecz and Koch, 2007).

There are two types of synoviocytes, macrophagic cells (type A cells) and fibroblast-like cells (type B cells). Type A synoviocytes are non-fixed cells that phagocytose cell debris and waste in the joint cavity, and possess antigen-presenting capability. These type A cells, derived from blood-borne mononuclear cells, can be considered resident tissue macrophages. Type B synoviocytes are characterized by the rich existence of rough endoplasmic reticulum, and dendritic processes which form a regular network in the luminal surface of the synovial membrane. The type B cells, which are proper synoviocytes, are involved in production of specialized matrix

constituents including hyaluronan, collagens and fibronectin for the intimal interstitium and synovial fluid. For an exact understanding of the mechanism of arthritis, we need to establish the morphological background of synoviocytes as well as their functions under normal conditions. (Iwanaga et al, 2000; Klippel, 2001; Szekanecz and Koch, 2007).

In the blood, mature monocytes eventually undergo transendothelial migration into tissues, such as the synovial tissue, become tissue macrophages and last about 60 days (Szekanecz and Koch, 2007). These cells can also give rise to osteoclasts, which play a crucial role in bone destruction (Klippel, 2001; Szekanecz and Koch, 2007). This process involves RANK/RANKL interactions, integrins and monocyte colony stimulating factor (M-CSF). Macrophages in RA patients are capable of transformation into osteoclasts, and stimulation with TNF-α or IL-1 induces bone resorption by osteoclasts (Klippel, 2001; Szekanecz and Koch, 2007).

IL-1 and TNF-α are the major proinflammatory cytokines that are secreted by the synovial macrophages. TNF-α is responsible for a cascade of products from this cell including IL-6, which is involved in cytokine release and effector functions on monocytes (Szekanecz and Koch, 2007). Although TNF appears to be the dominant cytokine, there are other cytokines or chemical mediators involved in the inflammatory process of RA, and blocking TNF does not benefit all patients or all tissues (lung disease and nodules may get worse). Blockade of IL-1, IL-15, and IL-16 also have beneficial effects and IL-17 may be important. Other cytokines are released by monocyte/macrophage lineage and contribute to RA. IL-10 induces TNF-α receptor expression on monocytes (Szekanecz and Koch, 2007). IL-12 and IL-15 promote maturation and development of osteoclasts (Szekanecz and Koch, 2007).   MIF is

involved in cytokine release from macrophages and angiogenesis. MIF induces TNF-α,

IL-1, IL-6 and MMP production, and MIF serum levels correlate with increased severity

in RA (Szekanecz and Koch, 2007). Growth factors released by macrophages are also

involved in angiogenesis, angiostasis and fibrosis in RA (Szekanecz and Koch, 2007).

They include platelet-derived growth factor (PDGF), basic fibroblast growth factor,

acidic fibroblast growth factor, vascular endothelial growth factor (VEGF), hepatocyte

growth factor and TGF-β (Klippel, 2001; Poole et al, 1995; Poole, 2001; Skerry and

Gowen, 1995; Szekanecz and Koch, 2007).

The proteases that are released from monocytes/macrophages include MMP and

cathepsins; these are mostly involved in extracellular matrix degradation, inflammation,

cell migration and angiogenesis (Klippel, 2001; Poole et al, 1995; Poole, 2001; Skerry

and Gowen, 1995; Szekanecz and Koch, 2007). In RA, MMP's are secreted by

macrophages, particularly, MMP-1 (collagenase), MMP-2 (gelatinase A), and MMP-9

(gelatinase B) (Szekanecz and Koch, 2007). Cathepsins B, L, S and K are expressed in

synovial tissue from RA patients and mediate cartilage and/or bone destruction (Poole et

al, 1995; Poole, 2001; Szekanecz and Koch, 2007). Cathepsin G mediates chemotaxis of

monocytes into the synovial fluid of affected joints in RA patients. Macrophages can be

activated by T cells, which lead to the release of IL-1 and TNF-α.

Abnormal Bone and Cartilage Remodeling in RA

Effects of RA on Bone

The primary effect of RA on bone is substantial local and systemic bone loss, as

well as altered bone formation. Bone remodeling includes osteophyte (bone spur)

formation and joint fusion in later stages of the disease. The dangers of these

16

pathological changes include altered function via collapsing subchondral bone, and/or limited joint movement. Bone formation is an attempt to restore normal morphology when the weight bearing surfaces of a joint fail and there is continual mechanical loading of the tissue (Skerry and Gowen, 1995). Formation usually occurs during remission, and not during flare ups, and therefore indicates that this process is reparative and not part of the pathogenesis (Skerry and Gowen, 1995).

Bone loss of about half the original length occurs in smaller bones, like the phalanges (Skerry and Gowen, 1995). Periarticular bone loss occurs for several reasons. Disuse- related loss will occur because of joint pain and subsequent loss of function. Joint effusion can alter the load across a joint and reduce stress on the subchondral trabeculae which results in remodeling (Skerry and Gowen, 1995). The cause of generalized osteoporosis is hard to understand, particularly because of difficulty in measuring whole body bone mass accurately. The main mechanism of local bone loss, however, is thought to be due to cytokine-mediated events. Both formation and resorption are elevated in RA, which suggests intervention may be directed at multiple control sites.

Multiple theories have been made about the impact of cytokines on bone remodeling (Cutolo et al, 2002; Klippel, 2001; Poole et al, 1995; Poole, 2001; Skerry and Gowen,1995). The reasons fall into three categories. First, few cytokines act alone, and therefore individual agents may be altered by the presence of another cytokine, which has an antagonistic or synergistic effect (Skerry and Gowen, 1995). Second, other molecules that are not cytokines modify the actions of the cytokines involved in bone remodeling (Skerry and Gowen, 1995). Finally, extracellular matrix components may bind to

cytokines, either to inhibit interactions with target cells, or to further increase their actions (Skerry and Gowen, 1995). Local and systemic effects result from the secretion of elevated cytokines into the synovial fluid in RA patients (Skerry and Gowen, 1995). One of the hypotheses for the presence of the cytokines, particularly in the synovium is to enhance bone resorption; however, measuring cytokine levels in the synovial fluid is not an accurate predictor of remodeling.

One of the main cytokines involved in the remodeling process is IL-1; it has been shown to have a positive action on bone resorption. It exists in two forms, alpha and beta. The method of signal transduction once binding occurs is not known, but is associated with a rapid rise in intracellular calcium. The effects of IL-1 on bone remodeling are due to direct or indirect stimulation of recruitment and activation of osteoclasts, while its effects on bone formation are due to effects on osteoblasts (Skerry and Gowen, 1995). *In vivo*, IL-1 induces bone resorption and is currently thought to be one of the causes of much of the pathological resorption in inflammatory diseases. IL-1 also up-regulates the expression of integrin subunits, which cause cell attachment, and therefore affects resorptive potential (Skerry Gowen, 1995).

TNF is the other cytokine involved in the destructive process of bone in RA. Even though there is little structural similarity between it and IL-1, the two share many functions. TNF also has two forms, alpha and beta. Two receptors exist for TNF which bind both forms despite marked structural differences in the receptor protein (Skerry and Gowen,1995). TNF's effects seem to be more variable than IL-1. These effects include proliferation of cultured bone cells, no effect, transient stimulation followed by inhibition, and inhibition only (Skerry and Gowen, 1995). This is occurs from post-

receptor factors. Therefore other unknown influences can modulate the responsiveness of cells. TNF and IL-1 do have a synergistic effect, in which suboptimal doses cause effects which are many times greater than the sum of their individual actions (Skerry and Gowen, 1995). This may be the reason for the profound effect in RA.

IFN-γ is produced primarily by T cells, natural killer cells and macrophages. IFN-γ can be a potent inhibitor of bone resorption in culture, and is stimulated by IL-1 and TNF. Its mechanism is not clear. It is thought to inhibit synthesis and release of metalloproteases used in matrix degradation (Skerry and Gowen, 1995).

Chemokines like IL-8 will lead neutrophil and monocyte infiltration to the site of their production. Tissue cells, when exposed to TNF and IL-1, will produce these chemokines (Skerry and Gowen, 1995). In addition to cartilage and bone, fibroblasts and endothelial cells have been known to release these chemokines (Skerry and Gowen, 1995). Monocytes chemoattractant MCP-1 is released by articular chondrocytes and osteoblasts when stimulated with IL-1 (Skerry and Gowen, 1995). This may propagate arthritis. Therefore, joint connective tissue cells such as osteoblasts and chondrocytes may act as effector cells in the induction and/or maintenance of the inflammatory process, rather than a responder or innocuous cell (Skerry and Gowen 1995).

Cellular causes of bone remodeling are thought to be due to synovial tissue's special ability to invade bone. This was especially supported by the invasive nature of fibroblasts which gain the ability to move and penetrate into cartilage and bone (Schett , 2006). Osteoclasts are responsible for the destruction of bone tissue, and are identified by tartrate-resistant acid phosphatase (TRAP) expression, cathepsin K, and calcitonin-receptors (Schett, 2006). These cells are multinucleated; however, mononucleated

osteoclast precursors are also found in the synovial membrane and express TRAP in RA patients. This is proof that cells designed for bone erosion are present in synovial inflammatory tissue and not only in bone marrow (Schett, 2006). Final proof that osteoclasts are essential for arthritis came from osteoclast-deficient models of arthritis. C-fos-deficient mice are free of osteoclasts because of a maturation arrest of the osteoclast lineage (Schett, 2006). Thus, RANK signaling is defective and no osteoclasts can develop. Bone resorption is absent in these mice, and they are completely resistant to the induction of arthritis. RANKL-deficient mice display no signs of bone erosion when standard methods are used to try to induce arthritis (Schett, 2006). These two models confirm the key role of osteoclasts in arthritic bone erosion, and can be a target for therapy.

Osteoclast formation is dependent on essential signals, which drive osteoclast precursors to differentiate into mature osteoclasts. These include M-CSF and RANKL (Imboden, 2009; Schett, 2006; Szekanecz and Koch, 2007). M-CSF is secreted by fibroblasts, and its receptor is expressed in osteoclast precursors (Schett, 2006; Szekanecz and Koch, 2007). RANKL is expressed in the synovial membrane, it is part of the TNF-α superfamily, and is structurally similar to TNF (Imboden, 2009; Schett, 2006). It is normally expressed by osteoblasts and drives osteoclast resorption. In RA, RANKL is also secreted by T cells and fibroblasts, thus providing a second signal to the osteoclast precursors (Schett, 2006). RANKL binds to its receptor, RANK, and elicits a cascade of signaling, which leads to the generation of mature and activated osteoclasts (Imboden, 2009, Schett, 2006). In the case where minimal amounts of RANKL are present, TNF-α supports the effects RANKL and allows for effective osteoclast formation (Schett, 2006).

The current model of bone erosion in chronic arthritis attributes an important role to RANKL. As in normal bone remodeling, bone erosion in RA is a multi-step process. First a microenvironment is formed, which will support osteoclast formation. This means a large amount of monocytes and/or osteoclast precursor cells from the blood move into the synovial membrane, with a concomitant rise in TNF-α (Schett, 2006). Next, RANKL expression is induced by mediators in cells of the synovial membrane like T cells and synovial fibroblast-like cells. The third step is the initiation of osteoclast differentiation by the engagement of RANK by RANKL (Schett, 2006). Finally, resorption of bone by osteoclasts allows the generation of an acidic pH, solubilizing calcium and the secretion of enzymes to remove bone matrix (Schett, 2006).

Systemic bone loss due to inflammation is also a problem in patients with RA (Skerry and Gowen, 1995, Schett, 2006). Osteoporosis develops in the majority of patients with the disease. This is associated with an increase in fracture risk. The reasons for this include increased age, gender (higher risk in females), decreased mobility secondary to functional limitations and systemic use of glucocorticoids (Skerry and Gowen, 1995, Schett, 2006). Disease activity is also a major predictor of osteoporosis in RA, independent of other concomitant factors, and suggests that the inflammation not only affects local bone, but also leads to bone loss in other areas. This is thought to result from disrupted cytokine balance with a negative net effect on bone (Schett, 2006), and can occur even when normal levels of PTH and 1,25 dihydroxyvitamin D exist (Skerry and Gowen, 1995). The over expression of cytokines may be the likely culprit in systemic bone loss (Schett, 2006).

The Effects of RA in Cartilage, Synovial Degradation, and Pannus Formation

The extracellular matrix of cartilage consists of ~70% water, largely in the superficial zone (Poole et al, 1995; Poole, 2001). Collagen molecules like type II, IX and XI are organized in fibrils that give cartilage its tensile strength (Poole et al, 1995; Poole, 2001). Resistance to compression is given by aggrecan, a large aggregating proteoglycan, and a component of the proteoglycan, glycosaminoglycan (Poole et al, 1995). The glycosaminoglycan chains are responsible for binding the massive amount of water (Poole et al, 1995). Macromolecular organization and retention of aggrecan in the matrix is determined by hyaluronan, an anionic, non-sulfated glycosaminoglycan that binds to the collagen fibrillar network (Poole et al, 1995; Poole, 2001). Articular chondrocytes embedded in the cartilage will differ in their response to mediators depending on what joint they come from (Poole, 1995).

Pannus is a sheet of inflammatory granulation tissue and synoviocytes that spreads from the synovial membrane; it is associated with cartilage loss as it invades the joint in RA. Some theories of its development include: (1) the concept of synoviocyte transformation into erosive immature mesenchymal cells; (2) the importance of neutrophils in early erosions of small joints; (3) the contributions of dedifferentiated chondrocytes in its early development and (4) the sequential progression from the erosive early pannus of fibroblastic/macrophagic cells to an end-stage fibrotic scar tissue (Wooley, 1995). When considering the process of cartilage erosion it is important to keep in mind which enzymes and specific cell types are responsible. Even though there is a recognizable sequence of events for damage and microenvironmental factors that control proteinase expression at erosion sites, at the same time it is also understood that

between specimens and within specimens a wide spectrum of histological observations of rheumatoid lesions are regularly seen (Wooley, 1995).

In the development of pannus and cartilage erosion in early RA, the junction between the synovial tissue, cartilage and bone is of prime importance, because it resembles adjacent synovial tissue with macrophages and type B synoviocytes. In this area, four common theories exist regarding the development of pannus.

The first theory was supplied by Fassbender, who suggested that fibrin exudates are necessary for the proliferation of local synovial tissue cells, which eventually invade cartilage matrix and subchondral bone (Fassbender, 1975, 1983; Wooley 1995). These cells have been described as immature mesenchymal cells that lack neovascularization, and have a tumor-like morphology and erosive capabilities. With the addition of vascularization, macrophages and lymphocytes become more fibroblast-like. As a result, pannus increases its collagen content, and becomes more fibrous, which substantially limits the joint's range of motion. This final product contains few fibroblasts, lymphocytes, mast cells or neutrophils and is characterized by dense collagenous scar tissue. Fassbender did not favor the idea of chondrocyte contribution to the developing erosive pannus tissue (Fassvender, 1975, 1983; Wooley 1995).

The second theory was developed by Shiozawa (1985) who, agrees with Fassbender that chondrocytes do not play a large role in the development of the pannus. However, they may contribute to the composition of the non-invasive, fibrous pannus, where the junction with cartilage is not clearly demarcated, and may be continuous with the cartilage matrix (Shiozawa, 1985; Wooley 1995). This observation may represent

healing or repair mechanisms, since they are often associated with fibrous, rather then quiescent, pannus tissue (Shiozawa, 1985; Wooley 1995).

Mitrovic (1985) attributes pannus development to fibrous metaplasia of hyaline cartilage, where chondrocytes activated by inflammatory cytokines dedifferentiate, enlarge their lacunae, coalesce and then break onto the cartilage surface to form a fibrous pannus (Mitrovic, 1985; Wooley 1995). The fibrous pannus becomes invaded by inflammatory cells from the synovial fluid. The chondrocytes lose their phenotype and acquire fibroblastic characteristics to destroy the cartilage (Mitrovic, 1985; Wooley 1995).

Lastly, many studies have discussed the role of neutrophils in cartilage destruction. They have been localized to the cartilage-pannus junction of small joint specimens showing early cartilage erosions. In contrast, many pathologists think their contribution to cartilage degradation is minimal, since they are not present extensively throughout the pannus.

Enzymes known to attack proteoglycans and cause cartilage erosion are produced from synoviocytes and chondrocytes; they include serine proteases and the metalloproteinase, stromelysin. The type II, IX and XI collagens are vulnerable to different enzymes, like collagenases. Once the collagen framework is destroyed, the cartilage's morphology and properties will not return. The cysteine proteinases, cathepsin B and cathepsin L, are derived from lysosomes, and will also break down type II, IX and XI collagen, as well as proteoglycan aggregates. Cathepsin B has been found in synovial cells in RA joints (Wooley, 1995).

At cartilage-pannus junctions, collagenase is present in 40% of cellular junctions examined in RA joints, whereas synovial tissue remote from the cartilage interface showed only a few cells producing collagenase (Wolley, 1995). This enzyme was more frequently found in cartilage erosion sites. Chondrocytes close to the cartilage-pannus junction occasionally express this enzyme, while deeper chondrocytes are more frequently collagenase-negative. Stromelysin is more frequently found in pannus tissue, most frequently at erosion sites (Wooley, 1995).

Macrophages are present at erosion sites, apparently attacking these sites with intracellular acid phosphatase. Macrophages found away from the erosion sites contain relatively little acid phosphatase (Wooley, 1995).

Subchondral cartilage erosions demonstrate a different cellular composition than synovial pannus tissue. Here, there are multiple multinucleated chondroclasts that show erosive attachments to the cartilage matrix. These cells are described as having multiple nuclei, acid-phosphatase-positive cells with ruffled borders associated with calcified or hyaline cartilage. Osteoclasts, in contrast, are associated with mineralized bone. Chondroclasts are observed in approximately 30% of large joint specimens, where they make a major contribution to the subchondral cartilage erosions of large joints, but are rarely found associated with small joint pathology (Wooley, 1995).

Serial sectioning of cartilage lacunae demonstrate that when they are not in continuity with the pannus, the cells entombed here still become activated and produce pannus and lytic activity. In contrast, adjacent areas in the same specimen show chondrocytes close to the pannus interface, with no signs of activity, and other chondrocytes that may repair earlier proteoglycan depletion. This finding demonstrates

the chondrocyte's role in both catabolic and metabolic activity, indicating responsiveness to different local signals and emphasizing the importance of the microenvironment in cartilage loss and repair (Wooley, 1995).

Cartilage is usually not close to a blood supply, and therefore, gets its energy from anaerobic glycolysis (Poole, 1995). It is an immunologically reactive tissue, with both humoral and cellular immunity. The extracellular matrix plays an important role in shielding chondrocytes from immune damage, like that caused by cytotoxic T lymphocytes and antibodies (Poole, 1995). It is immunologically privileged, because of its avascularity. A bidirectional attack on cartilage manifests, as cells erode both the surface and subchondral portion of articular cartilage concomitantly. This method of erosion may reflect changes in either the cartilage matrix components or their immunology, as judged by the production of autoantibodies to specific cartilage components. T lymphocytes found at the sites of cartilage erosions stimulate or recruit cells, such as macrophages, B cells, fibroblasts, mast cells, and neutrophils, especially in relation to the production of autoantibodies, cytokines and prostaglandins (Wooley, 1995).

The bidirectional attack observed in large joints demonstrates different types of cells above and below the cartilage. Macrophages and fibroblasts are the predominant cells of the cartilage-synovial pannus junctions, while multinucleated cells, macrophages and small blood vessels are the major components of the subchondral erosion sites (Wooley, 1995). Multinucleated cells with acid phosphatase activity have never been observed at cartilage-synovial pannus junctions (Wooley, 1995). However, no regular pattern of cartilage erosion has emerged, indicating that the cellular composition at sites

of cartilage erosion is variable. Adding to the variability, in comparison to the discontinuous pannus in large joints, small joints undergo a process called capping or underpinning, which demonstrates a continuous erosive front (Wooley, 1995). Adding to more confusion, other patterns also exist.

TNF-α and IL-1 play an important role in cartilage and bone degradation. In RA, most of the pro-inflammatory cytokine-containing cells are macrophages (Klippel, 2001; Szekanecz and Koch, 2007; Wooley, 1995). Proteinase production in the microenvironment is therefore contingent on a complex sequence of cellular events brought on by local signals derived from cells, extracellular matrix, and possibly immune complexes. These signals are capable of initiating activation, recruitment and proliferation of specific cells at the sites of erosion (Wolley, 1995).

The metalloproteases are synthesized and secreted into the extracellular matrix as inactive proenzymes, which requires a zinc atom at the active site and may involve changes in molecular conformation (Poole, 2001). On the other hand, procollagenase can be partly activated by plasmin to produce a molecule, which is further cleaved by stromelysin-1 to remove the prodomain resulting in superactivation of collagenase (Poole, 2001). In the presence of IL-1, plasminogen increases matrix degradation in culture. Because of its large size, it is unlikely that plasminogen can penetrate healthy cartilage. This implicates plasmin activity derived from plasminogen activator on plasminogen. Ordinarily, the proteoglycan, aggrecan, restricts permeability to molecules smaller than 60 kDa. In arthritis, loss of aggrecan would therefore favor plasminogen penetration. Thus, plasminogen activators have the potential to play an important role in matrix degradation (Poole, 2001).

Collagenase is the only proteinase that can cleave the triple helix of type II collagen in cartilage. In RA, type II collagen cleavage is usually first seen in pericellular and territorial sites adjacent to the calcified matrix and subchondral bone around chondrocytes of the deep zone. Early damage to the articular surface is substantially limited (Poole, 2001). Diffuse damage to the collagen fibrils through the cartilage matrix is a feature of more advanced stages in RA. This finding demonstrates that cellular events in adjacent bone, which produces an extensive osteopenia or osteoporosis, may result in the production of prodegradative cytokines, like IL-1 and TNF-α (Poole, 2001). These proinflammatory cytokines act not only on osteoblasts and osteoclasts, but also on deep zone chondrocytes close to the bone. In RA, considerable damage to type II collagen is observed in sites adjacent to pannus invading cartilage. Triple helical cleavage of type II collagen by activity from neutrophil collagenase on the articular surface may be of limited importance. Loss of aggrecan in acute inflamed joints has also been noted without the presence of neutrophil accumulation (Poole, 2001). Therefore, the role of the neutrophil is secondary to chondrocyte- and synovial-mediated cartilage degradation (Poole, 2001).

Stromelysin-1 and cathepsin B and G can also cleave collagen type II in the non-helical telopeptide region, where intermolecular crosslinks are located (Poole, 2001). Unwound triple helical collagen is readily cleaved by gelatinases, and also by interstitial collagenase and stromelysin-1. There is no evidence indicating that the other metalloproteases can degrade the triple helix of type II collagen.

Aggrecan and link proteins form macromolecular aggregates with hyaluronic acid. Aggrecan is secreted from chondrocytes (Poole, 2001), and is initially cleaved

proteolytically to release a very high-molecular-weight product essentially similar to its original form. It can also be cleaved by gelatinases, cathepsin B, and interstitial collagenase. Other cleavage sites, elsewhere in the molecule, such as in chondroitin sulfate-rich regions, have characteristics that suggest one common proteinase is responsible (Poole, 2001). Link protein is primarily fragmented by stromelysin-1, cathepsin B and G, stromelysin-2, collagenase, and gelatinases (Poole, 2001).

The proteoglycan, decorin, binds the collagen fibrils as they form, and can regulate fibril diameter (Poole et al, 1995; Poole, 2001). Collagen fibrils that form in the presence of decorin are of smaller diameter (Poole et al, 1995; Poole 2001). In normal articular cartilage, collagen fibrils are much thinner at the surface, where decorin is most concentrated (Poole et al, 1995; Poole, 2001). Here, the fibrils are aligned parallel to the surface (Poole et al, 1995; Poole, 2001), an important functional property, since this area is exposed to maximal shearing, compressive, and tensile forces. The intermediate zone consists of rounded cells surrounded by an extensive extracellular matrix. The deep zone cell volume is lowest, and cells here often form clusters, in contrast to the surface, where cell density is highest (Poole et al, 1995; Poole, 2001). These superficial cells are more susceptible to IL-1, and therefore damage (Poole et al, 1995; Poole, 2001).

The sequelae of RA are mediated by an interdependent network of cytokines and proteolytic enzymes. The main contributors in this mechanism are TNF-α and IL-1. Cytokines and growth factors obtain a balance between synthesis and degradation of matrix turnover. The net loss of structural matrix molecules results from an imbalance between the synthesis, activation, and inhibition of proteinases coupled with impaired synthesis and incorporation of molecules within the extracellular matrix (Poole et al,

1995; Poole, 2001). Controlled proteolysis occurs by the release of type II collagen and aggrecan fragments, and other cartilage matrix molecules, into healthy synovial fluid and peripheral blood (Poole et al, 1995; Poole, 2001). There is excessive damage and removal of resident molecules in arthritis, which involves a rapid turnover of the matrix in close proximity to the chondrocytes in the pericellular domain.

Insulin-like growth factor-1 (IGF-1) is one of the most potent anabolic molecules present in synovial fluid and serum, and can stimulate synthesis of major structural matrix molecules (Poole et al, 1995; Poole, 2001). TNF-α and IL-1 can individually or jointly, severely inhibit matrix synthesis of type II collagen and aggrecan (Poole et al, 1995; Poole, 2001). They cause damage by increasing transcription of metalloproteases, especially stromelysin-1, in articular cartilage, possibly by stimulating plasminogen activator synthesis. IL-1 can stimulate cathepsin B activity in articular cartilage cells. IGF-1 and TGF-β negate the harmful effects of IL-1 and TNF-α, protecting the tissue (Poole et al, 1995; Poole, 2001).

In addition to inhibiting matrix synthesis, IL-1 can cause degradation of type II collagen and aggrecan in articular cartilage (Pooleet al, 1995; Poole, 2001). IL-1 *in vivo* increases neutrophil infiltration and loss of aggrecan (Poole, 2001). Intra-articular TNF-α causes neutrophil infiltration as well, but is substantially less potent than IL-1 (Poole et al, 1995; Poole 2001). It can increase matrix degradation, and inhibit cartilage proteoglycan synthesis (Poole et al, 1995; Poole; 2001). Molecular mechanisms for the signaling of these cytokines in chondrocytes involve intermediary pathways using protein kinase C and transcriptional regulation of stromelysin and collagenase. Degradation products of matrix molecules can stimulate matrix destruction by chondrocytes and other

cells (Poole et al, 1995; Poole, 2001). Mechanical forces can also regulate matrix turnover.

Matrix degradation in RA involves global destruction of all tissues in the joint. The ingrowth of pannus may be related to cartilage collagen degradation and the stimulation by IL-1 and IL-8 synthesis, a potent angiogenic molecule (Poole et al, 1995; Poole, 2001). Adjacent to the edge of the pannus formation, destruction of type II collagen occurs in the presence of collagenases and stromelysin (Poole et al, 1995; Poole, 2001), and is associated with increased expression of proteinases by the synovium. The destruction of type II collagen in the deep zone near the subchondral bone may be due to the substantial turnover of subchondral bone in RA, which is associated with increased bone resorption.

Regulation of Bone Remodeling by the Central and Peripheral Nervous Systems

Cytokine-Mediated Brain Activation in RA Contributes to Pathophysiology

RA symptoms such as fever, malaise, loss of appetite and weight loss are due to cytokine release into the blood stream to affect brain regulation of these processes. Synthesis of cytokines can be induced in the brain by blood borne signals, such as circulating peripheral cytokines, and by neural signals induced with immune challenge (Lorton 2008). Glial cells and neurons are capable of producing cytokines, and express functional cytokine receptors. Peripheral immune activation induces the expression of cytokine mRNA and protein in the brain (Hopkins and Rothwell, 1995). Numerous studies have indicated that peripheral expression of cytokines by activated peripheral immune cells is consistently associated with delayed induction of cytokines in specific

brain regions known to be involved in sickness response (Crosby, 1988; Lorton et al, 2008). The cellular targets for proinflammatory cytokines produced in the brain are still not entirely clear, and the mechanisms by which the brain-derived cytokines signal target neurons remains to be elucidated (Crosby, 1988; Lorton et al, 2008). However, there is evidence that cytokines produced locally in the brain are responsible for the behavioral effect of peripheral cytokines (Lorton et al, 2008).

The proinflammatory cytokines released in the periphery by monocytes and macrophages activate peripheral afferent nerves to induce the synthesis and release of proinflammatory cytokines in the brain. Central cytokines then act on key neural circuits that are involved in the control of thermo-regulation, metabolism, psychological status and behavior (Crosby, 1988; Lorton et al, 2008; Thompson et al, 1992). The sympathetic nervous system (SNS) is one of two major routes through which the CNS regulate the immune system and its synthesis and release of peripheral cytokines. One role of the SNS is to provide negative feedback regulation thereby dampening the production of proinflammatory cytokines and promote the expression of anti-inflammatory cytokines to return to a homeostatic state. There are numerous reports of a stressful event preceding flairs in RA (Cutolo et al, 2002; Lorton et al, 2008; Lubahn et al, 2004), which suggests that stress, which in part mediated via the SNS, plays a role in inflammatory arthritis (Crosby, 1988, Lorton et al, 2008; Thompson et al, 1992), and that increased sympathetic tone reported in RA patients may promote, and contribute to, disease pathology (Lorton et al, 2008).

Stress and RA: the Hypothalamic-pituitary Adrenal Axis

The hypothalamic-pituitary-adrenal (HPA) axis is a complex set of direct influences and feedback interactions among the hypothalamus, the pituitary gland, and the adrenal glands. Its interactions constitute a major part of the neuroendocrine system that controls reactions to stress and regulates many body processes, including the immune system, emotions, energy storage and expenditure, digestion and sexuality.

Besides the SNS, the HPA axis is another major efferent pathway from the CNS that mediates the effects of stress on RA. It regulates the immune response through corticosteroids. Both systems promote humoral immunity by altering macrophage and T cell cytokine production after antigen challenge. This is done by inhibiting IL-12 and IFN-γ which drives cell-mediated immunity. They also both inhibit inflammation. These pathways enable the HPA axis and SNS to influence the course of RA (Lorton et al, 2003). In RA, the HPA axis is hypofunctional; it concomitantly has a poorly functioning peripheral and central region. The cause of the hypoactivity is unknown (Lorton et al, 2008).

Glucocorticoids from the HPA axis and NE from the SNS interact with immune cells by receptors that regulate the production of key cytokines (Lorton et al, 2008). Glucocorticoids modulate immune responses by binding to cytosolic glucocorticoid receptors within immune target cells, while catecholamines do so by interaction with plasma membrane β- or α-ARs. This binding promotes humoral immunity by altering macrophage and T cell cytokine production after immune challenge. The inhibition of IL-12 and IFN-γ drives cell mediated and humoral immunity by stimulating IL-10 production by macrophages via β_2-AR activation.

In patients with RA, changes in immune cell expression of β and α-ARs have been reported in peripheral blood mononuclear cells. The potential consequences of a shift from β to α-ARs expression by monocytes/macrophages in RA has been speculated because of altered disease outcomes after treating animal models with selective β and α adrenergic agonist and antagonist (Lorton et al, 2008). A β_2 to α-AR shift in receptor expression on macrophages would reduce the inhibitory effects of β_2-AR stimulation while augmenting the stimulatory effects of NE binding with α-1 ARs (Lorton et al, 2008). These changes accompanied by an increase in sympathetic outflow would be expected to drive inflammatory processes by promoting production of proinflammatory cytokines.

Catecholamines and gluccocorticoids inhibit inflammation by decreasing production of proinflammatory cytokines from macrophages/monocytes. This is how homeostasis is maintained. The dysregulation of these stress pathways in RA patients indicates that these homeostatic mechanisms are dysfunctional and contribute to the cytokine imbalance that propagates the chronic inflammatory response. Therapies that address these neural pathways and restore immune homeostasis could be helpful for RA patients. Such treatments would be expected to restore the balance of pro- to anti-inflammatory cytokines and reduce joint pathology.

Innervation of Bones in the Hind Limbs

Innervation of Joints of the Hind Limb and their Role in RA

Neurogenic inflammation, which is mediated via both autonomic and sensory nerves, plays an essential role in the joint pathology associated with RA. Neurotransmitters released by these nerves regulate vascular changes, chemotaxis and

activation of immune cells that mediate the inflammatory response as well as nociception. Recent studies indicate nerve signaling to bone cell receptors can regulate bone metabolism under normal conditions, but this same path can also contribute to bone and cartilage destruction in RA (Offley et al, 2005; Owan and Ibaraki, 1994; Schwab et al, 1997; Togari, 2002).

The joint capsule, synovium, subchondral bone, bone marrow, trabecular bone and periosteum are all innervated by primary sensory afferent neurons, whose cell bodies reside in the dorsal root ganglia (DRG), and by postganglionic, sympathetic efferent nerves. DRG neurons synthesize and secrete sensory neuropeptides, mostly notably substance P (SP) and calcitonin gene-related peptide (CGRP), whereas sympathetic neurons that innervate bone synthesize and secrete norepinephrine (NE), neuropeptide Y (NPY), and vasoactive intestinal polypeptide (VIP). The density and distribution of these nerve fibers varies in different bones.

The marrow of the distal rat tibia is innervated by sympathetic nerves. These nerves are often identified by immunohistochemistry for tyrosine hydroxylase (TH), the rate-limiting enzyme for synthesizing NE, the major neurotransmitter within these nerves. NPY and VIP co-localize with NE nerves. TH-ir (immunoreactive) fibers enter the proximal and distal tibial epiphysis, accompanying the intramedullary vessels. In contrast to the smaller sized vessels that the diaphyseal CGRP-ir fibers adhere to, the TH-ir fibers course along relatively large-diameter vessels. TH-ir fibers are present in the bone marrow of the metatarsal bones, but not in the region of the tarsus (Imai et al, 1997).

Both sensory and sympathetic nerves are also found in other tissues associated with joints; for example, the sublining layers of synovial membranes, tunica adventitia and

media of arteries, periosteum, vascularized fibrocartilage of menisci, perichondrium, Volkmann's canals of bone, ligaments, and particularly, ligamentous attachments. However, the lining layer of the synovium is not innervated by sympathetic nerves. (Schwab et al, 1997; Cherruau et al, 2003).

Neurotransmitters released from these nerves bind to their specific receptors expressed in bone cells to regulate bone cell function *in vivo*. Thus, the central and peripheral nervous systems play an important role in the complex regulatory mechanisms that control bone remodeling, particularly, the SNS, via release of NE to affect bone cell functions after subsequent binding with β_2-ARs. Neurons in the CNS receive information from bone cells in the periphery and process this and other information regarding homeostasis, glycemia, or reproductive signals with the regulation of bone remodeling, a process called negative feedback. Alternatively, osteoblasts and osteoclasts constitutively secrete diffusible axon guidance molecules that function as a chemoattractant or chemorepellent for growing nerve fibers (Togari, 2002).

Buma (2000) found lower numbers of neuropeptide-containing fibers in methylated bovine serum albumin-induced arthritis of mice knee joints, suggesting disease-mediated fiber depletion due to necrosis or proliferation of soft tissues. The synovial cavity was enlarged, but the most pronounced changes were in the pattern of CGRP, substance P, VIP, and TH fibers in the periosteum. This finding was confirmed by other authors (Cherruau et al, 2003; Imai et al, 1997). The SP and CGRP fibers in the periosteum were gradually depleted. These findings suggest that in the proliferative inflamed areas nerves die back and/or fail to grow into the inflamed regions (Buma et al, 2000).

Sensory Nerves in Bone

The sensory nervous system also regulates bone resorption. CGRP, although less potent than calcitonin, binds to calcitonin receptors on osteoclasts *in vitro* and *in vivo*, inhibiting bone resorption by a cAMP-dependent mechanism (Zaidi et al, 1987; Owan et al, 1994). CGRP inhibits precursor cell development and prevents the fusion of committed precursor cells to form multinucleated cells (Cornish et al, 2001). Adam and colleagues (2000) have found that reducing CGRP and SP fibers by 58 and 49% respectively, in the rat mandible, by using the neurotoxin capsaicin, decreases the number of actively resorbing osteoclasts without affecting the total number of osteoclasts, and it also lowers osteoclast precursor numbers. Capsaicin-sensitive sensory neurons are important for maintaining trabecular bone. Four weeks after capsaicin treatment that produced a 57% loss in unmyelinated sensory axons, bone mineral density (BMD) decreased in the metaphysis of the tibia and femur in rats. In the proximal tibia, osteoclast number and surface area increases, trabecular bone volume and connectivity are diminished, and bone formation is impaired (Offley et al, 2005).

Peripheral Nerves and RA

Sensory and sympathetic nerve densities increase and decrease, respectively, in the synovium of patients with longstanding RA depending on the severity of inflammation (Cutolo et al, 2002; Miller et al, 2000; Ahmedet al, 1995). This decrease in sympathetic nerves may be a compensatory mechanism to halt the bone destruction. Despite the loss of sympathetic nerves, NE levels are maintained by synovial macrophages (Cutolo et al, 2002).

CGRP-ir fibers directly appose osteoblasts and osteoclasts in the metaphysis and are near periosteal lining cells of normal rats. In AA rats, these small non-myelinated nerves are extensively degenerated. Numerous $CGRP^+$ fibers re-innervate the post-arthritic ossifying periosteum, eroded surface of metaphyseal bone and cartilage (Imai et al, 1997). AA rats show a considerable number of helper T cells and macrophages immunoreactive for nerve growth factor (NGF) invading the synovium and a dense plexus of $p75NGFR^+$ nerve fibers closely apposed to osteophytes (Wu et al, 2002). This suggests that NGF derived from immune cells may enhance the outgrowth of peripheral nerves. From their data, it also suggests that CGRP released from these nerves may cause osteophyte formation in the synovium.

The Role of the SNS in Bone Remodeling

Pharmacological manipulations and various genetic mouse models with autonomic dysfunctions have demonstrated the existence of a neuronal pathway between the hypothalamic neurons and osteoblasts. Lack of dopamine beta-hydroxylase, the enzyme generating NE, induces a late onset increase in bone mass. Consistent with this finding, mice and rats treated with the non-selective β-adrenergic blocker, propranolol, displayed an increase in bone mass (Elefteriou, 2008). Animals treated with non-selective β-agonists or $β_2$ adrenergic selective agonists exhibit a low bone mass (Elefteriou, 2008). Collectively, these findings demonstrate a role for the SNS in regulating bone formation.

The presence of multiple types of nerves, with each population containing and releasing a variety of neuromediators, in the bone and periosteum microenvironment, suggest multiple neuropeptides and their receptors expressed on cells within bone

regulate bone physiology (Adam et al, 2000; Ahmed et al, 1995; Akopian et al, 2000; Buma et al, 2000; Cherruau et al, 2003; Cornish et al, 2001; Elefteriou, 2008; Frediani et al, 1996; Imai et al, 1996 and 1997; Neugebaur et al, 1996; Nissalo et al, 2002; Offley et al, 2005; Togari, 2002; Wu et al, 2002; Zaidi et al, 1987). Other indirect pathways through which neural mediators affect bone metabolism exist, including neuropeptide influences on the function of osteoclasts, adipocytes and immune cells.

Sympathetic signaling inhibits bone formation via β_2-AR on osteoblasts (Elefteriou, 2008; Lubahn et al, 2004). The SNS also mediates the effects of hypothalamic leptin-induced inhibition of bone formation via a β_2-AR-mediated mechanism (Elefteriou, 2008). This is not induced through osteoblast apoptosis, but rather by inhibition of osteoblast proliferation and function (Elefteriou, 2008). Leptin is an adipocyte-derived hormone whose secretion in the hypothalamus is regulated by the SNS. Leptin binding with its receptor, ObRb (Elefteriou, 2008), enhances proliferation of chondrocytes and their synthesis of matrix (Poole, 2001), stimulates local bone resorption and inhibits bone formation by acting on the brain (Elefteriou, 2008). Leptin-deficient mice (despite their hypogonadism and hypercorticosteronemia) and lipodystrophic mouse models that express little or no serum leptin levels have a high bone mass (Elefteriou, 2008). Similarly, mice deficient in another hypothalamic neuropeptide, neuromedian U (NMU) whose release is regulated by leptin, also have high bone mass (Elefteriou, 2008). NMU deficient mice were resistant to the anti-osteogenic effect of leptin and β-AR agonists (Elefteriou, 2008). Intracerebroventricular (icv) infusion of leptin in leptin-deficient mice reduces bone mass to levels similar to their wildtype littermates after 28 days (Elefteriou, 2008). Additionally, destruction of the

ObRb-positive hypothalamic neurons in the wild type mice produces the high bone mass phenotype similar to leptin-deficient mice, and makes the lesioned mice resistant to the anti-osteogenic effect of icv infused leptin (Elefteriou, 2008). These findings further support a role for leptin as an inhibitor of bone formation *in vivo*, an effect indirectly mediated via its regulation of NMU expression in the hypothalamus and subsequent modulation of SNS outflow to affect osteoblast function (Elefteriou, 2008).

Encannabinoids also regulate bone homeostasis by signaling CB1 and CB2 receptors, which are highly expressed in the CNS, and increase after traumatic brain injury, suggesting that activation regulates sympathetic signaling at the pre-synaptic level in bone nerve endings by reducing NE release and inhibiting the anti-osteogenic function of the SNS (Elefteriou, 2008). This may be what leads to heterotrophic ossification in patients with nervous system damage like traumatic brain injury, spinal cord injury or burns.

Other nerve-derived peptides are likely to contribute to the growing list of molecules regulating bone remodeling, including endothelial nitric oxide synthase (eNOS) and inducible nitric oxide synthase (iNOS), which modulate osteoblasts (Elefteriou, 2008). Also, neuronal nitric oxide synthase (nNOS), which is highly expressed in the CNS and peripheral nervous system, performs a role in cell communication and is a negative regulator of bone remodeling (Elefteriou, 2008). Bioactive amines, like glutamine, dopamine, and serotonin, may also contribute to the regulation of bone metabolism. It is also possible that CGRP secreted by nerve terminals modulates osteoblast biology by a direct mechanism (Elefteriou, 2008).

NE released by sympathetic nerves influences bone resorption *in vitro*. This along with the expression of β- and α-AR on osteoblasts and sympathetic nerves that innervate osteoblasts, suggests that the catecholamines NE and epinephrine are involved in local bone metabolism. Catecholamines are reported to enhance the proliferation and differentiation of cultured osteoblast-like cells, such as MC3T3-E1 cells, a response that is able to be blocked by selective α_1-AR antagonists. Therefore, the SNS may alter bone metabolism by altering the numbers and differentiation of osteoblasts in arthritic joints (Lorton et al, 2003).

SNS Effects on Osteoblasts

Catecholamines alter bone metabolism by affecting bone formation and resorption regulatory proteins produced by osteoblasts and osteoclasts, including osteocalcin. For example, osteocalcin, an extracellular calcium-binding protein, is synthesized by osteoblasts and binds with high specificity to bone mineral crystals to promote bone formation. Decreases in plasma osteocalcin observed after major abdominal surgery are attributed in part to increased circulating catecholamines, as well as cortisol. While considerable literature supports glucocorticoid regulation of osteocalcin, data regarding catecholamines' effects on plasma osteocalcin levels are limited and mainly confined to animal studies. In these studies, increased catecholamines following restraint stress decreased osteocalcin levels. The absence of sympathetic neural function or adrenal cortisone production following sympathetic ganglia blockade or adrenalectomy increased osteocalcin levels by 50% (Takeuchi et al, 2000). Stress-induced release of both corticosterone and NE, but not epinephrine, were required to return plasma osteocalcin levels to baseline values after restraint stress, suggesting that both corticosterone and NE

regulate plasma osteocalcin and osteocalcin release from bone, at least under certain types of stress (Takeuchi et al, 2000). Similarly, catecholamines can affect alkaline phosphatase production, which is necessary for bone formation. Alkaline phosphatase is found in the membrane of osteoblasts and is released into the circulation during bone formation. With surgery, a major stressor, circulating alkaline phosphatase levels are either increased or decreased. Bone-specific alkaline phosphatase levels are not increased with increased glucocorticoid secretion. Stress-associated decreases in bone-specific alkaline phosphatase levels are mediated by catecholamines or cytokines. Similarly, treatment of osteoblast-like cells with isoproterenol, a β-AR agonist, increases alkaline phosphatase. This effect is blocked by the non-specific β-AR antagonist, propranolol. In contrast, epinephrine increases alkaline phosphatase activity in differentiating osteoblast-like cells (MC3T3-E1 cells) by stimulating α_1-AR (Takeuchi et al, 2000).

Regardless of the specific AR involved in each of these studies, they suggest that NE alters bone formation by reducing osteoblast activity. While the functions of alkaline phosphatase are not entirely clear, it is thought to initiate bone mineralization. Alkaline phosphatase is responsible for local increases in inorganic phosphate ion concentrations by its action on the organic phosphate supplement, but it is not required for mineralization to proceed once initiated. High alkaline phosphatase activity may result in "ectopic mineralization", where calcium phosphate crystals are deposited in cultures, but without the intimate relationship of crystals to matrix. Therefore, the increases in sympathetic tone through release of NE could contribute to changes in bone metabolism

and the calcification of soft tissues that occur in arthritic joints, by altering osteoblast

alkaline phosphatase production.

SNS Effects on Osteoclasts

Catecholamines modulate osteoblast regulation of osteoclast differentiation. The

effects of catecholamines on osteoclast differentiation may result from catecholamine-

induced increases in production of osteoclast differentiation factor (ODF) also known as

RANKL and osteoclastogenesis inhibitory factor (OCIF) also known as osteoprotegerin

(OPG). Treatment with epinephrine rapidly increases ODF and OCIF mRNA levels in

osteoblast-like MC3T3-E1cells (Takeuchi et al, 2000). A β-AR antagonist inhibits

epinephrine-induced increases in ODF, while an α-AR antagonist blocks epinephrine-

induced increases in OCIF mRNA levels. The epinephrine-induced osteoclast

differentiation factor increases were mediated by catecholamines, and indirectly by

catecholamine-induced changes in IL-11 and PGE_2 production (Takeuchi et al, 2000).

These findings suggest that catecholamines have both direct effects and indirect effects

through IL-11 and PGE_2 and ODF and OCIF mRNA expression in osteoblasts in order to

induce osteoclastogenesis (Takeuchi et al 2000). The effects of catecholamines on

osteoblast regulation of osteoclast differentiation via β-ARs is also supported by an

increase in TRAP-positive multinucleated cells upon treatment of mouse bone marrow

cells with isoproterenol, a β agonist, or epinephrine (Takeuchi et al, 2000). TRAP is a

reliable marker for osteoclasts *in vivo*, and is expressed in late osteoclast development.

Additionally, AR agonists efficiently activate β-AR on osteoblast cells, and stimulate

bone resorption in intact mouse calvaria in organ cultures (Takeuchi et al, 2000).

Consistent with these findings, chemical sympathectomy in rats by treatment with

guanethidine, a sympathetic neurotoxin, impairs bone resorption, reduces the number of osteoclasts, impairs osteoclast access to the bone surface, and decreases TRAP+ mononuclear preosteoclasts (Cherruau, 2003). Collectively, these findings support a role for the SNS in regulating osteoclast differentiation and bone resorption. Therefore, SNS dysregulation in RA and AA could impact bone destruction through effects on osteoclast differentiation and bone resorption. Similarly, effects of adrenergic drug treatments on bone destruction in AA could result from altered osteoclast differentiation and therefore inhibition of bone resorption.

Indirect SNS Effects on Bone Metabolism

SNS signaling of immunocytes also could alter bone metabolism indirectly by changing immune cell cytokine production, which then influences osteoblast and osteoclast function. For example, inflammatory cytokines elevated in RA patients during flares, such as TNF-α and IL-1, are potent inhibitors of osteocalcin synthesis. IL-6, which also is elevated in RA patients, promotes the development of both osteoclasts and osteoblasts. Since catecholamines modulate proinflammatory cytokine production, including TNF-α and IL-1, their effects on osteocalcin release from bone could be mediated indirectly by altering cytokine production.

Additionally, target cells of sympathetic nerves in the joint include resident macrophages, mast cells, synoviocytes, fibroblasts, small non-myelinated afferent fibers, and vasculature. Sympathetic modulation of these cells could impact disease outcome. For example, vascular changes can promote fluid and immune cell infiltration into the joint (edema), and reduce clearance of destructive components from the joint capsule. Therefore, the SNS could impact bone metabolism through multiple indirect pathways.

Sympathectomy by treatment with guanethidine increases osteoblastic activity and reduces osteoclast number and activity in rats (Cherruau et al, 2003). The effect on the osteoclasts may be from decreased VIP release from sympathetic nerves. VIP-ir fibers are positioned close to the most peripheral and less differentiated osteogenic cells. In the absence of osteoblast/stromal cells, VIP induces a rapid cytoplasmic contraction and decreases motility of osteoclasts. However, when osteoblasts/stromal cells are present, VIP increases the number of resorption pits and total bone area resorbed. Therefore, VIP regulates osteoclast activity by specific binding sites on both osteoclasts and osteoblasts. VIP receptors on differentiated osteoclasts transiently inhibit osteoclast activity, while VIP receptor activation on stromal cells/osteoblasts indirectly promotes osteoclastic resorption (Lundberg et al, 2000; Ransjo et al, 2000). The inhibitory effects of VIP on osteoclast recruitment may be due to regulation of key proteins involved in the later stages of osteoclast differentiation, such as ODF and OCIF expressed in osteoblast/stromal cells (Togari et al, 2002).

Osteoblasts and osteoclasts possess α- and β-ARs. β-Adrenergic agonists increase the number of TRAP$^+$ multinucleated cells from mouse bone marrow cells (Takeuchi et al, 2000), and bone resorbing capabilities in human osteoclast-like multinucleated cells in the absence of osteoblastic/stromal cells (Arai et al, 2003). *In vitro* studies have demonstrated that catecholamines can induce osteoclast maturation and stimulate osteoclast activity via a β_2-AR-mediated mechanism. Catecholamines increase TRAP activity, IL-6 production, multi-nuclearity, and response to calcitonin in human osteoclast precursors (Frediani et al, 1996). β-AR stimulation activates osteoblasts to secrete ODF. Similarly, treatment with epinephrine rapidly increases ODF and OCIF in

MC3T3-E1 osteoblast-like cells.   It also increases cyclooxygenase (COX)-2, IL-11 and PGE$_2$, cytokines which increase ODF and OCIF, but not as rapidly as epinephrine. These findings suggest both direct and indirect effects of epinephrine on ODF and OCIF secretion, and supports indirect stimulation of osteoclastogenesis via osteoblastic cells and direct stimulation of bone resorbing activity of osteoclasts.

 Human bone marrow cells that constitutively express mRNA for α and β- AR also expressed characteristic markers for mature osteoclasts. The resorbing activity by these cells as indicated by f-actin rings and resorption pits is substantially increased by isoprenaline (β-adrenergic agonist), moderately increased by epinephrine (an α and β adrenergic agonist), and poorly increased by phenylephrine (an α$_1$-adrenergic agonist) (Arai et al, 2003), suggesting that this effect is primarily mediated via β-AR. β-AR-mediated bone resorbing activity may be mediated by up-regulating the α V chain of integrin, carbonic anhydrase II, and cathepsin K, which results in attachment, demineralization and collagen degradation, respectively. These findings indicate that sympathetic nerves in bone play an important role in the control of bone cell activity.

 SNS dysfunction in RA is also supported by our findings showing a parallel reorganization of sympathetic innervation and immune cell populations in spleens from AA rats. In severe disease, we have demonstrated that sympathetic nerves are lost in spleen compartments where immune target cells reside (white pulp). In contrast, sympathetic nerves sprout abnormally into compartments where more mature or activated immune cells reside (red pulp), suggesting that nerve remodeling takes place in lymphoid organs with development of inflammatory arthritis.

Clinical Evidence of Autonomic Dysfunction in RA

Autonomic neuropathies comprise a collection of syndromes and diseases affecting either parasympathetic or sympathetic neurons, or both. In patients with autoimmune rheumatic disease, both neurological and cardiac manifestations occur, and significantly affect the clinical course of the disease (West, 1994; Riboldi et al, 2002). Autonomic nervous system (ANS) dysfunction is a complication of many chronic diseases, but is most extensively studied in diabetic populations (Vinik et al, 2003), and as it pertains to oncology (Lorusso, et al, 2007). ANS dysfunction in autoimmune-mediated rheumatic diseases has been recently reviewed by Stojanovich (2009). Manifestations of parasympathetic and sympathetic dysfunction have been reported in variable proportions ranging between 24% and 100% of patients with autoimmune-mediated rheumatic disease, depending on the methods used (Mravec, 2007; Cutolo and Straub, 2008; Hogarth et al, 2002; Mori et al, 2005).

Cardiac ANS dysfunction occurs in patients with autoimmune-mediated rheumatic disease, and is closely associated with autoimmune rheumatic disease, such as systemic lupus erythematosus, RA, primary Sjögren's syndrome, scleroderma, and fibromyalgia, even in the absence of any cardiological and neurological manifestations (Mravec, 2007). The most commonly used tests to evaluate autoimmune-mediated rheumatic disease are the 24-hour heart rate variability, Valsalva maneuver, slow deep breathing, cold face test, heart rate response to standing, hand grip test, and mental arithmetic stress test. Other measures have been baroreflex sensitivity, and cardiovascular reflex tests to evaluate for autonomic dysfunction. Testing of 24-hour variability in heart rate have been most commonly employed, and usually reveal abnormal results; often in the absence of cardiac disease.

Still, involvement of the ANS in patients with RA has been poorly studied. In the studies that have examined a role for the ANS in RA, conflicting results have been reported, because of the way in which controls were selected, and varying criteria used to evaluate ANS dysfunction (Mravec, 2007; Toussirot et al, 1993). There is evidence of autonomic dysfunction in many RA patients, including cold, clammy, cyanotic extremities, peripheral vasospasm, tachycardia, changes of the skin, hair and nails, and, rarely, orthostatic hypotension. The majority of patients with disabling RA develop absence of sweating in many areas of body, defective cardiac responses to deep breathing, standing and Valsalva's maneuver, and altered or absent sympathetic skin responses (Stojanovich et al, 2007; Toussirot et al, 1993). Abnormalities in parasympathetic regulation of cardiovascular reflexes have also been reported in a third of RA patients (Edmonds et al, 1979. In these patients, four out of nine patients with abnormal tests also had symptoms suggesting ANS dysfunction, and more than half of the patients with abnormal tests showed signs of peripheral neuropathy. Parasympathetic cardiovascular ANS dysfunction in RA patients has also been confirmed in a later study (Toussirot E et al, 1993). Toussirot and colleagues (1993) have found ANS dysfunction in 60% of 50 RA patients, as defined by abnormal results on two of the three cardiovascular reflex tests, but with no correlation between ANS dysfunction and disease duration, inflammatory syndrome, titers of RF, or destruction of articular joints (Stojanovich et al, 2007). In contrast to these reports, Bekkelund et al. (1996) have reported no cardiovascular ANS abnormality or other ANS symptoms in a study of 43 RA patients.

In a recent study by El-Sayed et al. (2009), clinical evidence reveals cardiovascular and autonomic dysfunction in 65 and 40% of lupus and juvenile idiopathic arthritic (JIA) patients, respectively, but not in healthy controls. Lupus and JIA patients also have significantly lower serum NPY and VIP than controls, and patients with cardiovascular and autonomic dysfunction have significantly lower serum NPY and VIP concentrations than control subjects. All of five autonomic function test scores assessed in this study have significant negative correlations to NPY and VIP. Clinical evidence of cardiovascular and autonomic dysfunction can also be found in 41.7 and 14.3% of asymptomatic lupus and JIA patients, respectively. These findings support and extend other findings showing that cardiovascular and autonomic dysfunction is common in lupus and JIA patients, even in absence of relevant symptoms. Despite reported associations between variants in the gene encoding the β_2-AR and autoimmune disorders, such as RA, Pont-Kingdon et al. have failed to find an association between JIA and alleles, genotypes, or haplotypes of β_2-AR in patients with JIA or any of the major JIA subtypes. Specifically, the haplotype that has demonstrated a strong association with RA (R16/Q27) is not associated with JIA. These findings suggest that although JIA and RA share several clinical and pathological features, but JIA and RA have unique genetic associations.

The pathogenesis of the ANS dysfunction in RA patients is not clearly understood. Recently, circulating autoantibodies against nerve growth factor, cervical ganglia, and the vagus nerve has been reported in RA patients with cardiovascular and ANS dysfunction (Cutolo and Straub, 2008; Di Comite et al, 2007). The role of autoantibodies against the ANS in the pathogenesis of ANS dysfunction in RA, as well as cardiovascular and ANS

dysfunction, remains to be verified (Stojanovich et al, 2007; Sitia et al, 2008). These studies suggest that the prescription of drugs that affect ANS regulation of the cardiovascular system to RA patients should be considered carefully, and ANS regulation of cardiac function carefully monitored (Cutolo and Straub, 2008). Diagnosis of ANS dysfunction is non-invasive, and given the available literature is warranted in rheumatic patients, because increased sympathetic tone is associated with the development of ventricular tachyarrhythmia and greater incidence of sudden cardiac death. Serum autonomic neuropeptides (NPY and VIP) are also easily tested, and the therapeutic effects of NPY and VIP are recommended in these patients. Finally, further studies investigating the role of the ANS in rheumatic diseases are necessary in order to fully understand the clinical significance of autonomic dysfunction uncovered by clinical laboratory testing. It is likely that ANS dysfunction is nonspecific, extremely varied, and pertains to many organ systems, not just the cardiovascular system.

Changes in SNS Innervation of Affected Joints in RA

In RA or animal models for RA there may be an increase in sympathetic tone, suggesting that dysregulation of the SNS is part of the disease sequelae (Harle et al, 2006). Given the role of the SNS in the maintenance of homeostasis of most organ systems, and its role in regulating immune responses, dysfunction in the SNS is likely to contribute to the altered bone metabolism that drives the disease (Lubahn et al, 2004; Levine et al, 1986).

In AA, an animal model for RA, the density of nerves in the joint synovium and bone is altered as the disease progresses, such that sensory and sympathetic nerves increase and decrease in density, respectively (Levine et al, 1986). The consequences of

altered nerve distribution in these tissues are not entirely clear, nor is it known whether this condition persists after the inflammatory response is reported to wane.

AR Expression and Function in RA

Gene Variants

β2-ARs form a link between the immune system and the SNS and are involved in RA. The gene for β2-ARs is located at chromosome 5 q31-32 and contains three single nucleotide polymorphisms at amino acid positions 16, 27 and 164. Variations that occur on lymphocytes will alter the regulation of the immune responses for both autoantibody production and cytokine profile. Alterations of this receptor are associated with asthma, hypertension and obesity (Xu et al, 2005). Malysheva et al, demonstrated that arginine was present at codon 16 in patients with RA 89.7% of the time compared to controls at 66.2% of the time. They also found homozygosity for Arg 16 present in 107 patients with RA compared to 14 controls. Furthermore, 93.3% of patients with homozygosity for Arg 16 were positive for anti-cyclic citrullinated peptide antibodies compared to 75% of patients with homozygosity for glycine16 (Malysheva et al, 2008). Xu et al, found that down regulation promoted by agonists was enhanced in receptors homozygous for glycine 16 as compared with those homozygous for arginine 16. Receptors homozygous for glutamic acid 27 were resistant to such down regulation when compared with those homozygous for glutamine 27. The receptors homozygous for isoleucine 164 had markedly decreased ligand binding and coupling properties compared with those homozygous for threonine 164 (Xu et al, 2005). In patients with RA of recent onset, a diminished ANS response could be demonstrated, most clearly in patients with severe pain. It is possible that in these genetically predisposed individuals an imbalance

between the interaction and homeostasis of the SNS and immune system develops over a long preclinical phase and eventually leads to the outbreak of the disease (Wahle et al, 2002).

ARs and Bone Cell Signaling

An increasing body of evidence suggests that nerve-derived signals play an important role in the regulation of bone metabolism. The first observations suggesting this theory were based on patients who had suffered traumatic brain injuries, who showed an increase in osteogenic activity, and reflex sympathetic dystrophy patients who displayed localized sympathetic hyperactivity and osteopenia. Stroke patients and spinal cord patients also demonstrated osteopenia, bone fragility and poor fracture healing. Decades later, these initial reports, and a number of in vitro and in vivo studies using experimental models confirm the notion that bone homeostasis is under the influence of central and peripheral neuronal control (Elefteriou, 2005).

TH-containing fibers found close to blood vessels and localized in the periosteum suggest that this enables them to get close to osteoclasts and osteoblasts which both contain β_2-AR's (Aitken, 2009; Elefteriou, 2005; Michitugu et al, 2003). These receptors belong to a large family of membrane proteins that transduce signals through G-proteins. Activated β-ARs stimulate adenylyl cyclase, which increases cAMP intracellular levels. This causes protein kinase A (PKA), to phosphorylate various protein targets including transcription factors, kinases and cell surface receptors, including β-ARs (Elefteriou, 2005). In actuality, however, the existence of close contact between bone cells and nerve endings is sparse.

This discrepancy suggests that signal transduction by neuropeptides could be non-synaptic and/or that neurotransmitter primary signals are transduced to groups of osteoblasts via intercellular junctions (Elefteriou, 2005). The propagation of neuronal signals is plausible given the well known theory of osteoblast/osteocyte communication via exchange of molecules and signals through gap junctions. This also brings up questions as to how nerve distribution in bone communicates with osteoclasts, since they are very mobile and isolated cells that attach to trabeculae (as opposed to units of functional osteoblasts). It is likely that the neves would use a diffusion mechanism to transmit signals to osteoclasts rather than direct synaptic contact (Elefteriou, 2005).

***Direct and Indirect Effects of ARs on Ostoblasts and
Bone Metabolism***

β-ARs are largely known for their role in cardiovascular regulation, uterine and airway smooth muscle functions; however, this receptor is essential in bone metabolism. The direct involvement of the SNS in the regulation of bone mass has been demonstrated by an increase in osteoblast number and activity and subsequent increase in bone mass in mice characterized by low sympathetic tone (Elefteriou, 2005). These mice were treated with the β-blocker propanolol or deficient in dopamine β-hydroxylase, the step limiting enzyme responsible for catecholamine synthesis. Mice treated with the β agonist isoproterenol, as a surrogate for SNS hyperactivity, demonstrated a marked decrease in osteoblast number, activity and bone mass. Therefore, $β_2$-AR activation decreases bone formation by osteoblasts. It is the main mediator of sympathetic signaling in osteoblasts, and interfering with them increases bone formation and bone mass (Elefteriou, 2005). The downstream target genes in these receptors in osteoblasts are not completely

characterized (Elefteriou, 2005). Osteoblast growth and differentiation does not seem to be affected by stimulating these receptors (Aitken et al, 2009)

RANKL is a well characterized gene whose expression has been shown to be regulated by β_2-AR signaling in osteoblasts (Elefteriou, 2005). RANKL is a critical factor inducing osteoclast differentiation. It is secreted by osteoblasts and its action on osteoclasts is antagonized by a soluable receptor called osteoprotegerine (OPG). Adrenergic signaling stimulates osteoclast differentiation indirectly by increasing RANKL expression in osteoblasts via β_2-ARs (Elefteriou, 2005). Both PTH and β_2 agonists can upregulate RANKL expression in osteoblasts and subsequently bone resorption by osteoclasts.

Aitken et al, suggests there are other plausable indirect methods for bone formation since they were unable to detect any direct effect of adrenoreceptor ligands on osteoblast differentiation and function, which suggests that effects on bone formation may be indirect and mediated by a neurogenic mechanism or other pathway that remains unidentified (Aitken, 2009).

No matter what direction the intracellular signaling takes, the pathway is stimulated by activating the β_2-AR on the osteoblast. These studies indicate that increased sympathetic signaling influences both arms of remodeling, decreasing bone formation and increasing resorption, by acting on one cell type, the osteoblast (Elefteriou, 2005).

Direct and Indirect Effects of ARs on Osteoclasts and Bone Metabolism

β-AR agonists have been shown to directly stimulate bone resorption and

therefore reduce bone mass, demonstrating the importance of the SNS in bone metabolism; however, the cellular mechanisms responsible are not completely understood. Aitken el al. found that while β_2-AR are expressed by mature osteoblasts and osteoclasts, the highest numbers were found on bone marrow cells and M-CSF dependent bone marrow macrophages (Aitken et al, 2009). They also found that expression of mRNA for dopamine beta hydroxylase was virtually undetectable in bone cells, suggesting that catecholamines are unlikely to be produced endogenously by osteoblasts or osteoclasts and instead derived from the circulation or innervating neurons. The mRNA for monoamine oxidase-α was highly expressed in all bone cells and monoamine oxidase β mRNA was detectable in osteoblasts, indicating bone cells can metabolize catecholamines (Aitken et al, 2009).

Treatment with β_2-AR agonists can result in the formation of large multinucleated osteoclasts. This suggests that β_2-AR agonists might affect fusion of osteoclast precursors, but more work is still needed to confirm this theory (Aitken et al, 2009). Frediani et al. found that catecholamines act as inducers of osteoclast maturation in vitro and as stimulators of osteoclast activity through the binding of β_2-ARs (Frediani et al, 1996). They found catecholamines increase TRAP activity, IL-6 production, multi-nuclearity and response to calcitonin in undifferentiated osteoclast precursors. Osteoclast resorbing activity was also increased with the beta adrenergic agonist isoprenaline as evident by actin rings, which suggests high bone resorbing activity, that was clearly observed in an osteoclast like multinucleated cell line (Arai et al, 2003). These findings demonstrate that catecholamines and beta adrenergic agonists regulate osteoclasts function directly via β_2-ARs.

55

An indirect way to inhibit bone formation can occur by stimulating the

hypothalamus sympathetic neurons with leptin. This can be nullified with the use of beta

blockers which also inhibit receptors of the hypothalamic adrenergic neurons (Wlodarski

and Wlodarsi, 2009).

Direct and Indirect Effects of IL-1, TNF-α and RANKL on Osteoclasts and Bone Metabolism

IL-1 and TNF-α stimulate synovial fibroblasts and chondrocytes to produce

proteinases that degrade cartilage. Blocking these cytokines can significantly reduce

bone erosions, cartilage degradation, synovitis, and reduce joint space narrowing (Strand

and Kavanaugh, 2004). Polzer et al., demonstrated that by using human TNF-α mice

crossed with mice lacking IL-1, that IL-1 is essential for TNF-mediated bone loss. By

using CT scanning, histomorphometry, and serum markers, they concluded that systemic

bone loss is fully protected by the absence of IL-1. This suggests that IL-1 is essential for

inflammatory osteopenia (Polzer et al, 2010). With the understanding thought that

lymphocyte-monocyte interactions increase bone resorption by using TNF-α and IL-1 to

increase RANKL expression by osteoblasts, Gradaigh et al., found that TNF-α is a potent

enhancer of RANKL which mediated osteoclast activity. Interactions between TNF-α

and IL-1 also resulted in osteoclastic activity, but independent of RANKL (Gradaigh et

al, 2004). T cells can also release RANKL which can induce osteoclastogenesis and is

enhanced by TNF-α, IL-1, and IL-17. This mechanism can be inhibited by OPG

(Saidenberg-Kermachac'h et al, 2004).

RANK is a membrane bound TNF receptor which is expressed on lymphocytes

and osteoblast precursors and binds to RANKL via a direct cell to cell interaction

(Bezerra 2005; Mundy, 2007). This process is essential for precursor osteoclast cells to differentiate into mature osteoclasts. These precursors have been demonstrated to consist of macrophages or synoviocytes if M-CSF, TNF-α, or IL-1 is also present (Adamopoulos et al, 2006; Saidenberg-Kermachac'h et al, 2004). RANKL also prolongs the survival of osteoclasts and promotes resorbing activity. OPG or other selective inhibitors are capable of blocking RANKL's interaction with RANK, therefore inhibiting bone destruction (Jimi, 2004; Mundy, 2007). The interplay between RANKL and OPG is considered to be the major regulation of osteoclasts. Hirayama et al, by using isolated monocytes from RA patients and normal controls in culture with M-CSF and RANKL, found that it may not be this increase in osteoclast number which is responsible for bone remodeling, but rather an increase in osteoclast functional activity (Hirayama et al, 2002).

**Direct and Indirect Effects of IL-1 and TNF-α on Osteoblasts and
Bone Metabolism**

An indirect effect of these cytokines on bone resorption is proposed by Tsutsumimoto et al, who demonstrated that by examining the effects of TNF-α and IL-1 on cell adhesion molecules in osteoblastic MC3T3-E1 cells, that these cytokines compromise the cell-cell adhesion of osteoblasts which cover the bone surface. This may in turn facilitate the direct adhesion of osteoclasts on the calcified bone matrix surface. These results implicate an indirect role for osteoblasts in the promotion of bone resorbtion by TNF-α and IL-1 (Tsutsumimoto et al, 1999).

Polyphosphoinositide-dependent signaling plays a central role in the regulation of many cellular processes including cell shape, adhesion, apoptosis, and proliferation. The disruption of this pathway can occur in inflammatory states, such as in RA. Zini showed

57

that nuclear phospholipase C β_1 and phosphatidylinositol 4,5-bisphosphate, two key elements of the polyphosphoinositide signal transduction system, increase in primary osteoblast cultures of RA patients when compared to post-traumatic after fall patients (Zini et al, 2003). They also demonstrated that these alterations can be induced in the fall patients' osteoblasts by IL-1 and TNF-α. This suggests that proinflammatory cytokines from mononuclear cells can modulate the nuclear polyphosphoinositide signaling pathway of osteoblasts involved in bone remodeling. The proinflammatory factors released in the bone marrow of RA patients constantly act on osteoblasts modulating gene expression and upregulates chemokine expression resulting in an inflammatory response (Zini et al, 2003).

Osteoblasts from RA patients express IL-1 and TNF-α in basal conditions, but do not release detectable amounts. It has been reported that these cytokines alone or in combination strongly stimulate chemokine release by osteoblasts (Lisignoli et al, 1999; Zini et al, 2003). These chemokines could directly or indirectly effect bone remodeling mechanisms and cartilage destruction. This suggests that osteoblasts are capable of autocrine/paracrine regulation that affects bone remodeling in RA (Lisignoli et al, 2003; Zini et al 2003).

Effects of Adrenergic Drug Treatment on RA

The SNS could play a role in AA and RA by extension, by directly or indirectly altering bone metabolism. The SNS's role in bone metabolism is supported by osteoblasts' and osteoclasts' expression of adrenergic receptors, and reports that stressors that increase circulating levels of catecholamines alter bone turnover (Skerry and Gowen, 1995; Lorton et al, 2008).

58

Drugs that block adrenergic receptors, destroy sympathetic nerves, or alter sympathetic outflow in RA patients or animal models for RA alter bone destruction, supporting an important contribution of the SNS in altered bone metabolism that contributes to joint injury (Cherruau et al, 2003; Lorton et al, 2003; Lubahn et al, 2004). Treatments which alter SNS outflow or block adrenergic receptors in arthritic animals or RA patients can alter disease severity. These findings suggest an important contribution of the SNS to joint injury in RA. We have explored the effects of the specific β_2-adrenergic receptor agonist, terbutaline, the α-adrenergic agonist, phentolamine, and an investigational drug, which is a combination of these, named SH1293, at different time points on disease outcome using the AA model of RA in Lewis rats. These treatments significantly decrease inflammation and radiographic scores if treatment was started at disease onset and continued through severe disease. The effects of these drugs are not mediated through the HPA axis, as plasma cortisol levels are not altered with the adrenergic drug treatments.

The inability to effectively process and eliminate the antigen, resulting in RA occurs via the continuous availability of high local and circulating proinflammatory cytokines. It has also been reported that sympathetic dysregulation occurs in RA and in animal models for RA. Dysregulation of the neural signaling to the immune system, in turn, helps perpetuate the disease (Harle et al, 2006).

Purpose of Study

Only a few studies in the 1960's describe the pathology of AA in rats. One of the best representations was by Pearson and Wood (1963) who described, in detail, the histologic characteristics of the disease. They also noted that no experimental disease is

sufficient as an ideal model for RA and that this may be because of differences in species. They were also aware of the variable responsiveness of the rats to the adjuvant injection, which they think is due to "technical factors" and "variations in the components of the adjuvant". With this in mind, they still commented on the significant number of overlapping clinical and histological similarities that exist between the diseases. Their observations are based on the description of almost 100 animals between the time points of 24 hours within the clinical onset through the 350th post-inoculation day. These observations include onset of the disease in the hind paws which appears suddenly at about the 14th day post-inoculation. In the Long-Evans strain that they used, there was a penchant for involvement of the tarsal joints, the heel and the metatarsal phalangeal joints. One or several digits may have gotten swollen, while other areas remain normal. In the Wistar strain the greatest tendency was towards fusiform swelling of the proximal interphalangeal and metatarsal phalangeal joints. There were variations in the severity from one animal to another; very few showed mild transience of the disease, most had moderate damage, and a few had lasting severe arthritis. In general, an average of 90% of the animals inoculated developed arthritis to some degree. The main difference among animals was in location. The animals that had an initially severe onset also showed a tendency to have persistent changes with time. These changes developed slowly over a period of 6 weeks to 3 months after the initial onset and led to chronic enlargements, flexion deformities and ankylosis. Nonarticular lesions were found in other tissues in about 25% of the animals.

The disease demonstrated arthritis (synovitis) concomitantly with periarthritis, tendinitis and peritendinitis, bursitis, and periostitis. On the first day, the major changes

included an edematous, relatively hypocellular separation of the connective tissue planes.

The edema was primarily found in the para-articular subsynovial tissues and along the

periosteum, about tendon sheaths and occasionally between muscle planes. There was a

moderate increase in synovial fluid volume with a slight increase in the number of

inflammatory cells. Connective tissue cells included fibroblasts and monocytes. Small

round mononuclear undifferentiated cells may have included lymphocytes. Only a

paucity of neutrophils was found.

On the second through fourth days, synovitis and intra-articular alterations were

noticed in a number of joints, and there was proliferation of the synovial lining cells.

There were compact masses of fibrin which adhered to the hyperplastic synoviocytes. A

few neutrophils, macrophages and desquamated synoviocytes were found in the joint

space. Fibroblastic invasion of the fibrin masses appeared as the earliest evidence of

organization. Tissue cellular responses were intensified and were composed mainly of

monocytes, lymphocytes, and fibroblasts. Again only a few neutrophils were scattered

among these cells.

Between the fifth and tenth days, a para-articular granulation tissue began to

emerge, known as pannus. This invaded and destroyed the bone in the subchondral

region and occasionally along the shaft of the bone. Similar findings were observed

along the tendons, especially around the ankle. The makeup of the joint's synovial fluid

was changing to consist more of monocytes and macrophages. At this point an intense

cellular reaction occurs in the subsynovial layer, around tendon sheaths and bursae and

occasionally along periosteal surfaces. After the seventh day, fibrin deposits were not

found in the connective tissue as previously reported. This may be due to organization

and invasion of cellular infiltrate, or to lysis. In some cases, an intense periosteal new

bone was in the process of being formed. This seemed to occur closer to the joints, but in

some animals it involved the entire surface of one or many of the small bones in the

paws.

During the eleventh through the twentieth days this periosteal bone formation and

pannus development, as well as other cellular processes seemed to intensify. Within the

periarticular or peritendinous connective tissue, the predominant inflammatory cell

becomes the lymphocyte, with an occasional small collection of plasma cells.

Proliferation of connective tissue elements in the bone marrow's subchondral region

invaded and dissolved articular cartilage components. This area was not connected to the

marginal pannus of the joint.

Between the twenty-first and thirtieth days, synovial villi projected into some

joints. Pannus penetrated the subchondral zone and often invaded the cortical bone at the

margins of the articular cartilage, then spread out into the marrow spaces. It also

extended from the marginal synovial reflexion across the surface of the cartilage for a

variable distance, eroding or completely replacing portions of the cartilage. A thin layer

of hyalinized fibrin occasionally covered the articular cartilage. The active periosteal

new bone formation was diminishing and the numbers of activated osteoblasts were much

fewer. An outer marginal rim of immature cartilage was often found near the osteoid

layer. The connective tissue reaction was less aggressive, but foci of very active

appearing fibroblasts were still seen and foci of metaplastic cartilage were found in some

areas of intense fibroblastic activity. The predominant inflammatory cell was still the

lymphocyte. Dense clusters of lymphocytes in the form of lympoid nodules without germinal centers were occasionally found in the periarticular tissues.

Between the thirty-first and sixtieth days, marrow spaces and articular cartilage continued to become filled with pannus, but in a less aggressive manor. The intent of the invasion of the pannus from below the articular cartilage and above seriously compromises its viability. No boney bridges occur at this time, however, so this does result in a fibrous ankylosis. Inflammatory cells that are present are mainly the lymphocytes and plasma cells.

During the sixtieth day to the three-hundred and fiftieth day, there was decreasing evidence of all the inflammatory and connective tissue reactions. The newly formed periosteal bone assumed the general appearance of calcified cortical bone with enclosed marrow spaces. Chronic inflammatory cells persisted in some areas about tendons and in the subsynovial regions. Fibrous ankylosisng persisted and the pannus lost its aggressive characteristics and is relatively inactive. Sclerotic bone was found under areas of fibrous ankylosis or thinned or destroyed articular cartilage.

About 25% of the animals that previously demonstrated arthritis continued to demonstrate small or occasionally large cellular foci even up to the twelfth month. Also actively proliferating connective tissue cells persisted in some areas.

Pearson and Wood make note that no matter how closely pathologic lesions resemble each other, the synovial and periarticular tissues have a limited capacity to respond to a variety of insults. They also mention points of dissimilarity between AA and RA which include (1) the absence of an initial vasculitis and perivasculitis in the articular lesions of the AA model; (2) an absence of lymphoid follicles in the syniovial

villi for the most part in AA; (3) a greater tendency for the occurrence of periosteitis and new bone formation in AA and (4) the absence of characteristic nodules in AA.

In recent studies, we have observed signs and symptoms (increased pain sensitivity, redness and swelling) in AA rats up to 18 weeks after disease induction. This finding is consistent with the literature, which describes the disease as having an acute inflammatory phase and a chronic inflammatory phase. The time point at which these phases change is around 28-30 days after adjuvant challenge and the disease cannot be induced a second time by repetitive treatment with complete Freund's adjuvant (CFA) (Levine et al, 1986).

Additionally, our research on the role of the SNS in RA suggests that the SNS shifts the balance of the immune system response to adjuvant challenge toward cell-mediated immunity and alters bone destruction. While the effects of the SNS on bone destruction may be mediated indirectly through SNS induced changes in immune cell responses, they also could be mediated by direct effects of catecholamine interaction with osteoblast and osteoclast adrenergic receptors.

Neurogenic inflammation is believed to play an essential role in joint pathology that occurs in RA for several reasons. (1) Stress and altered CNS activity can modulate the course and clinical outcome of RA (Crosby, 1988; Thomason et al, 1992). (2) Autonomic dysfunction occurs in RA and treatment with adrenergic drugs effect the progression of arthritis (Lorton et al, 2003). (3) In experimental models of AA, transection of innervating peripheral nerves attenuates hyperalgesia, swelling and joint destruction (Levine et al, 1986). (4) Finally, there is symmetrical joint involvement due

to cross-spinal reflexes and predominant involvement of heavily innervated small joints of the hand and feet (Niissalo et al, 2002).

Both classes of neurons (sensory and sympathetic) have been implicated in many processes that underlie nociception and neurogenic inflammation, including peripheral vasodilation and plasma extravasation, inflammatory cell chemotaxis and activation (Partsch and Matuciecerinic, 1992), pain neurotransmission (Oku et al, 1987; Neugebauer et al, 1996; Sluka et al, 1997; Otsuka and Yoshioka, 1993), and spinal processing (Murase et al, 1989; Randic et al, 1990). Additionally, neurotransmitters released by these nerves by interacting with bone cells, and by affecting cytokine release by infiltrating inflammatory cells, affect bone metabolism. Therefore, dramatic changes in innervation of the inflamed joint results in pathologic consequences. It is not clear whether altered nerve density persists after the inflammatory response subsides.

Sensory and sympathetic nerves traveling in neurovascular bundles within bone tissue coupled with the presences of specific receptors on bone cells for neurotransmitters released by these nerves strongly suggests a functional role for these nerves in local bone metabolism. Since the literature presented above indicate that activation of AR on bone cells can affect bone metabolism, it will be important to identify changes in sympathetic nerve density and distribution in the distal tibia in AA rat ankles and examine changes in their spatial relationships with potential target cells in the inflamed joint. This information is critical for understanding how dysregulation of the nervous system during the course of AA contributes to joint destruction and deformity. The literature sited above is critical for understanding the nervous system's role in altering normal bone remodeling, the role of various hormones, neurotransmitters and cytokines, their direct or

65

indirect effect with bone cell or immune cell receptors in the pathogenisis and maintenance of RA and most importantly the potential for novel and effective drug treatment.

The purpose of this study is two-fold. The first purpose is to develop techniques in order to characterize changes seen in the joints of AA rats at various time points up to 18 weeks. This will allow observation of disease associated changes in SNS activity during active disease and to determine at what time points SNS activity is elevated. The second purpose is to use these techniques to characterize changes seen in adrenergic drug treated AA rats. This will determine if blocking the increased SNS activity that occurs after disease onset alters bone metabolism in AA and whether the effects are mediated by reduced norepinephrine interaction with adrenergic receptors peripherally. Previous studies have demonstrated by our laboratory in collaboration with Drs. Lorton and Lubahn that treatment with adrenergic agents that interact with α and β-AR after disease onset prevent joint destruction by X-ray (Lubahn et al, 2004; Lorton et al, 2003). The ultimate goal of this study is to determine whether SNS drug treatments targeting specific ARs can be used to prevent bone destruction associated with RA.

The studies performed for this dissertation use the AA rat model for RA. The use of a number of experimental rat and mouse autoimmune erosive arthritis models are widely accepted as models for studying the pathophysiology of RA that could be used for this study. Some popular rat models include the use of cartilage oligomeric matrix protein (COMP)-, avridine, pristane, mineral oil and streptococcal cell wall to induce arthritis. However, the more widely used models are the collagen-induced arthritis (CIA) model in mice and the AA model in rats. CIA introduces type II collagen into susceptible

66

strains, inducing arthritis within 10-14 days after injection. AA is produced in genetically susceptible rats by injecting 0.1 ml of CFA containing 10 mg/ml *Mycobacterium butyricum*. The disease appears in a similar time period after injection as in CIA, and is characterized by lymphocytic infiltration into the synovium, as well as cartilage and bone erosion. Even with all these experimental models that have been developed, none reflect all the articular, systemic features, immunological profile and genetic factors typical of the human disease (Di Paola 2008). In the present study, we chose to use the AA rat model, because there is preponderance of overlapping clinical and histological similarities between this model and RA. Clinically these similarities include acute and recurrent arthritis of the peripheral and spinal joints, chronic deforming arthritis, joint destruction detectible by x-ray, conjunctivitis, and progressive joint disease. Histologically the similarities include acute or subacute synovitis with fibrin deposition, periarthritis, lack of abscess formation, primary mononuclear inflammatory response, inflammatory exudation into joint fluid, lymphoid follicles in synovium or adjacent tissue, synoviocyte proliferation, synovial villus hypertrophy, invasion of subchondral bone and joint space by pannus, periostitis and osteitis, bursitis and tendinitis or peritendinitis, fibrous ankylosis, and bony ankylosis.

We predict that altering the result of the increased tone in SNS activity during disease development will have a profound effect on bone metabolism that will reflect the amount of bone destruction. We hypothesize that changes in SNS activity and/or SNS dysfunction contribute to bone destruction in RA. The effects of increased SNS activity could alter bone functions indirectly by altering production of key cytokines involved in bone cell differentiation for development of osteoblasts and osteoclasts, as well as the

functions of these cells. Alternatively, increased sympathetic activity could act directly via ARs present on osteoblasts and osteoclasts to alter their functions and differentiation. Findings from our labs and others have found evidence for dying back of sympathetic nerves in lymphoid organs and affected joints.

Micro computerized axial tomography image analysis and serial reconstruction of the ankle joint will provide a sensitive measure of bone volume changes seen in arthritic rats as compared to controls. Histological data will demonstrate marked changes in connective tissue as well as both the density and distribution of autonomic nerves in sites within the ankle joint displaying indications of disease activity. Therapies with adrenergic agents will prevent the disease associated rise in inflammatory infiltrates and osteoclast activity with consequent reduction in bone and cartilage destruction and maintenance in the bone volume and distribution of autonomic nerves in the ankle joint.

CHAPTER TWO

SYMPATHETIC MODULATION OF JOINT ALTERATIONS IN AA

Introduction

Rheumatoid arthritis (RA) is characterized by an increase in proinflammatory cytokines in the synovium of affected joints and bloodstream, which are directly involved in the disease's pathophysiology. Increased cytokine production, particularly tumor necrosis factor-alpha (TNF-α) and interleukin-1 (IL-1), plays a key role in sympathetic nervous system (SNS) activation in RA and adjuvant-induced arthritis (AA), a model for RA. The inability to effectively process and eliminate the antigen resulting in RA eventually causes dysregulation of SNS outflow, via the continuous availability of high local and circulating proinflammatory cytokines. Dysregulation of the neural signaling to the immune system, in turn helps perpetuate the disease (Elefteriou 2008; Imboden 2009).

SNS pathways activated in response to hypothalamic effects of proinflammatory cytokines during disease progression regulates synthesis and release of peripheral cytokines. This acts as a negative feedback loop to dampen production of proinflammatory cytokines and promote expression of anti-inflammatory cytokines. Hypothalamic neurons that regulate sympathetic outflow to bone cells are responsive to leptin, an adipocyte-derived hormone that inhibits bone formation by osteoblasts. Thus, leptin indirectly affects sympathetic nerve activity in bone, causing release of

norepinephrine from these nerve terminals, which binds with β_2-adrenergic receptors (ARs) on the osteoblasts and may inhibit their activity (Elefteriou, 2008).

Numerous reports of a stressful event just prior to subsequent disease flair ups typically occur in RA (reviewed in Cutolo et al., 2002; Lorton et al., 2008; Lubahn et al., 2004). These findings suggest that stress and the SNS play a role in inflammatory arthritis (Crosby 1988; Lorton et al., 2008; Thompson et al., 1997). Additionally, it provides a possible mechanism through which increased sympathetic tone in RA patients may promote and contribute to disease pathology (Lorton et al., 2008).

Increased sympathetic tone in RA indicates dysregulation of the SNS. Given the role of the SNS in maintenance of homeostasis of the body's functions and its role in regulating immune responses, dysfunction of the SNS is thought to contribute to the altered bone metabolism that drives the disease. There is strong evidence that indicates the presence of sympathetic nerves in bone and joint structures (Imai et al., 1997 b; Schwab et al., 1997; Cherruau et al., 2003) as well as the presence of α- and β-ARs on osteoblasts and osteoclasts (Takeuchi et al., 2000). This is possibly due to diffusible axon guidance molecules by osteoblasts and osteoclasts that function as a chemoattractant or chemorepellent for sympathetic, as well as, afferent nerve fibers (Togari, 2002). Drugs that block ARs, destroy sympathetic nerves, or alter SNS outflow in RA patients or animal models for RA, alter bone destruction (Lubahn et al., 2004; Cherruau et al., 2003; Harle et al., 2006). Collectively, these findings support an important contribution of the SNS in altered bone metabolism that leads to joint injury.

In vitro studies have demonstrated that catecholamines can induce osteoclast maturation and stimulate osteoclast activity via a β_2-AR-mediated mechanism (Frediani

et al.,1996). The resorbing activity by osteoclasts as indicated by the presence of f-actin rings and resorption pits was substantially increased by isoprenaline (β-AR agonist), moderately increased by epinephrine (an α- and β-AR agonist), and only slightly increased by phenylephrine (an α_1-AR agonist) (Arai et al., 2003), suggesting that this effect is primarily mediated via β-AR. It has also been shown that sympathectomy by treatment with guanethidine increases osteoblastic activity and reduces osteoclast number and activity in rats (Cherruau et al., 2003).

Finally, neurogenic inflammation, which is mediated via both autonomic and sensory nerves, plays an essential role in the joint pathology associated with RA. Neurotransmitters released by these nerves regulate vascular changes, chemotaxis and activation of immune cells that mediate the inflammatory response and nociception. In RA, the density of nerves in the joint synovium and bone are altered with disease progression; there is an increase in sensory nerves and decrease in sympathetic nerves (Weidler et al., 2005). The consequences of altered nerve distribution in these tissues are not entirely clear, nor is it known whether this condition persists after the inflammatory response is reported to wane.

We have explored the effects of the specific β_2-AR agonist, terbutaline, the nonselective α-AR antagonist, phentolamine, and an investigational drug which acts on both α- and β-ARs, SH1293, on disease outcome across time using the AA model in Lewis rats (Lubahn et al., 2004). The rats were given two intraperitoneal injections per day of phentolamine or terbutaline (1200µg per day), initiated at adjuvant challenge or disease onset, and continued through severe disease. The data revealed that treatment with phentolamine or terbutaline, started at adjuvant challenge worsened the disease.

However, SH1293 did not exacerbate the disease when given at adjuvant challenge. Treatment with phentolamine, terbutaline or SH1293 initiated at disease onset attenuated joint inflammation and dramatically reduced bone destruction. This supports the fact that the SNS plays different roles in pathology preclinically and after onset. All of the treatments significantly decreased inflammation in the paws and radiographic scores from the hind limbs of animals with AA if treatment was started at disease onset and continued through severe disease, but the effects were most marked with SH1293. These data support the hypothesis that the SNS plays different roles in pathology of AA preclinically and after onset.

Stimulation of α_2-ARs promotes the release of IL-1 and TNFα from immune cells which in turn perpetuates chronic inflammation and increases osteoclast differentiation and activation (reviewed in Lorton et al., 2003; Klippel 2001). Stimulation of β_2-ARs decreases the release of these pro-inflammatory cytokines and decreases inflammation (Lorton et al., 2003). Terbutaline treatments mimic the effects of an increase in sympathetic tone via increase NE availability and subsequent interaction with β_2-ARs. Stimulation of β_2-ARs activates cAMP second messenger pathways which is largely inhibitory to cell-mediated immune effector functions. Phentolamine modulates proinflammatory cytokine production by two different routes: 1) by directly blocking NE interaction with α_2-ARs expressed on macrophages and other immune cells which would decrease pro-inflammatory cytokines and 2) indirectly by blocking NE interaction with presynaptic α_2-ARs expressed on sympathetic nerve terminals, which would reduce sympathetic outflow. Treatment with terbutaline would counteract, at least to some extent, lowered sympathetic tone induced by the presynaptic α_2-AR blockade.

Despite the SNS's role in regulating key cytokines involved in driving inflammation and reports of SNS dysfunction in RA patients, no studies have adequately determined if the combination of proposed drugs protects rat ankle structures. A time course of the disease that correlated joint destruction with SNS activity has already been established by our lab. Of particular interest to our lab is the distal tibia where most of the cellular activity occurs. The purpose of this study was to characterize changes in the joints of AA rats at various time points up to 28 days post-immunization, to examine disease-associated changes in the SNS, and to investigate the effects of adrenergic drug treatments aimed at lowering sympathetic signaling via α-AR and increasing signaling via β_2-AR in AA rats. The overall hypothesis is that correcting the disease-related shift in SNS signaling away from β- and/or toward α-AR mechanism will alter bone metabolism in AA.

NE released from sympathetic nerve terminals will bind to α and β ARs on macrophages and lymphocytes. When the α-AR is stimulated, it will release the cytokines IL-1 and TNF-α. When the β-ARs are stimulated, it inhibits the release of IL-1 and TNF-α. These cytokines can affect bone cells. By using SH1293, phentolamine blocks the release of cytokines from macrophages and lymphocytes while terbutaline perpetuates inhibition of the cytokines. Phentolamine also binds to the α-AR on the terminal bouton which decreases the release of NE.

I hypothesize that disease-related changes in SNS signaling contribute to bone destruction in RA. I predict that changes in SNS signaling via α- and β-ARs during disease development will have a profound effect on bone metabolism that will be reflected in the amount of bone destruction. The effects of increased SNS activity with

73

disease development and altered signal transduction mediated by sympathetic neurotransmission could alter bone function indirectly by altering the production of key cytokines involved in bone stem cell differentiation into osteoblasts and osteoclasts, as well as functions of these mature bone cell populations. Additionally, increased sympathetic activity could act directly via ARs present on osteoblasts and osteoclasts to alter their functions and differentiation. The ultimate goal of this study is to determine whether a SNS drug treatment targeting specific ARs can be used to prevent bone destruction associated with RA.

Data obtained from morphometric techniques will be used to determine how changes in nerve density and distribution correlate with measures of disease pathology. Performing these types of analyses in animals treated with adrenergic drugs that facilitate and inhibit β_2-AR and α-AR activation, respectively will indicate more directly the effects of sympathetic nerves in disease pathology. This is because terbutaline may perpetuate β-AR mediated inhibition of the release of IL-1 and TNF-α while at the same time phentolamine may inhibit the release of IL-1 and TNF-α from lymphocytes. This potential alteration in cytokine release from lymphocytes can inhibit osteoclast activity, and therefore bone resorption. A finding that our drug treatments reversed or prevented the changes in bone pathology and nerve density and distribution, would support our hypothesis that the SNS acts directly on bone and/or immune cells to produce their bone sparing effects in the affected joints.

Material and Methods

Reagents and Adjuvant

SH1293, a patented investigational adrenergic compound that interacts with α- and β_2-AR was dissolved in 0.01mM ascorbic acid in 0.9% sterile, endotoxin-free saline. SH1293 (600 μg) was administered by intraperitoneal (i.p.) injections twice a day (morning and evening) in a total volume of 250 μl per injection, based on a previous report by our laboratory demonstrating predictable ameliorating pharmacological effects of this drug on AA in young male Lewis rats (Lubahn et al., 2004). The CFA (0.03 g dried and heat killed *Mycobacterium butyricum* (*M. butyricum*) Difco, Detroit, MI) was emulsified in 10 ml sterile mineral oil by grinding the *M. butyricum* with a mortar and pestle until the bacterial cell walls turn from light beige to an eggshell white powder. The mineral oil was then slowly worked into the bacterial cell wall powder using the mortar and pestle. The suspension was treated with a sonic dismembraner for 5 min to ensure that the bacterial cell wall powder remained suspended in the mineral oil for animal injections. All animals received the same batch of CFA. Treatment of animals with CFA prepared with this protocol produces arthritis in 100% of the animals, although there is variability in the severity of the disease that develops between different preparations of CFA.

Animals

Young adult male Lewis rats (200-250 gm) were obtained from Charles River Laboratories (Wilmington, MA). Rats were housed in plastic cages with soft CareFresh bedding (Absorption, Bellingham, WA) in the vivarium at Sun Health Arthritis Research Institute, where they were given food (Purina Lab Diet 5001) and water *ad libitum,* and

placed on a 12-h-on and 12-h-off lighting schedule. Rats were housed in the vivarium for 1 week before undergoing any manipulations. For AA rats, food was placed inside the cage, and water was supplied by using long-stemmed sipper tubes. This allowed easy access to food and water. All rats were observed to eat and drink throughout the course of the experiment. Animals were weighed and observed daily to monitor weight gain and ensure good general health of the animals. AA was induced by an intradermal injection of 100 μl CFA (0.3 mg/rat) into the base of the tail. Rats typically develop arthritis between 11 and 14 days post-challenge with CFA. To control for the effects of vehicle and stress associated with handling, to establish baseline data, and to determine disease-related effects on test parameters, control groups received the same volume of (1) mineral oil alone, (2) *M. butyricum* suspended in sterile saline, (3) sterile saline or (4) no treatment. On day 12 post-challenge, immunized or control rats were randomly assigned into appropriate drug treatment groups, and treated twice daily with SH1293 or vehicle until sacrifice at 14, 21 or 28 days after immunization, as described above.

Preparation of Tissues

At sacrifice, rats were deeply anesthetized with 1.0 ml of an 8% solution of chloral hydrate in sterile saline (overdose), and then perfused transcardially with phosphate-buffered saline (PBS) containing 0.5% sodium nitrite (pH 7.2) followed by 250 ml of 4% paraformaldehyde in the same buffer (pH 7.2). The left ankles of each rat, were imaged with soft tissue intact using micro-computed tomography (MicroCAT II, Siemans Medical Solutions USA, Inc., PA). The right ankles from each rat were stripped of their skin immersed in the same fixative overnight at 4 °C, then washed with PBS and decalcified in 10% ethylenediaminetetraacetic acid (EDTA) (pH 7.2) for 5 weeks at 4 °C.

After decalcification the ankles were rinsed in deionized water for 3 min. and cut

midsagitally from the calcaneus to the interspace between the 2nd and the 3rd phalanx and

embedded in paraffin with the cut side down. Next, the ankles were sectioned at 5 μm for

standard bone histology or 16 μm for immunocytochemistry (ICC) to localize tyrosine

hydroxylase (TH), the rate-limiting enzyme for the synthesis of norepinephrine. For all

regular histology sections, the tissue was mounted onto Fisher Superfrost Plus slides

(Statlab, Louisville, Texas). For all immunocytochemistry, tissue sections were mounted

onto subbed slides (Vectabond reagent, Vector Laboratories Inc, Burlingame, Ca).

Tissue sections cut at 5 μm were stained with (1) hematoxylin & eosin (H&E) for general

observations and to examine lymphocytic cellular infiltration; (2) tartrate-resistant acid

phosphatase (TRAP) to visualize cells of the osteoclast lineage and assess bone area; (3)

toluidine blue to characterize cartilage changes and (4) trichrome staining to assess

pannus formation. After staining, tissue sections were dehydrated through series of

graded ethanol solutions, cleared with xylene, and cover slipped with Cytoseal 28

(Stephens Scientific, div. of Richard Allan Scientific, Kalamazoo, MI) for ICC slides or

Acrymount solution (Statlab, Louisville, Texas) for standard histological evaluation.

TRAP Staining

TRAP staining was performed on tissue sections using a post-coupling procedure.

Briefly, tissue sections were incubated at 37 °C for 1 h in sodium acetate buffer (pH 5.0)

containing the substrate, naphthol AS-BI phosphate as the substrate; sodium salt (0.05%;

Sigma Chemical Co, St. Louis, MO), and 0.05 M sodium tartrate (source). Then, the

slides were placed in a pararosaniline dye solution in the presence of 0.05 M sodium

tartrate for 10 min. Slides then were rinsed with deionized water, and counterstained

with methyl green. Finally, the slides were dehydrated through series of graded ethanol solutions, cleared with xylene and mounted with Acrymount solution.

ICC for TH

Tissue sections, cut at 16 μm, were stained with ICC for TH and used to visualize TH-positive (TH+) sympathetic nerves using a polyclonal rabbit anti-TH antibody (Chemicon International) was used.   Nickel sulfate intensification of the 3,3'diaminobenzidine (0.04%; DAB) chromagen reaction product (Hancock, 1986) was used to form a blue/black reaction product in TH+ nerves. All steps were carried out in 0.15 M phosphate buffer (pH 7.4) at 25 °C using gentle agitation, unless otherwise indicated. Sections were rinsed thoroughly in buffer and incubated for 30 min in 10% normal goat serum (NGS). The anti-TH primary antibody was diluted 1:500 in 0.15 M phosphate buffer containing 0.4% Triton X-100 and 0.25% bovine serum albumin. Incubation in the primary antibody was carried out at 4 °C for 24 h. Negative control sections were incubated in 0.15 M phosphate buffer in the absence of the primary antibody.

On day 2, sections were rinsed 6 x 10 min in PBS, incubated for 30 min in 10% NGS, and then incubated in the secondary goat anti-rabbit antibody (Vector Elite kit) diluted in PBS (1:2,000) for 90 min. sections then were rinsed 4 x 10 min in buffer and incubated in 2.5% methanol with 8% hydrogen peroxide for 30 min to remove endogenous peroxidase activity. Following 6 x 10 min rinses, sections were incubated in an avidin-biotin-peroxidase complex (ABC) (Vector Elite kit; 1:4,000 dilution in PBS) for 90 min. Sections were rinsed 4 x 10 min in PBS buffer, followed by 2 x 10 min in 0.05 M acetate-imidazole buffer, pH 7.2, and then developed in acetate-imidazole buffer

containing 0.25 g/100 ml nickel (II) sulfate, 0.04 g/100 ml DAB, and 0.005% hydrogen

peroxide for 15 to 20 min. All sections then were rinsed 2 x 10 min in acetate-imidazole

buffer, followed by 4 x 10 min rinses in phosphate buffer. Then the slides were

coverslipped as described above.

3-D Image Analysis using μCT

With 3-D imaging methods available in the μCT equipment, the left ankles from

each animal were used to determine tibial bone volume within a region of interest (ROI)

using an Amira software program (Visage Imaging, Inc., Carlsbad, CA). The imaging

equipment consisted of an 80keV X-ray source. The μCT's camera used a 2048^2 matrix,

4x4 binning with an exposure time of 200 ms. The x-ray parameters were 75 kVp at 100

μA with a 0.5 mm Al filter. The CT scan included 360 rotation steps for a total scan time

of 10 min and 45 sec. The reconstructed image was 512^3 for a voxel size of 0.126^3 μm.

The distal tibias were evaluated for thickness by quantifying the number of slices

from medial to lateral. From this measurement, the middle of the tibia was determined.

By using the Point Probe function in the Amira program, it was possible to discern a

difference between bone and soft tissue. This was accomplished by selecting a spherical

ROI with a radius of 1 mm just proximal to the apex of the distal articular cartilage in the

middle slice.

Morphometric Analysis of Histologically-Stained Tissue

TH-stained sections through the talocrural joint were visualized using an Olympus

BH-2 photomicroscope. RGB color images were captured and digitized at X200 using a

high image resolution Olympus CCD video capture system at a resolution of 300 pixels

per inch and were used for automated measurement of the mean area of TH+ nerves in the joint capsule and synovial lining. Three (nonarthritic rats) or five to seven (arthritic rats), non-overlapping fields (200 μm x 100 μm or 20 mm^2 per field) within the joint capsule were captured from each rat per treatment group for quantitation using Image-Pro Plus$^®$ imaging software (version 5.0; Media Cybernetics, Inc., Silver Spring, MD, USA). A greater number of fields were captured for analyses in arthritic rats, because the volume of the joint capsule is greater in arthritic compared with nonarthritic rats. Sampling was carried out blinded to the treatment group, and biased towards qualitatively selecting fields with the greatest density of nerve fibers. TH+ nerve fibers were selected by the Image-Pro Plus software based upon their RGB color value and intensity. The staining intensities in all images were filtered by applying a threshold value to remove low intensity pixels that represent nonspecific/background values. The threshold value was determined with mean and standard deviation pixel intensity values obtained from a histogram analysis of all images sampled. This threshold process was applied in a consistent manner to all images to remove nonspecific background staining. Non-neural TH+ staining was excluded based on profile size and/or their non-linear profile. Data were expressed as percent area of TH+ nerves per field, then all fields per rat were averaged, and finally, the mean percent area of TH+ nerves ± SEM for each treatment group was calculated (i.e., a mean of a mean).

In H&E-stained tissue, the overall infiltration of lymphocytes throughout the whole ankle section was examined. The site for sampling of the inflammatory cell infiltration in the distal tibia is demonstrated in Figure 1B, (shown by the open black box). Cellular infiltration was evaluated using a grading scale of + (1 plus), ++ (2 plus), or +++ (3 plus),

representing low cellular infiltration (<300 lymphocytes), moderate cellular infiltration (~300 to 600 lymphocytes), or high cellular infiltration (>900 lymphocytes).

Images from trichrome sections were captured by digital photography with an Olympus BH-2 microscope and analyzed with the Image-Pro Plus® software. Trichrome-stained images were used to determine the percentage of pannus in the section compared with the total tissue. The whole section was used because of the pervasive nature of the pannus. An example of one region in the anterior tibial joint capsule is demonstrated in Figure 1A (open blue box). For the toluidine blue-stained tissue sections, the articular cartilage of the whole distal tibia and trochlea of the talus were traced and quantified using the semiautomated Osteomeasure image analysis system and its digitizing pad to obtain the total area (OsteoMetrics, Inc., Atlanta, GA). An example of the sample site is demonstrated in Figure 1B, (open light blue box).

The TRAP-stained sections were observed for bone area and analyzed with the semiautomated OsteoMeasure image analysis system and digitizing pad. Three sample sites (zones 1 through 3), each consisting of a 350 x 350 μm^2 area were examined from the distal tibia of each rat. Zone 1 (Figure 1A, in open red box closest to the joint), encompassed tibial articular cartilage/cartilage remnants and the subchondral bone located proximally. Zone 2 (middle red box) encompassed any subchondral bone and trabecular bone. Zone 3 (in open red box most distal to the joint), encompassed the trabecular bone located most superiorly in the sampling site. The bone that was present in each zone was outlined using the digitized pad and the area was then computed using the program. TRAP-positive osteoclasts were also counted in these zones.

For all morphometric analysis the examiner was blinded to the treatment groups. Where appropriate, histological data was expressed as a mean $\pm$ SEM and treatment groups were compared using one-way analysis of variance (ANOVA) with subsequent post-hoc comparison performed using the Tukey method for significant differences ($p<0.05$) as determined my ANOVA. All p values are reported from the post-hoc comparison. Through statistical analyses, we found that there was no difference between any of these control groups. For the purposes of this study, all of the control groups have been collapsed into one group designated as the control group. On day 14, the control group consisted of 15 rats, and an AA group consisting of 5 rats. On day 21, the control group consisted of 8 rats, an AA group that consisted of 10 rats and a SH1293 group consisting of 12 rats. On day 28, the control group consisted of 8 rats, the AA group consisted of 6 rats and the SH1293 group consisted of 8 rats.
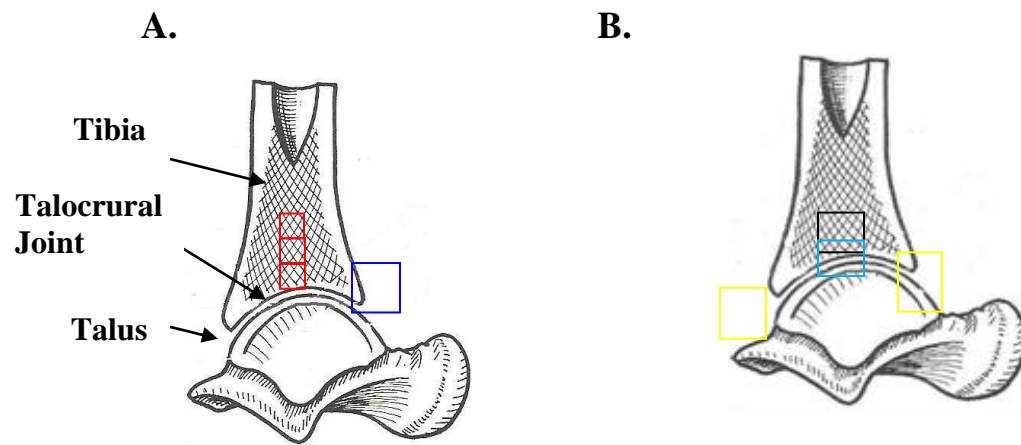
Figure 1. Schematic Illustration of Sampling Sites. Schematic diagram of the talocrural joint between the tibia and talus illustrating the regions of interest (ROI) for evaluating the pannus and cellular infiltration (open blue box) (A), bone resorption and osteoclast number (open red boxes) (A), cartilage (open light blue box) (B), inflammatory infiltration (open black box) (B) and TH+ staining (open yellow boxes) (B).

Results

Assessment of Arthritis

There was marked increase in swelling and redness of some animals (Fig. 2A). The X-rays demonstrated that at 14 days there was very little difference between the animals (Fig. 2B.). By 21 and 28 days, the AA animals demonstrated remodeling of the bones in the ankle (Fig. 2C and E); however, there is variability in its severity (Fig. 2D). Qualitative evaluation of the ankle joint revealed that administration of SH1293 reduced the severity of destruction of the bones in the ankle (Fig. 2E and G), but this drug-induced affect was variable depending on the animal and on the bones in the ankle (Fig. 2F and H).

Sympathetic Nerves

At 14 days no significant difference existed between the controls and the AA rats (Fig. 3A, B and C). On day 21 the sympathetic nerve density in the AA rats averaged 0.02% ($\pm$0.005%, $p<0.05$) of the total pixels sampled for the nerve stain (Fig. A). The SH1293 rats averaged 0.045% ($\pm$ 0.01, $p<0.05$), while the controls averaged 0.1975% ($\pm$0.05) (Fig. 3A and D). By 28 days the nerve density in the AA rats was 0.026% ($\pm$0.012, $p<0.05$), the SH1293 rats averaged 0.013% ($+0.003$, $p<0.05$) and the controls averaged 0.2125% ($\pm$0.04) (Fig. 3A and E). At both 21 and 28 days both the AA rats and SH1293 rats showed a significant decrease in sympathetic nerve density compared to the controls (Fig. 3A). There is no correlation between the TH+ stained nerves and any other variable that was measured.

Figure 2. Observations and X-rays Figure. 2A. Gross observations of inflammation and swelling in AA rats.

Figure 2B. 14 Day X-ray films AA, SMB, Saline, MO.

Figure 2C. Day 21 X-ray films AA, SMB, Saline, MO.

Figure 2D. 21 Day arthritis variability in the same animal.

Figure 2E. 21 Day X-ray films AA, SH1293, MO.
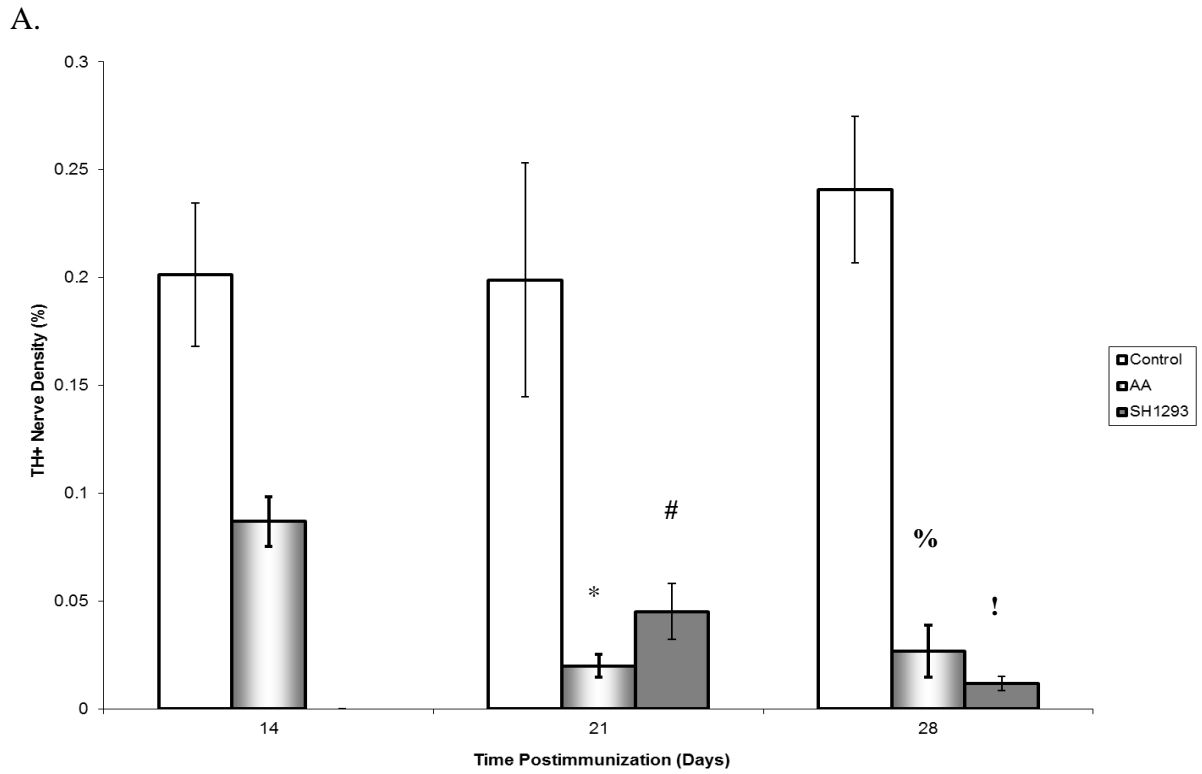
Figure 2F. 21 Day SH1293 variability in the same animal.

Figure 2G. 28 Day X-ray films AA, AA/Saline, SH1293, no treatment.

Figure 2H. X-ray SH1293 variability in the same rat.

A.

Figure 3. TH+ Nerve Density in the Distal Tibia
* AA rats showed a significant difference in TH+ staining (p<0.05, n=10) compared with the control rats. (n=11)
# SH1293 rats showed a significant difference in TH+ staining (p<0.05, n=8) compared with the control rats (n=11)
% AA rats showed a significant difference in TH+ staining (p<0.05, n=6) compared with the control rats (n=11)
! SH1293 rats showed a significant difference in TH+ staining (p<0.05, n=8) compared with the control rats (n=11)
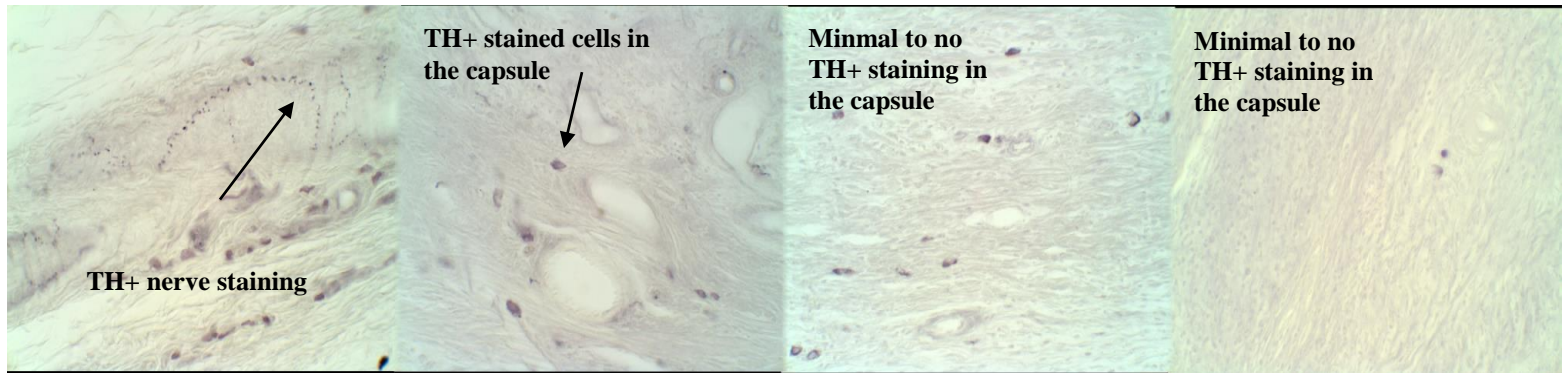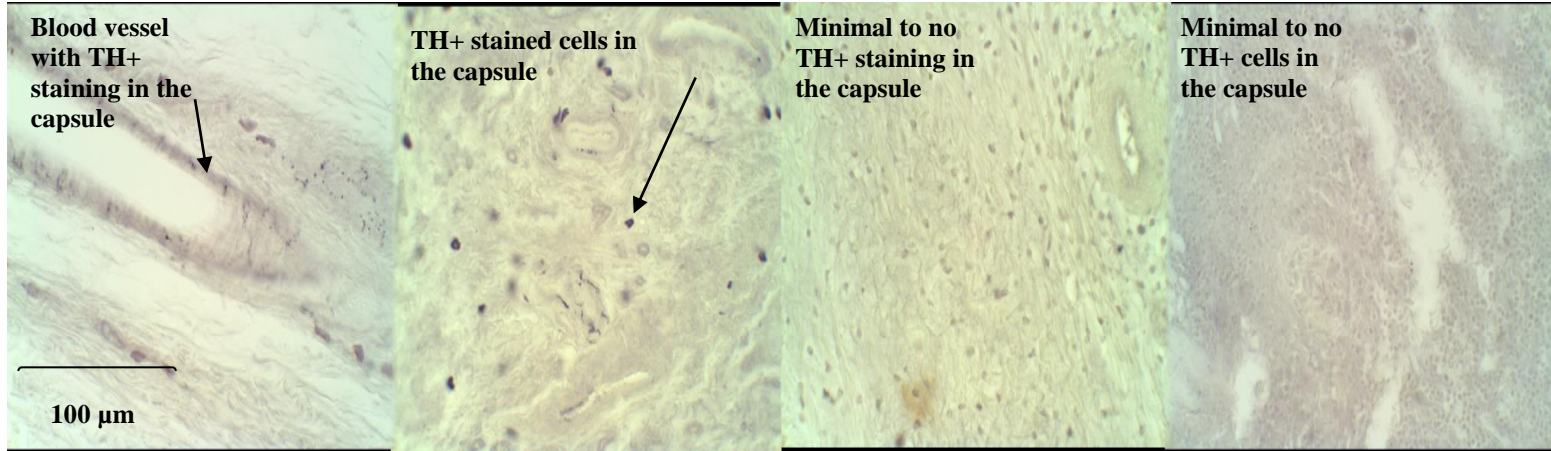
Figure 3. TH+ nerves in the capsule

Bone Volume

Figure 4A is an example of a control rat 14 days after the start of the experiment using μCT and 3D reconstruction. This image demonstrates the preservation of the talocrural joint. The trochlea of the talus and the articular surface of the tibia are seen to have regular boarders and smooth articular surfaces. There is an absence of bone erosion and osteophyte formation. Figure 4B demonstrates an AA rat 14 days after challenge with CFA with preservation of the talocrural joint, as the disease has not advanced very far at this time point. Figure 4C is an AA rat 21 days post-challenge demonstrating bone resorption at the talocrural joint. Here it is evident that there is broken continuity between the tibial diaphyseal cortical bone and the tibial articular cartilage, as well as other erosion sites in the other tarsal bones. Figure 4D demonstrates a 21 day SH1293 rat with complete preservation of the talocrual joint. Figure 4E demonstrates a 28 day AA rat with severe ankle and tarsal bone resorption. Figure 4F demonstrates a 28 day SH1293 rat with similar severe ankle and tarsal bone resorption.

At 14 days, the AA rats showed a significant decrease in bone volume, 3,939.0 voxels per sphere ($\pm$ 234.0, $p<0.0003$), compared with controls 4659.3 voxels per sphere ($\pm$ 43.58). On day 21, the mean bone volume was measured in the AA rats at 2,413.0 voxels per sphere ($\pm$ 188.01, $p<0.0001$), the SH1293 rats were measured to be 4,154.8 voxels per sphere ($\pm$ 96.42, $p<0.05$), while the controls were measured to be 4,560.5 voxels per sphere ($\pm$ 47.80). There was no significant difference in bone volume between the control rats and the SH1293 rats. By day 28, mean voxels in AA rats were measured at 2,523.7 per sphere ($\pm$ 276.79, $p<0.0001$), the SH1293 rats mean voxels were measured at 2,382.7 per sphere ($\pm$ 262.65, $p<0.0001$), while the controls measured 4,190.1 voxels

per sphere ($\pm$ 32.85). At day 28, there was a significant decrease in bone volume between the AA and SH1293 rats compared to the control rats (Figure 4G).

At 14 days, the AA rats showed a significant ($p<0.05$) and inverse correlation between bone volume and the presence of osteoclasts (-0.99). At 21 days, the AA rats bone volume correlated ($p<0.05$) with an increased presence of lymphocytes (0.78) and an increase presence of pannus formation (0.72). The SH1293 animals showed no significant correlations at this time point or at 28 days. On day 21, there was a 41.9% preservation of bone volume in the AA rats that received SH1293 compared with the AA animals. By day 28, there was a 5.6% decrease in bone volume in the AA animals that received SH1293.
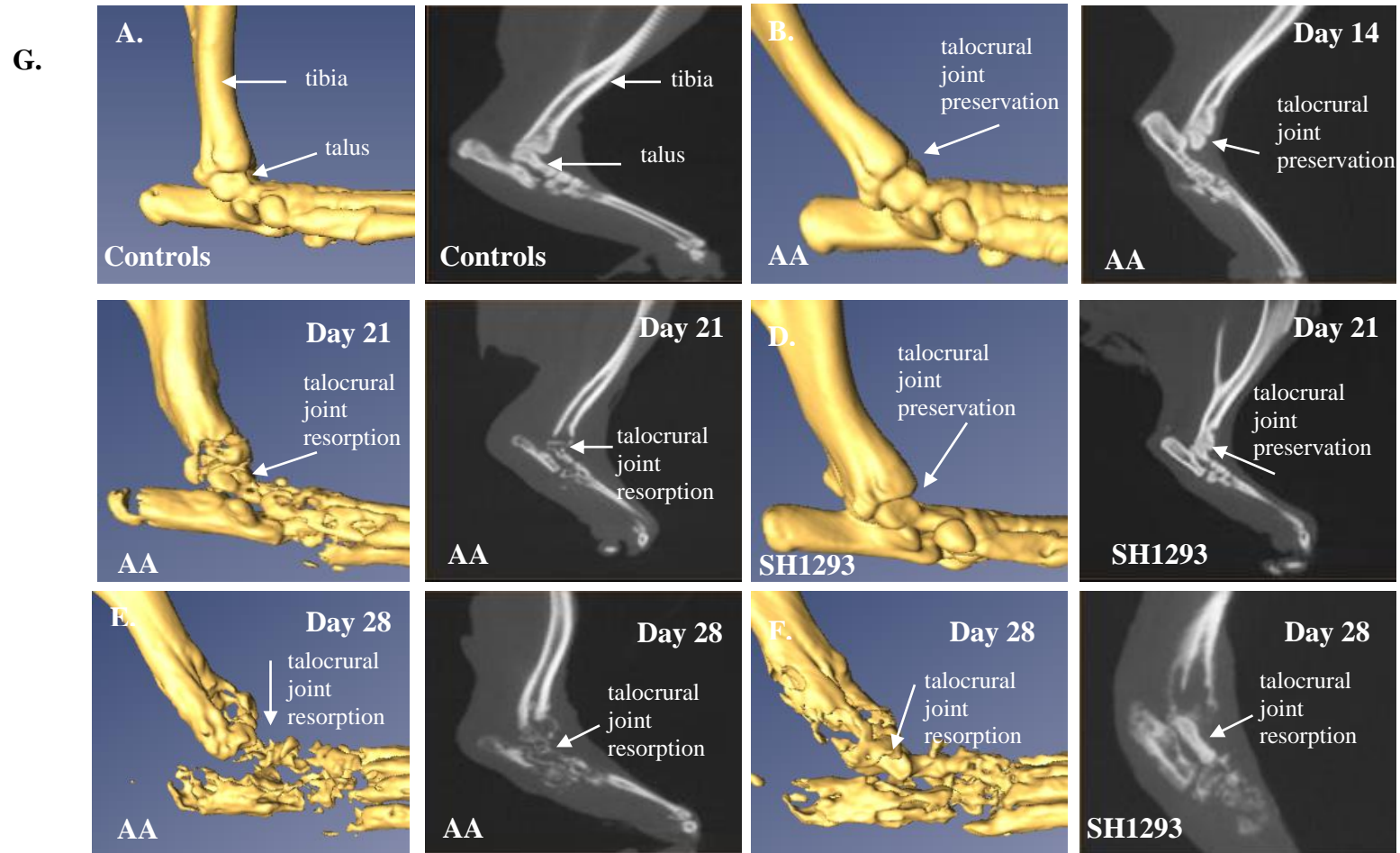
Figure 4. µCT imaging of the Ankle A.-F.
A. A 14 day control rat demonstrating preservation of the talocrural joint.
B. A 14 day AA rat demonstrating preservation of the talocrural joint.
C. A 21 day AA rat demonstrating bone resorption at the talocrural joint.
D. A 21 day SH1293 rat demonstrating bone preservation at the talocrural joint.
E. A 28 day AA rat demonstrating severe ankle and foot bone resorption.
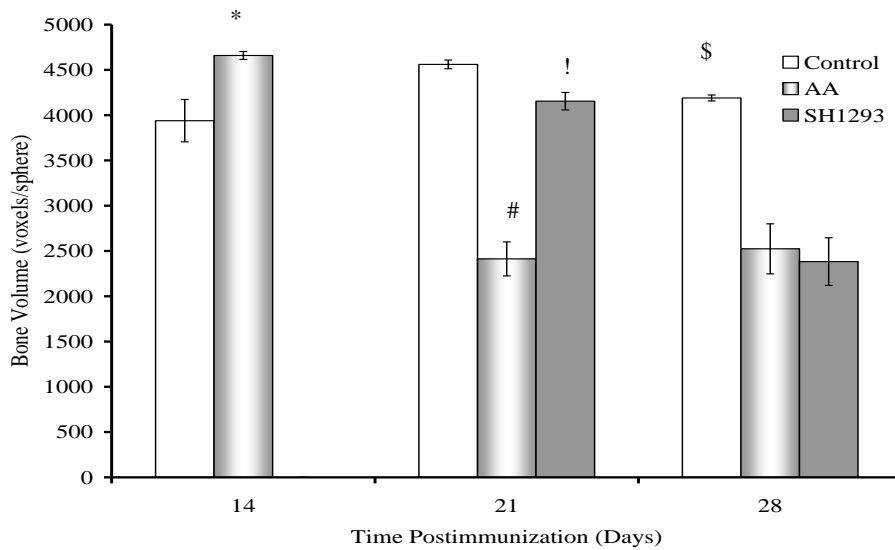F. A 28 day SH1293 rat demonstrating severe ankle and foot bone resorption.

Figure 4. G.

*AA rats showed a significant decrease in bone volume (p<0.0003, n=5) compared with the control rats (n=15)

AA rats showed a significant decrease in bone volume (p<0.0001, n=9) compared with the control rats (n=10) and the SH1293 rats (n=9)

! SH1293 rats (n=9) showed no significant difference in bone volume compared with the control rats (n=10)

$ Control rats (p<0.0002, n=8) show a significant difference compared with both AA rats (n=6) and SH1293 rats (n=6)

Lymphocytic Infiltration

Figure 5A demonstrates a 14 day control rat with intact collagen fibers forming the capsule of the talocrural joint. Synoviocytes and minimal cellular infiltration is also apparent. Figure 5B demonstrates a 14 day AA rat with intact collagen fibers forming the capsule of the talocrural joint, but with increased cellular infiltration. Figure 5C demonstrates a 21 day AA rat with distal tibial bone resorption and a large osteophyte with severe increase in cellular infiltration. Figure 5D demonstrates a 21 day SH1293 rat without osteophytes or erosion, intact collagen fibers forming the capsule and an increase in cellular infiltration, but still contained within the joint. Figure 5E demonstrates a 28 day AA rat with distal tibial bone resorption, a large osteophyte and increased cellular infiltration that has breached the capsule. Figure 5F demonstrates a 28 day SH1293 rat with distal tibial bone resorption, osteophyte formation and increased cellular infiltration. The next series of images demonstrate the trabecular bone infiltration. Figure 5G represents a 14 day control rat with intact trabecular bone just proximal to the subcortical bone on the distal tibia. Figure 5H represents a 14 day AA rat with intact trabecular bone and an increase in cellular infiltration. Figure 5I shows a 21 day AA rat demonstrating complete trabecular bone resorption and a celluar nodule. Figure 5J demonstrates a 21 day SH1293 rat with trabecular bone preservation and an increase in cellular infiltration. Figure 4K demonstrates a 28 day SH1293 rat with trabecular bone resorption and increased osteoclasts as well as other inflammatory cells.

At 14 days, a significant increase in lymphocyte infiltration was shown in the AA rats which averaged a score of 3.0 ($\pm$ 0.0, $p<0.0001$) compared with the control rats 1.13 ($+0.09$, $p<0.0001$). At 21 days post-challenge, the lymphocytic infiltration score was

significantly greater in rats with AA which averaged 2.78 ($\pm$ 0.139, $p<0.0001$) compared with the controls 1.0 (± 0.0, $p<0.0001$) and the SH1293 group 2.0 (± 0.0, $p<0.0001$). In addition, lymphocytic infiltration into the bones from the SH1293-treated AA rats was significantly ($p<0.0001$) increased from the control rats. At 28 days, lymphocytic infiltration scores in the bones from the AA rats averaged 2.7 ($\pm$ 0.21, $p<0.0001$) while the score of the SH1293 rats was 2.4 ($\pm$ 0.18, $p<0.0001$). The control rats scores remained at 1.0 ($\pm$ 0.0, $p<0.0001$). By day 28, both the AA and the SH1293 rats showed a significant increase in mean scores from the control rats (Figure 5O).

By day 21, the AA rats lymphocyte infiltration showed a significant and positive correlation ($p<0.05$) with pannus development (0.84) and bone volume (0.78), and negatively correlated with sympathetic nerve density (-0.78). At 21 days, there was a significant correlation ($p<0.05$) between lymphocyte presence and pannus formation (0.65) in AA rats treated with SH1293. At 28 days, the AA rats' lymphocyte infiltration was associated with greater osteoclast numbers (0.84). At 28 days, there was a significant inverse correlation ($p<0.05$) between lymphocytes and bone area (-0.83), as well as, sympathetic nerves (-0.71) in rats treated with SH1293. By 21 days, there was a 28.6 % decrease in mean lymphocyte scores with SH1293 treatment compared with the AA animals. By day 28, treatment with SH1293 result in an 11.2% decrease in mean lymphocyte scores compared with the AA animals.

Pannus Development

Figure 5L demonstrates a 14 day control rat with an intact capsule arising from the distal tibia and no presence of pannus development (this connective tissue is what ends up being measured on the controls). Figure 5M demonstrates a 14 day AA rat with a severe increase in pannus development and destruction of the capsule. Figure 5N demonstrates a 28 day SH1293 rat with an increase in pannus development and osteophyte formation on the distal tibia. The biggest difference between the images is between the 14 day controls and the 14 day AA rats, as there is increased pannus that is evident. The 21 and 28 day AA and SH1293 specimens look similar to what is depicted in 5N so for brevity, they were not shown.

At 14 days, the AA rats showed a significant increase in pannus development, 70.57% ($\pm$ 2.08%, $p<0.0001$) from the control rats, 23.86% ($\pm$ 2.12%). On day 21, the mean pannus percentage in the AA rats was measured at 55.9% ($\pm$ 5.28%, $p<0.001$) while the mean in the SH1293 rats was measured at 47.2% ($\pm$ 3.96%, $p<0.01$) and the mean in the controls was measured at 25.3% ($\pm$ 5.64). At 21 days, the AA rats and the SH1293 rats showed a significant increase in pannus percentage compared with the control rats. At day 28, the mean percentage of pannus in the AA rats was 76.9% ($\pm$ 0.88%, $p<0.0001$) and 69.9% ($\pm$ 2.97%, $p<0.0001$) in the SH1293 animals while the controls rats were measured at 29.0% ($\pm$ 1.31). At 28 days the AA rats and the SH1293 rats showed a significant increase in pannus percentage compared with the control rats (Figure 5P). The trichrome stained the normal amount of collagen outside the bone (capsule and ligaments) on the controls which was accounted for here.

At 14 days, the AA rats showed a significant inverse correlation ($p<0.05$) between the pannus development and the amount of bone area (- 0. 96). At 21 days, the AA rats showed the pannus development correlated with the presence of bone volume (0.72), and with the lymphocytes (0.84). At 21 days, rats treated with SH1293 showed pannus formation significantly correlated ($p<0.05$) with lymphocyte infiltration (0.65), and sympathetic nerve density (-0.62). At 28 days, there was a significant correlation ($p<0.05$) between pannus and bone area (0.86) in AA rats. On day 21, treatment with SH1293 reduced pannus formation by 15.6% compared with the AA animals. By day 28, SH1293 treatment reduced pannus formation by 9.1% compared with the AA animals.
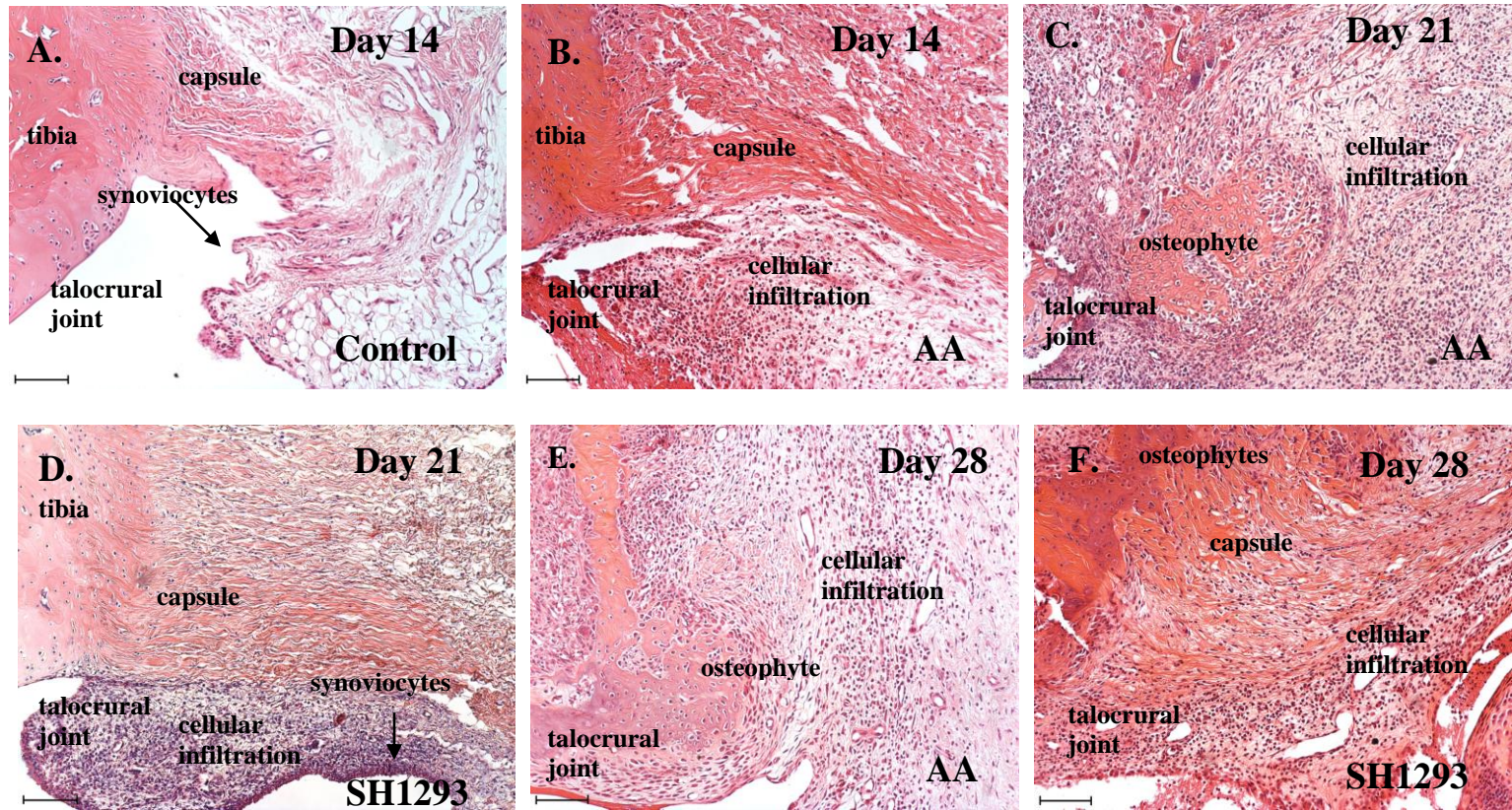
Figure 5. Inflammatory Cell Infiltration and Pannus Formation A.-K.

A. A 14 day control rat demonstrating intact collagen fibers forming the capsule of the talocrural joint and synoviocytes and minimal cellular infiltration.

B. A 14 day AA rat demonstrating intact collagen fibers forming the capsule of the talocrural joint, but with increased cellular infiltration.

C. A 21 day AA rat demonstrating distal tibial bone resorption with growth of a large osteophyte and severe increase in cellular infiltration.

D. A 21 day SH1293 demonstrating intact collagen fibers forming the capsule with an increase in cellular infiltration, but still contained.

E. A 28 day AA rat demonstrating distal tibial bone resorption, a large osteophyte formation and increased cellular infiltration.

F. A 28 day SH1293 rat demonstrating distal tibial bone resorption, osteophyte formation and increased cellular infiltration.
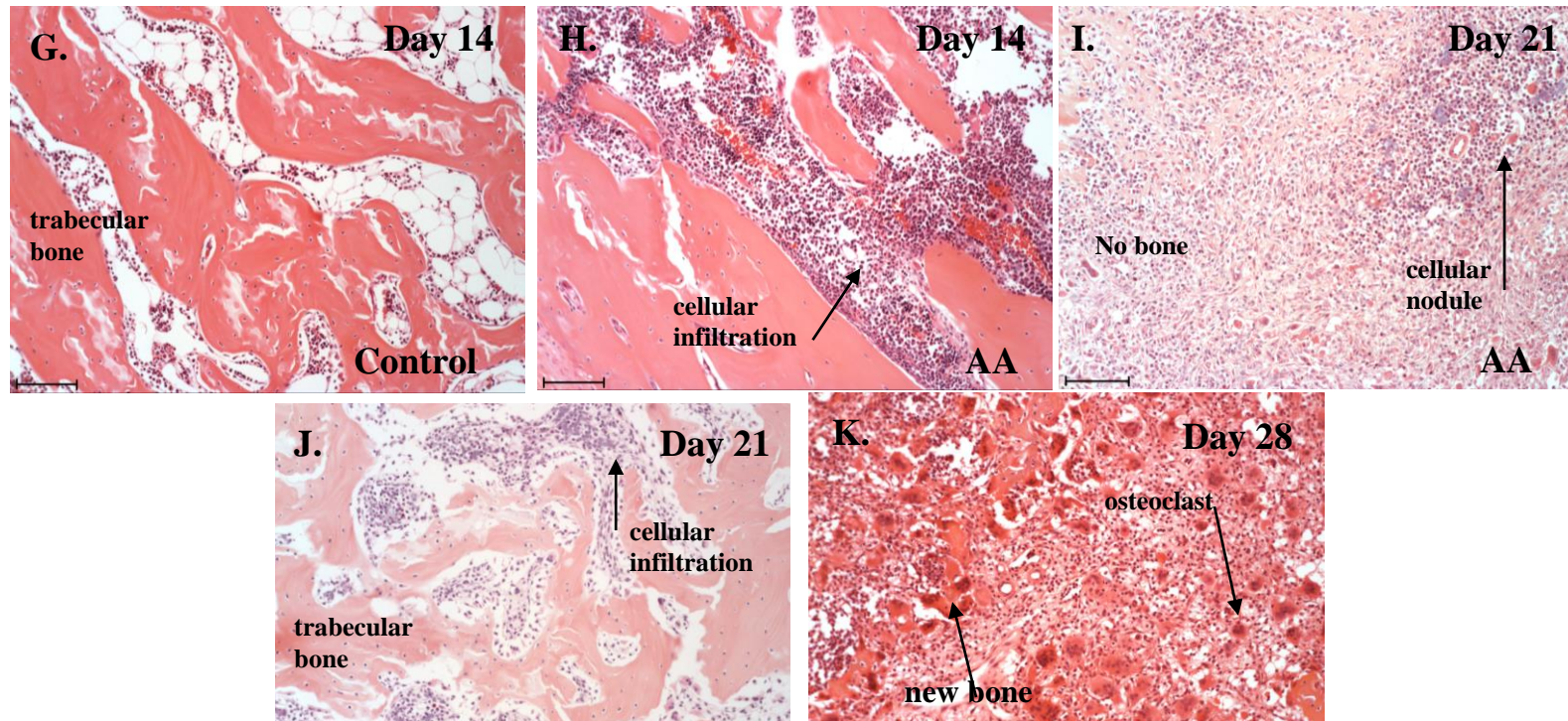
G. A 14 day control rat demonstrating intact trabecular bone just proximal to the subcortical bone on the distal tibia.

H. A 14 day AA rat demonstrating intact trabecular bone with an increase in cellular infiltration.

I. A 21 day AA rat demonstrating complete trabecular bone resorption and a cellular nodule.

J. A 21 day SH1293 rat demonstrating trabecular bone preservation with an increase in cellular infiltration.

K. A 28 day SH1293 rat demonstrating trabecular bone resorption and an increase in osteoclasts as well as other inflammatory cells.
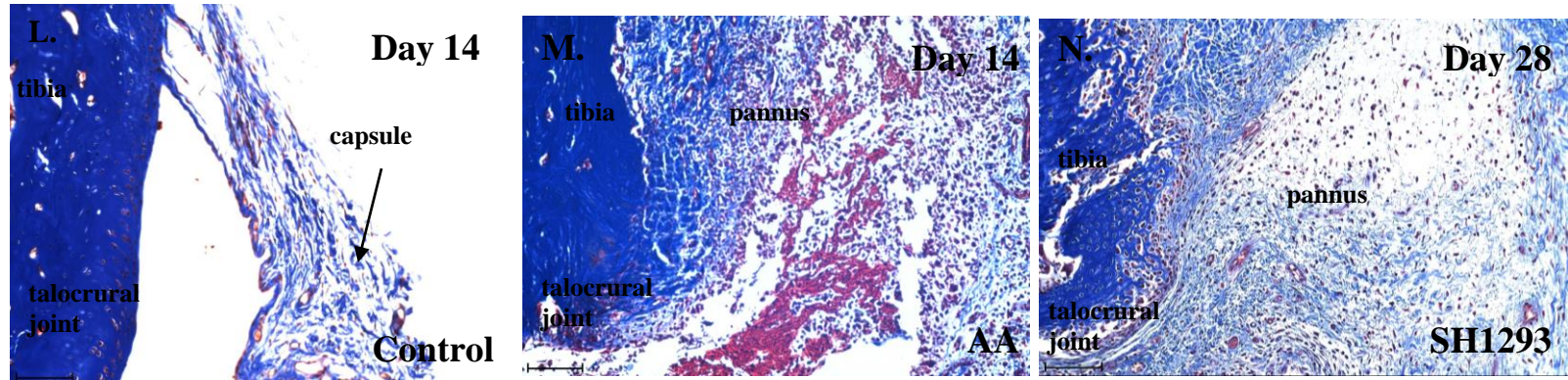
Figure L. – N.

L. A 14 day control rat demonstrating an intact capsule arising from the distal tibia and no presence of pannus development.

M. A 14 day AA rat demonstrating the severe increase in pannus development and destruction of the capsule.

N. A 28 day SH1293 rat demonstrating an increase in pannus development and osteophyte formation on the distal tibia.
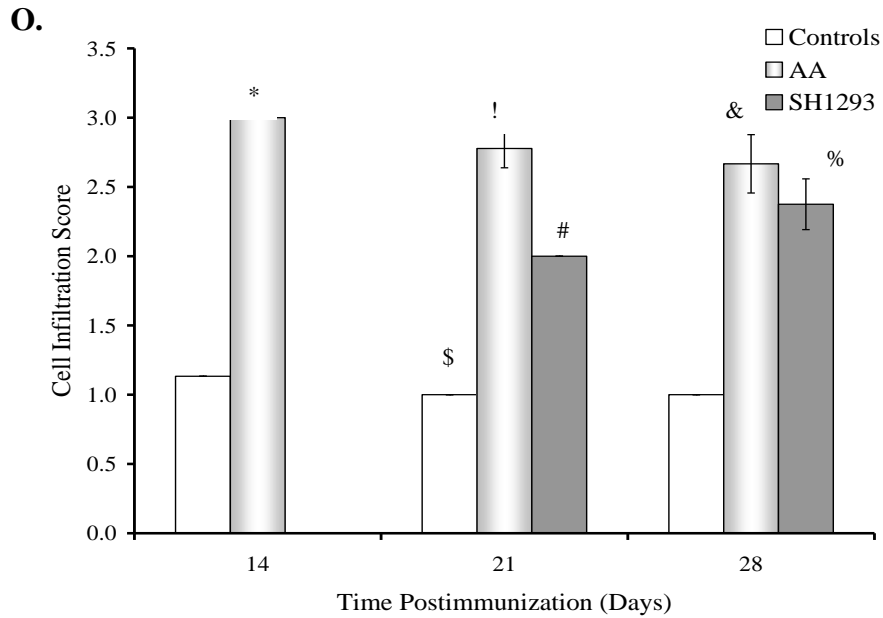
O.

Figure 5. O.
* AA rats showed a significant increase in lymphocyte infiltration (*p*<.0.0001, n=5) compared to the control rats (n=15)
$ Control rats showed a significant decrease (*p*<0.0001 and 0.0004) from both the SH1293 rats and the AA rats
! AA rats showed a significant increase (*p*<0.0001 and 0.02) from both the Control rats and the SH1293 rats.
SH1293 rats showed a significant difference (*p*<0.0001, and 0.0001, n=10) from both the Control rats (n=8) and AA rats (n=9)
& AA rats showed a significant increase (*p*<0.0001, n=6) in lymphocyte development compared to the control rats (n=8)
% SH1293 rats showed a significant increase (*p*<0.0001, n=8) in lymphocyte development compared to the control rats (n=8)
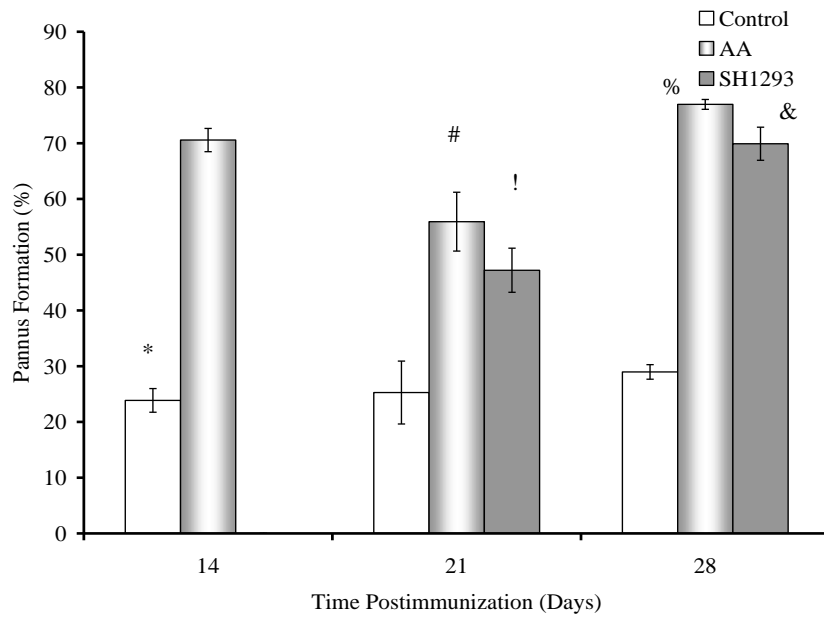
P.

Figure 5. P.
* AA rats showed a significant increase (*p*<0.0001, n=5) in pannus formation compared to Control rats (n=20)
# AA rats showed a significant increase (*p*<0.001, n=10) in pannus formation compared to the Control rats (n=7)
! SH1293 rats showed a significant increase (*p*<0.01, n=12) in pannus formation compared to the Control rats (n=7)
% AA rats showed a significant increase (*p*<0.0001, n=6) in pannus formation compared to the Control rats (n=6)

Articular Cartilage Area

Figure 6A demonstrates a 14 day control rat with no resorption of the subchondral bone or cartilage at the apex of the distal tibial concavity. Figure 6B demonstrates a 14 day AA rat with resorption of the subchondral bone, but not the articular cartilage at the apex of the distal tibial concavity. Figure 6C demonstrates a 21 day AA rat with subchondral bone and articular cartilage resorption at the apex of the distal tibial concavity. Figure 6D represents a 21 day SH1293 rat demonstrating no resorption of the subchondral bone or articular cartilage at the distal tibial concavity. Figure 6E demonstrates a 28 day AA rat with subchondral bone and articular cartilage resorption at the distal tibial concavity. Figure 6F represents a 28 day SH1293 rat with subchondral bone resorption and very mild articular cartilage resorption of the distal tibial concavity.

At 14 days, there was no significant difference in the mean articular cartilages at the talocrural joint between the controls, which was measured at 0.75 mm^2 ($\pm$ 0.03) and the AA rats which measured 0.7 mm^2 ($\pm$ 0.05). On day 21, the mean articular cartilage in AA rats was measured to be 0.61 mm^2 ($\pm$ 0.028, $p<0.009$) and mean of the SH1293 rats was measured to be 0.73 mm^2 ($\pm$ 0.032, $p<0.02$) while the controls measured 0.76 mm^2 ($\pm$ 0.033). The mean articular cartilage in the talocrural joint did not differ between SH1293-treated rats and controls ($p>0.05$), but there was a significant ($p< 0.009$ and 0.18 respectively) decrease in the articular cartilage in AA rats from the control and SH1293 rats. By day 28, mean articular cartilage in the AA rats measured 0.57 mm^2 ($\pm$ 0.037, $p<0.02$) and the SH1293 rats mean was measured at 0.69 mm^2 ($\pm$ 0.059), while the controls were measured at 0.78 mm^2 ($\pm$ 0.043). No significant ($p>0.05$) differences were

observed between the SH1293 rats versus the control or AA rats; however, there was a significant decrease between the AA rats and the control rats (Figure 6G).

There was a significant negative correlation (-0.94) between the sympathetic nerves and the articular cartilage ($p<0.05$). On day 21, 16.5% of articular cartilage was preserved in rats treated with SH1293 compared with the AA animals. By day 28 there was a 17.4% preservation of articular cartilage by using the drug compared to the AA animals.
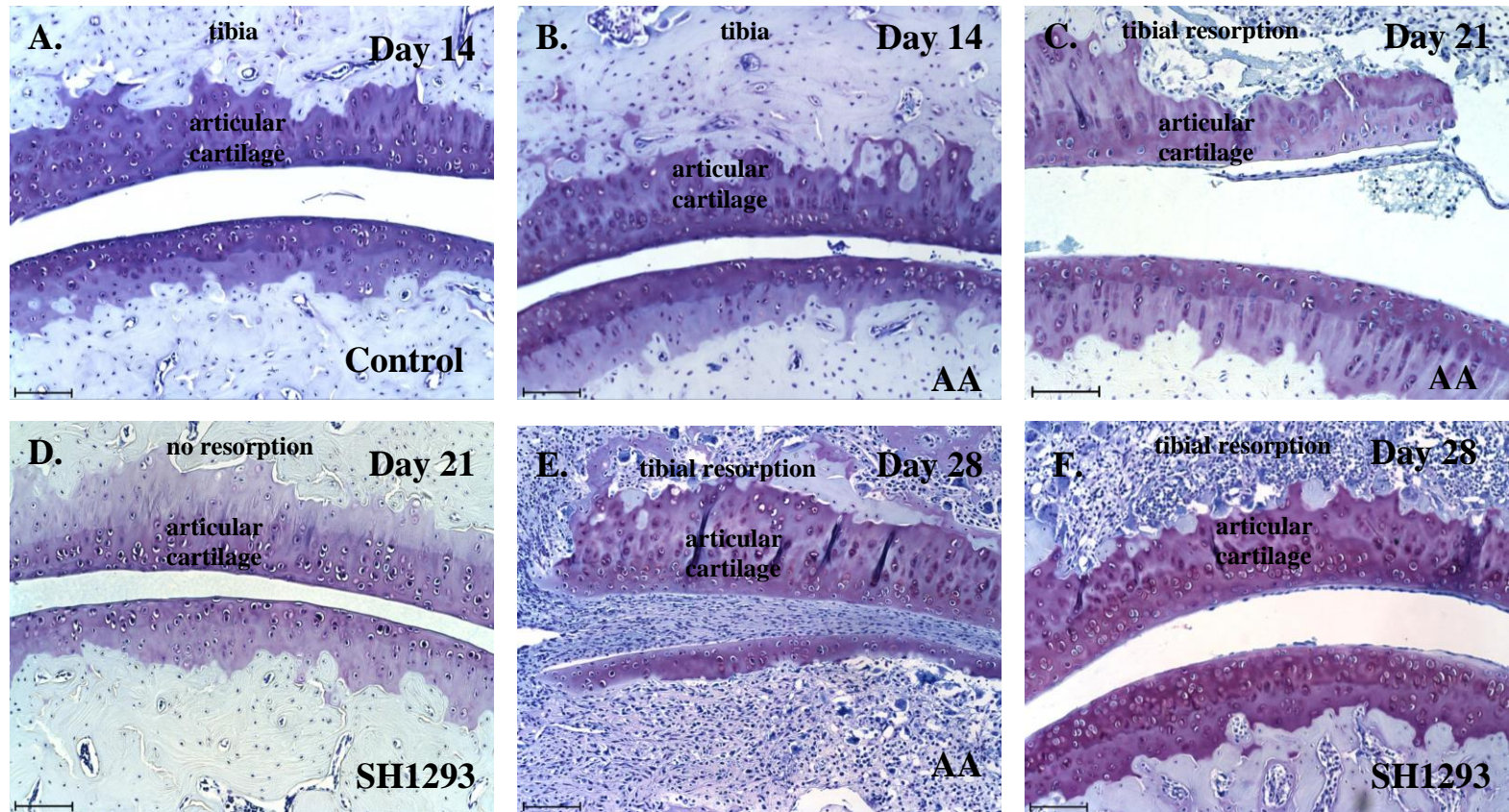
Figure 6. Talocrural Joint Articular Cartilage A.-F.

A. A 14 day control rat demonstrating no resoption of the subchondral bone or cartilage at the apex of the distal tibial concavity.

B. A 14 day AA rat demonstrating resorption of the subchondral bone, but not the articular cartilage at the apex of the distal tibial concavity.

C. A 21 day AA rat demonstrating subchondral bone and articular cartilage resorption at the apex of the distal tibial concavity.

D. A 21 day SH1293 rat demonstrating no resorption of the subchondral bone or articular cartilage at the distal tibial concavity.

E. A 28 day AA rat demonstrating subchondral bone and articular cartilage resorption at the distal tibial concavity.

F. A 28 day SH1293 rat demonstrating subchondral bone resorption and articular cartilage resorption of the distal tibial concavity.
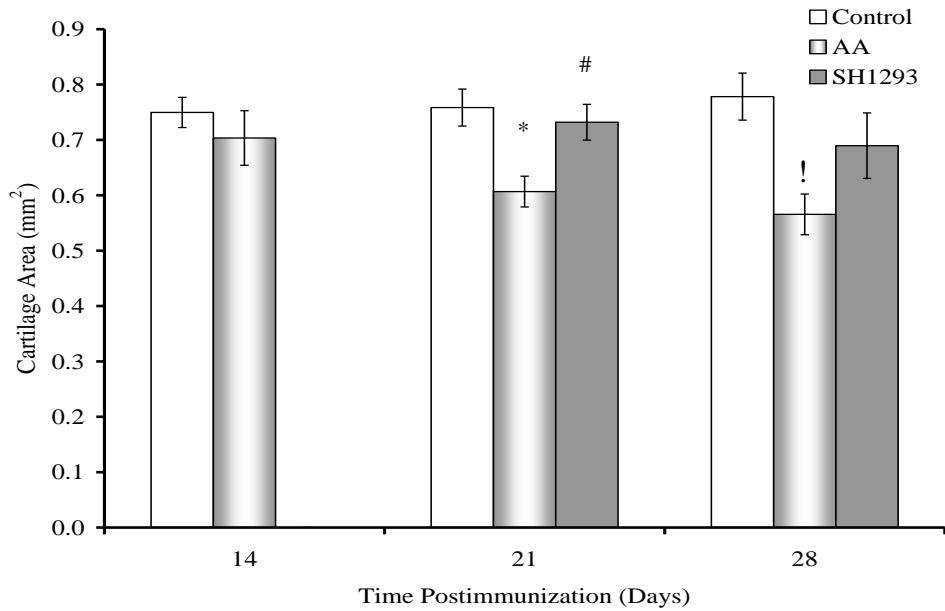
Figure 6. G.
* AA rats showed a significant decrease in distal tibial cartilage area ($p<0.009$, n=10) compared to the control rats (n=8)
#SH1293 rats showed a significant increase in distal tibial cartilage area ($p<0.02$,n=12) compared to the AA rats (n=10)
! AA rats showed a significant decrease in distal tibial cartilage area ($p< 0.02$, n=5) than the control rats (n=8)

Bone Area and Osteoclasts

For the bone area and osteoclasts, there were two very different groups that became evident by using a scatter plot. Of the animals that received SH1293, some responded more like the controls and some responded more like the AA animals. They were given the following labels. If they responded more like the controls, they were given the label SH1293h, h representing a high response. If they responded more like the arthritic rats, they were given the label SH1293l, l representing a low response.

Figure 7A represents a 14 day control rat with minimal osteoclast activity and the presence of trabecular bone in the second zone. Figure 7B represents a 14 day AA rat demonstrating minimal osteoclast activity and the presence of trabecular bone in the second zone. Figure 7C represents a 21 day AA rat with osteoclasts present and severe trabecular bone resoption in the second zone. Figure 7D represents a 21 day SH1293 rat with a low response to the drug and a similar response to the 21 day AA rat, where osteoclasts are present and severe trabecular bone resorption occurred in the second zone. Figure 7E represents a 21 day SH1293 rat with a high response to the drug and shows no osteoclasts and the complete preservation of the trabecular bone in the second zone. Figure 7F represents a 28 day AA rat with osteoclast presence and the resorption of trabecular bone and new bone deposition in the second zone. Figure 7G represents a 28 day SH1293 rat with a low response to the drug and a similar response to the 28 day AA rat. It has osteoclasts present and new bone deposition in the second zone. Figure 7H demonstrates a 28 day SH1293 rat with a high response to the drug and no presence of osteoclasts and intact original trabecular bone.

At day 14, there was no significant ($p>0.05$) difference between the mean bone area of the control rats 0.344 mm^2 ($\pm$ 0.052) and the AA rats 0.244 mm^2 ($\pm$0.03). On day 21, the mean bone area in the AA, SH1293h and SH1293l rats were 0.07 mm^2 ($\pm$ 0.0087, $p<0.0001$ and $p<0.0001$), 0.27 mm^2 ($\pm$ 0.011, $p<0.0001$ and $p<0.0001$), and 0.06 mm^2 ($\pm$ 0.013, p<0.0001 and 0.0001), respectively, while the control group was 0.31 mm^2 ($\pm$ 0.006). Bone area was significantly ($p<0.0001$, $p<0.03$, $p<0.0001$) less preserved in AA, SH1293h, and SH1293l rats compared with control rats. Mean bone area in the SH1293h rats was significantly ($p<0.0001$) increased compared with AA and SH1293l rats. By day 28, mean bone area in AA rats was 0.13 mm^2 ($\pm$ 0.031, $p<0.0002$ and 0.03), the SH1293h rats mean was 0.23 mm^2 ($\pm$ 0.018, $p<0.03$ and 0.001), the SH1293l rats mean was 0.08 mm^2 ($\pm$ 0.014, $p<0.0001$ and 0.0001), while the controls measured 0.3 mm^2 ($\pm$ 0.013). AA and SH1293l rats had significantly lower mean bone area than the control rats (Figure 7I).

For regression analysis, the SH1293 group was not divided into high or low responders. At 21 days, there was a significant ($p<0.05$) inverse correlation between bone area and osteoclasts (-0.83) and direct correlation between bone area and sympathetic nerves (0.84) in rats treated with SH1293. At 28 days, there was a significant correlation in the AA rats between mean osteoclast number and lymphocyte infiltration (0.84), and between mean bone area and percent pannus formation (0.86). At 28 days, in rats receiving SH1293 treatment, a significant inverse correlation between the mean bone area and the osteoclasts (-0.72) existed. The mean bone area was inversely correlated with lymphocytes (-0.83). The bone area at this time point also showed a significant correlation with sympathetic nerves (0.93).

On day 21, there was a 74.1% increase in mean bone area from rats that received SH1293 and were high responders, compared with a 14.3% decrease in bone area from rats administered SH1293 and were low responders. By day 28, there was a 43.5% increase in bone area of SH1293-treated high responders compared with a 38.5% decrease in SH1293-treated low responders.

At day 14, there was a significant difference ($p<0.033$) in the amount of osteoclasts between the control group and the AA rats. The controls averaged 2.27 cells per 3 zones ($\pm$ 1.91) while the AA rats averaged 13.4 cells per 3 zones ($\pm$ 19.40). On day 21, no significant difference existed between the control rats and SH1293h rats ($p>0.05$). There was also no significant difference between the AA rats and SH1293l rats ($p>0.05$). There was a significant difference between the control rats and the AA/SH1293l rats ($p<0.0002$, 0.0002), as well as the SH1293h rats and the AA/SH1293l rats ($p<0.0005$, 0.0002). The mean osteoclast numbers in AA rats averaged 20.6 cells per 3 zones ($\pm$ 3.27), the SH1293h rats averaged 1.9 cells per 3 zones ($\pm$ 1.01), the SH1293l rats averaged 26.6 cells per 3 zones ($\pm$ 6.02), while the controls averaged zero cells per 3 zones ($\pm$ 0.0). At day 28, there was no significant difference between the control group and the SH1293h group ($p>0.05$). There was a significant difference between the controls and the AA group ($p<0.0005$) as well as the SH1293l group ($p<0.02$). There was also a significant difference between the SH1293h group and the AA group ($p<0.002$) as well as the SH1293l group ($p<0.04$). By day 28, the AA rats averaged 45.2 cells per 3 zones ($\pm$ 10.8), the SH1293h rats averaged zero cells per 3 zones ($\pm$ 0.0), the SH1293l rats averaged 30.8 cells per 3 zones ($\pm$ 10.9), while the controls averaged a half a cell per 3 zones ($\pm$ 0.5).
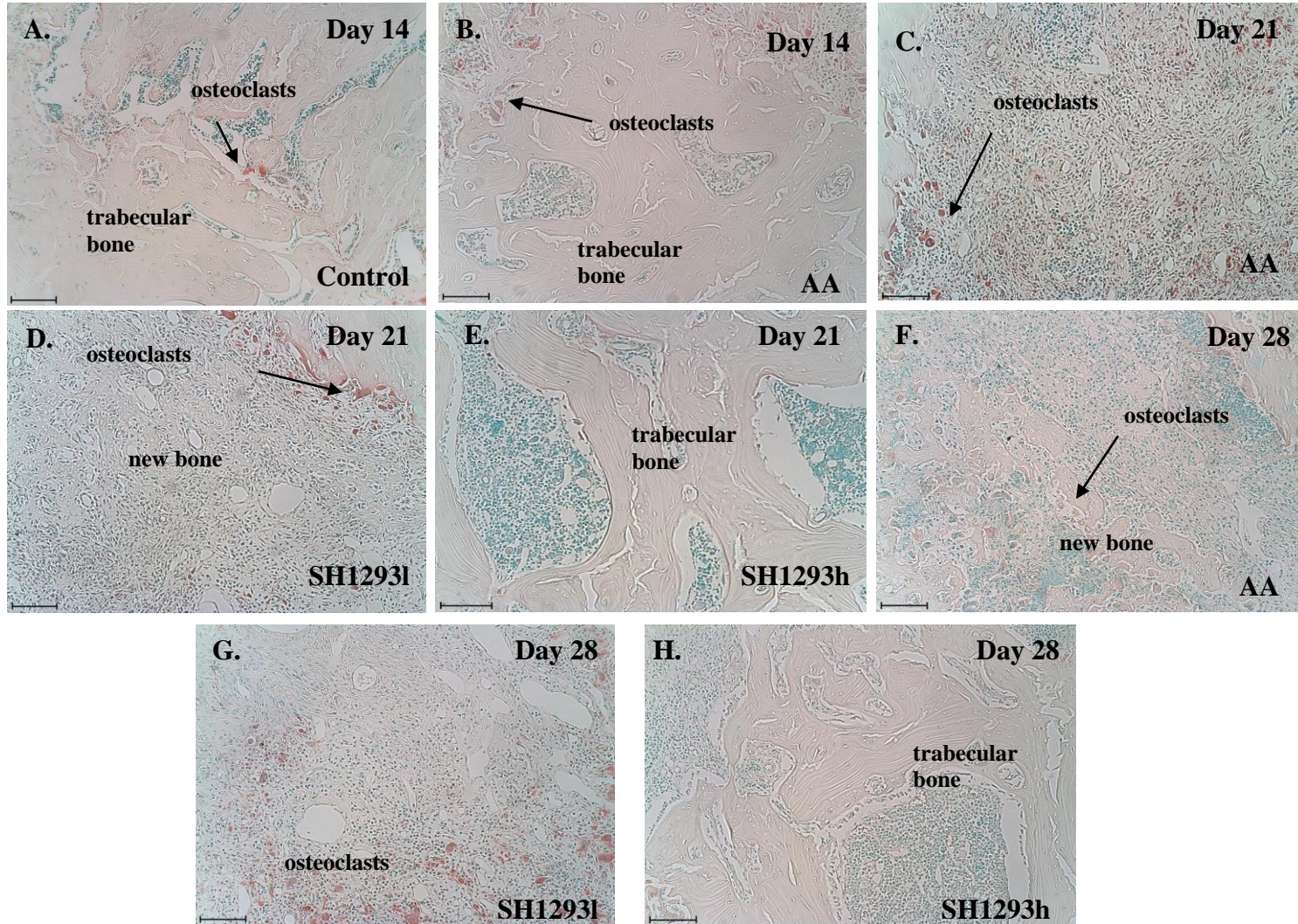
Figure 7. TRAP+ staining for osteoclasts in the distal tibia A.-H.

A. A 14 day control rat demonstrating minimal osteoclast activity and the presence of trabecular bone in the second zone.

B. A 14 day AA rat demonstrating minimal osteoclast activity and the presence of trabecular bone in the second zone.

C. A 21 day AA rat demonstrating osteoclasts presence and severe trabecular bone resorption in the second zone.

D. A 21 day SH1293 demonstrating a low response to the drug and a similar response to the 21 day AA rat, osteoclast presence and severe trabecular bone resorption in the second zone.

E. A 21 day SH1293 rat demonstrating a high response to the drug which shows no osteoclasts and the preservation of the trabecular bone in the second zone.

F. A 28 day AA rat demonstrating osteoclast presence and the resorption of trabecular bone and new bone deposition in the second zone.

G. A 28 day SH1293 rat demonstrating a low response to the drug and a similar response to the 28 day AA rat, osteoclast presence and new bone deposition in the second zone.

H. A 28 day SH1293 rat demonstrating a high response to the drug and no presence of osteoclasts and intact original trabecular bone
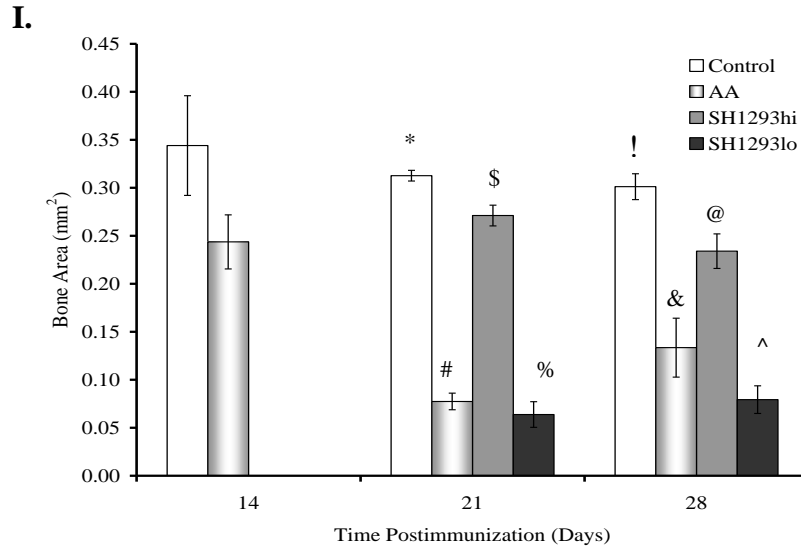
I.

Figure 7. I.

* The Control rats showed a significant increase ($p<0.0001$, .03, .0001 n=8) in Bone Area compared to the AA, SH1293h and SH1293l rats (n=8,7,5).

\# The AA rats showed a significant decrease ($p<0.0001$, .0001, n= 8) in Bone Area compared to the Control and SH1293h rats. (n=8,7).

\$ The SH1293h rats showed a significant increase ($p<0.0001$, .0001 n= 7) in Bone Area compared to the AA and SH1293l rats (n=8,5) and a significant decrease ($p<0.03$) compared to the Control rats (n=8).

% The SH1293l rats showed a significant decrease ($p<0.0001$, .0001 ,=5) in Bone Area compared to the Control and SH1293h rats (n=8, 7).

! The Control rats ($p<0.0002$, .0001, n=8) showed a significant increase in Bone Area compared to the AA and SH1293l rats (n=5, 4).

& The AA rats showed ($p<0.0002$, .03 n=5, 4) a significant decrease in Bone Area compared to the Control and SH1293h rats.

@ The SH1293h rats ($p<0.03$, .001, n=4) showed a significant increase in Bone Area compared to the AA and SH1293l rats (n=5, 4).

^ The SH1293l rats ($p<0.0001$, 0.001, n=4) showed a significant decrease in Bone Area compared to the Control and Sh1293h rats (n=8, 4).
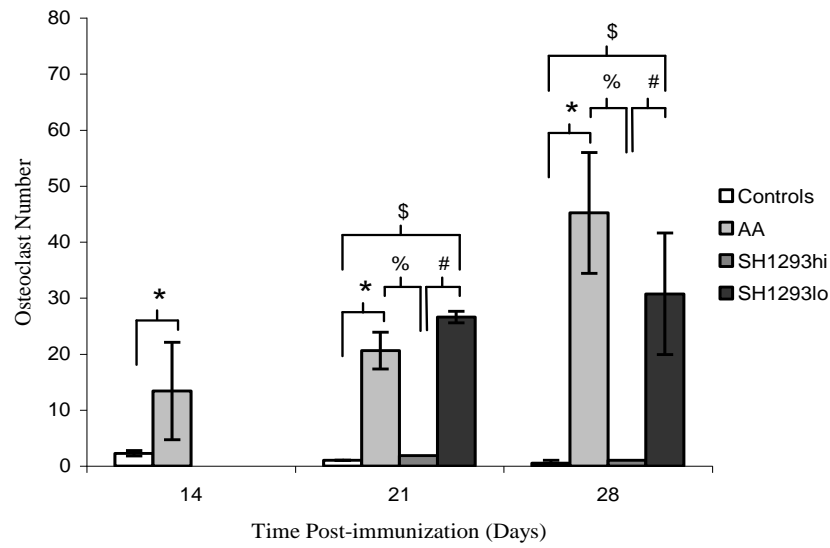
Figure 7. J.

No significant difference between control rats and SH1293h rats

No significant difference between AA rats and SH1293l rats

*Significant difference between control rats ($p<0.0002$, n=8) and AA rats (n= 8)

$ Significant difference between control rats ($p<0.0002$, n=8) and SH1293l rats (n=5)

% Significant difference between SH1293h rats ($p<0.0005$, n=7) and AA rats (n=8)

Significant difference between SH1293h ($p<0.0002$, n=7) and SH1293l rats (n=5)

No significant difference between control and SH1293h rats. No significant difference between AA and SH1293l rats

*Significant difference between control ($p<0.0005$, n=8) and AA rats (n= 5)

$ Significant difference between control ($p<0.019$, n=8) and SH1293l rats (n=4)

% Significant difference between SH1293h ($p<0.002$, n=4) and AA rats (n=5)

Significant difference between SH1293h ($p<0.04$, n=4) and SH1293l rats (n=4)

Discussion

Lymphocyte infiltration gradually increased between 14 and 28 days in the AA rats. This finding is consistent with DiPaola and Cuzzocrea's description of the AA model (2008). Treatment with SH1293 resulted in short term benefit to the rats at 21 days where they displayed less lymphocytic infiltration than the AA rats, but more than the controls.

At every time point the AA rats showed an increase in pannus development at each time point investigated. When the rats received SH1293, there was not a significant change in the amount of pannus present at any time point. The diverse cell types here are consistent with the description of Pearson and Wood (1963).

It has been well documented that the disease process can begin in the bone and progress into the joint. This is known as a bidirectional attack since cells erode both the surface and subchondral bone concomitantly (Wooley 1995). We have observed primarily the erosion of the diaphyseal region with preservation of articular cartilage as it was one of the last parts of bone to be effected in the AA rats. Different cell types above and below the cartilage were also observed as described by Wooley (1995). Macrophages and fibroblasts were the predominant cells of the cartilage-synovial pannus junctions, while multinucleated cells, macrophages and small blood vessels are the major components of the subchondral erosion sites. As described by Wooley (1995), and substantiated by our observations, no regular pattern of cartilage erosion has ever emerged. This indicates the cellular composition at sites of cartilage erosion is variable.

At 21 days the AA rats begin to show the removal of the articular cartilage; however, if given the SH1293, a short term benefit of decreased lymphocytes and cartilage preservation at this time point and beyond can be seen. By 28 days there is

significantly less cartilage in the AA rats compared to the control rats and the SH1293 rats. It is important to note here that there is still no significant difference between the controls and the SH1293 rats. It is also important to note here that even though there is preservation of the articular surface, in some animals the distal third of the cortical bone had been removed completely resulting in the articular surface being held to the mid shaft of the tibia solely by fibrotic connective tissue and pannus. Many pathologists think the contribution of the neutrophil to cartilage erosion is negligible since their presence in the pannus is negligible. This cartilage destruction method was seldom observed in our specimens and our animals favored the proximal to distal progression of the bidirectional attack which starts within the diaphysis where the sympathetic nerves are located and progresses towards the articular cartilage. It is also understood that between specimens and within specimens a wide spectrum of histological observations of the rheumatoid lesion are regularly seen. This was definitely the case in our animals, which caused a lot of variability in our data. Further evidence supporting the SNS's role in the destruction of the bone is the fact that early damage to the articular surface is substantially limited as described by Poole (Poole et al., 1995, Poole 2001). Diffuse damage to the collagen fibrils in the deeper zones of the cartilage, is a feature of more advanced stages in RA. This demonstrates that cellular events in adjacent bone which produce an extensive osteopenia, or osteoporosis, may result in the production of prodegradative cytokines like IL-1 and TNF-α (Poole 2001). These cytokines not only act on osteoblasts and osteoclasts, but also on deep zone chondrocytes close to the bone. In RA considerable damage to type II collagen is observed in locations adjacent to pannus invading cartilage. Triple helical cleavage of type II collagen by activity from neutrophil collagenase on the

articular surface may be of limited importance as described earlier. Loss of aggrecan in

acutely inflamed joints has also been noted without the presence of neutrophil

accumulation (Poole 2001). Therefore, the role of the neutrophil appears to be secondary

to other cells in AA cartilage degradation (Poole 2001) and the SNS seems to play a more

important role.

The TRAP staining demonstrated unanticipated findings. The SH1293h rats

showed improvements of many dependent variables, while the dependent variables of the

SH1293l rats looked strikingly similar to the AA rats. This discrepancy may have also

been responsible for the similar outcome of previous data obtained by our lab regarding

the positive effects observed on x-ray scores and footpad widths.

At 14 days, there was no difference in bone area between the control rats and AA

rats. At both 21 and 28 days, the SH1293h rats showed a significant decrease in bone

area compared to the controls. However, they also showed a significant reduction of

bone loss compared to the AA and SH1293l rats. These data are somewhat misleading

because in the animals that showed arthritic changes (AA and SH1293l), there was also

new bone being laid down. The way we obtained the data was not sensitive enough to

discern the difference between the different types of bone. We are aware this is a

limitation in our study and discerning a difference is crucial to the future outcomes.

Another confounding factor of the study was obtaining a count of the osteoclasts

at a particular time point. The difficulty was how to identify the cells to be included in

the count. We believe that there was a high osteoclast turnover rate at 21 and 28 days.

During our quantifying process, it was difficult to determine which cells were apoptotic

and which cells had been sliced through an oblique plane. Our answer for this was to

only count what we considered viable osteoclasts. We counted only cells which were

multinucleated, have a ruffled boarder and a Howship's lacunae.   However, sometimes

bone had been removed so fast that there was nothing for the cell to lie upon. This led to

some variability in the study. It seems the general trend was for the bone resorption to

begin near the trabecular bone, where the sympathetic nerves are most dense and progress

distally from there towards the articular cartilage.   This was consistent with Imai's (Imai

et al., 1997 b) findings of the location of the nerves in the bone marrow and bone

cartilage interface as well as Schwab (Schwab et al., 1997) and Cherruau's (Cherruau et

al., 2003) findings of the nerves being present in the tunica adventitia and media of

arteries and periosteum. At 14 days, no significant difference existed between the

amount of osteoclasts in the AA rats and controls. However, at day 21 and 28, the

SH1293h animals showed tremendous improvements over the AA and SH1293l animals.

At 14 days, there appeared to be no difference between the sympathetic

innervation of the AA rats compared with the SH1293 rats. By 21 and 28 days, there was

no significant difference in the mean percent area of sympathetic nerves between

treatment groups or any correlation. The trend is not an isolated loss of nerve, but rather

the nerves are destroyed by osteoclasts during bone resorption since the nerves are

housed within the bone.

One of the weaknesses of the study is that we had to use one limb for measuring

bone volume, while we used the contralateral limb to look at the histology of the bone.

At 14 days there was already a significant difference between the control rats and the AA

rats bone volume. By day 21, the AA rats continued to show a decline in bone volume,

while once again, as with the lymphocytes and cartilage, the SH1293 rats showed a short

term benefit in preserving bone volume. By day 28 this preservation seemed to lessen. We would have expected the bone volume to be similar to the bone area, but it seems there is a difference in degree of severity from side to side or we haven't found a way to correlate bone volume as measured by CT with bone surface area as measured using histological techniques.

There appeared to be many correlations within the AA animals. At the disease onset at 14 days, it seems that the more pannus is formed, the more bone area is removed, the more osteoclasts are present, and more bone volume is removed. By day 21, the increase in lymphocyte numbers strongly correlates with an increase in pannus amount, and the formation of new bone. It seems that as the new bone is being laid down, it is still not yet innervated by the sympathetic nervous system. Based on a net bone loss, there appears to be an incredibly strong response of the osteoclast cell line that is much faster than the osteoblasts ability to keep up. Eventually new bone is formed between 14 and 21 days. The new bone that is laid down is not the same morphology as the original architecture, but resembles mostly trabecular bone in nature, even in the cortical region. There is still the strong presence of osteoclasts with the formation of the new bone. In the chronic phase at 28 days, it seems that there is a stronger correlation between the lymphocytes and osteoclasts as well as between the pannus and bone area formation.

At 21 days, a positive and significant correlation occurred between the lymphocytes and the pannus of rats recieving the drug SH1293. As the lymphocytes decreased due to the effects of the drug, so did the pannus. There was also a strong inverse and significant correlation between osteoclasts and bone area.   As we have

described previously there were limitations in this aspect of our study that had changed our expected outcome.

At 28 days, the lymphocytes and bone area showed an inverse and significant correlation in SH1293 treated rats. As the lymphocytes decreased following administration of the drug, the bone area tended to increase as well. The osteoclasts showed a strong inverse correlation with the bone area. As the osteoclasts became more prevalent, the bone showed less area.

Previous studies are conflicting in their results in elucidating the effects of α antagonists and β agonists on AA. Many authors have studied the effects of β-AR agonists on non AA rats (Takeuchi et al., 2000). Collectively, they found that stimulating β-ARs causes a substantial increase in number of TRAP-positive multinucleated cells, as well as increased bone resorbing capabilities of these cells. When an α_1-AR agonist was used, these same cells showed a moderate increase in resorbing activity. Cherruau, (Cherruau et al., 2003) who achieved a decrease in sympathetic tone by performing sympathectomies in rats using guanethidine, showed an increase in osteoblastic activity as well as a decrease in osteoclast number and activity.

A few authors (Lubahn et al., 2004, Lorton et al., 2003, Levine et al., 1988) have studied these receptors in isolation and together in AA subjects. Levine used guanethidine to cause a sympathetic block on RA patients and showed a decrease in various subjective complaints and an increase in pinch strength over a 2-week period. He also used reserpine, a nonspecific catecholamine depletor on AA rats after disease onset and was able to favorably alter the course of the disease (Levine et al., 1988). In a third study, performing sympathectomies in AA rats by using guanethidine again, he

attenuated joint injury by depleting catecholamines peripherally (Levine et al., 1986).

We have found similar ameliorating effects on AA by altering peripheral catecholamine concentrations.

Our findings are also consistent with Lubahn et al, (2004) who studied the contribution of the β_2- and α-AR subtypes on AA disease pathology at different stages in rats. They demonstrated that if phentolamine and terbutaline were combined and given at the same time as adjuvant challenge, there was no exacerbation of the disease. When they were given at disease onset, there were significant and favorable outcomes for x-ray scores and footpad width. The x-ray scores improved by about 60% and the soft tissue swelling as measured by foot pad width improved about 55%. Together, these findings suggested that sympathetically-mediated effects via NE interaction with both α and β-ARs regulate late immune responses to CFA antigen challenge that affect disease severity.

Overall, the bone changes are greater than the cartilage changes and these changes are more related to nerve damage than pannus. Bone remodeling and formation was increased along with resorption. A consistent dose of SH1293 delays changes rather than prevented changes. It demonstrates the greatest effect on bone and the least effect on pannus. This effectiveness was variable. There were no long term effects on bone, and the remodeling was extensive. Not all arthritic rats had active arthritis at the time of euthanasia which demonstrates evidence of the episodic nature of the disease.

Conclusion

In conclusion, there is crucial information to be gained by this study in order to perpetuate the fight against this disabling disease. Our study demonstrates a strong trend

towards the SNS interacting with α- and β-ARs and playing a role in RA. This enhances the need for further investigation to clarify the mechanisms and explore the potential for adrenergic drug therapies that target α- and β- ARs in the cure for RA. The general trend clearly demonstrates over half of the animals given the drug showed preservation of the original architecture of the tibia and talocrural joint with minimal or absent deleterious cellular activity. Objectively, it can be said that the drug can limit the inflammatory response that activates the sequelae of the disease process, as well as preserve cartilage and bone volume up to the midpoint of the disease. There are also many strong trends showing that blocking the increased SNS activity that occurs after disease onset alters the bone physiology for the better. This study demonstrates steps in the right direction for preservation of tissue in this disease process as in nearly all animals receiving SH1293 showed positive changes compared with the animals that developed arthritis. These strong correlations enlighten us as to the relationships between these cells and tissues that were previously poorly understood. Future studies are currently focused on altering the amount of SH1293 given in order to observe the benefits of different doses. Additional studies may measure the amount of circulating IL-1 and TNF-α and investigate the ARs on the osteoclasts.

CHAPTER THREE

EFFECTS OF ADJUVANT ARTHRITIS OVER TIME

Introduction

Rheumatoid arthritis (RA) is characterized by increased local synovial and systemic

levels of proinflammatory cytokines, which are directly involved in the disease's

pathophysiology. Increased cytokine production plays a key role in sympathetic nervous

system (SNS) activation in RA and adjuvant-induced arthritis (AA), a model for RA. The

inability to effectively process and eliminate the relevant antigen is believed to result in

RA, and eventually causes dysregulation of sympathetic outflow and the continuous

availability of high local and circulating proinflammatory cytokines. Dysregulation of the

neural signaling to the immune system, in turn helps perpetuate the disease and is also

likely to have a direct effect on bone cells.

A consistent finding in RA is increased sympathetic tone, suggesting dysregulation of

the SNS. Given the role of the SNS in maintaining homeostasis of body functions and its

role in regulating immune responses, sympathetic dysfunction is likely to contribute to the

altered bone metabolism that drives the RA. There is strong evidence that supports the

presence of sympathetic nerves in bone and joint structures (Imai et al. a, 97, Schwab et al.,

97, Cherruau et al., 03), as well as, the presence of α- and β-adrenergic receptors (AR) on

osteoblasts and osteoclasts (Takeuchi et al., 00). Drugs that block ARs, destroy

sympathetic nerves, or alter sympathetic outflow in RA patients or animal models for RA

alter bone destruction. This supports an important contribution of the SNS in altered bone metabolism that contributes to joint injury.

In vitro studies have demonstrated that catecholamines can induce osteoclast maturation and stimulate osteoclast activity via a β_2-AR-mediated mechanism (Frediani et al., 96). Further supporting evidence includes findings that osteoblasts and osteoclasts secrete diffusible axon guidance molecules that function as chemoattractants or chemorepellents for sympathetic nerve fibers (Togari 02). It has also been shown that sympathectomies, by treatment with guanethidine, increase osteoblastic activity and reduce osteoclast number and activity in rats (Cherruau et al., 03). Finally, the resorbing activity by osteoclasts, as indicated by f-actin rings and resorption pits, was substantially increased by isoprenaline (β-adrenergic agonist), moderately increased by epinephrine (an α- and β-adrenergic agonist), and poorly increased by phenylephrine (an α_1-adrenergic agonist) (Arai et al., 03), suggesting that this effect is primarily mediated via β-AR.

Neurogenic inflammation, which is mediated via both autonomic and sensory nerves, plays an essential role in the joint pathology associated with RA (Levine et al., 85). In RA, the density of nerves in the joint synovium and bone is altered with disease progression with an increase in sensory nerves and decrease in sympathetic nerves (Miller et al., 00). In the chronic stages of AA no other changes are thought to occur. The consequences of altered nerve distribution in these tissues are not entirely clear, nor is it known whether this condition persists after the inflammatory response is reported to wane.

We have explored the effects of the specific β_2-adrenergic receptor agonist, terbutaline, the α-adrenergic agonist, phentolamine, and an investigational drug, which is a combination of these, SH1293, at different stages on disease outcome using AA in Lewis

124

rats (Lubahn et al., 04). These treatments significantly decreased inflammation and improved radiographic scores, showing a general trend of improvement if treatment was started at disease onset and continued through severe disease.

Despite the SNS's role in regulating key cytokines involved in driving inflammation and reports of SNS dysfunction in RA patients (Miller et al., 00), few studies have adequately investigated joint pathology with routine histology and μCT, or sympathetic innervation of affected joints at any time points after the disease is thought to come to a halt at 60 days (Pearson and Wood 63).

The goal of this study is to investigate changes that occur in the bone after inflammatory processes in AA is reported to resolve. Our lab, which had previously used these animals to study SNS in earlier disease phases, have observed skeletal changes as far out as 18 weeks after immunization. Most studies in AA rats stop their observation at 28 days, and report that there are no further changes seen. Identifying and describing these changes seen after 28 days, will add to the current body of literature already in existence. Of particular interest to our lab is the distal tibia where the terminals of the sympathetic nerves are housed and subsequently where most of the inflammatory activity occurs.

Materials and Methods

Adjuvant.

The complete Freud's adjuvant (CFA) (0.03 g dried and heat killed *Mycobacterium butyricum* (*M. butyricum*); Difco, Detroit, MI) was emulsified in 10 ml sterile mineral oil) by grinding the *M. butyricum* with a mortar and pestle until the bacterial cell wall turns from light beige to an eggshell white powder. The mineral oil was then slowly worked into

the bacterial cell wall using the mortar and pestle. The suspension was treated with a sonic dismembraner for 5 min to ensure that the bacterial cell wall remained suspended in the mineral oil for animal injections. Treatment of animals with CFA prepared with this protocol produces arthritis in 100% of the animals, although there is variability in the severity of the disease that develops.

Animals.

Young adult male Lewis rats (200-250 gm) were obtained from Charles Rivers (Wilmington, MA). Rats were housed in plastic cages with soft CareFresh bedding (Absorption, Bellingham, WA) in the Sun Health vivarium, where they were given food (Purina Lab Diet 5001) and water *ad libitum* and placed on a 12-hours-on 12-hours-off lighting schedule. Rats were housed in the vivarium for 1 week before undergoing any manipulations. For AA rats, food was placed inside the cage, and water was supplied by using long-stemmed sipper tubes for easy access to food and water. All rats were observed to eat and drink. Animals were weighed and observed daily to ensure adequate weight gain and good general health of the animals. AA in male Lewis rats, a routinely used animal model for RA, was induced by an intradermal injection of 100 μl CFA (0.3 mg) into the base of the tail. Rats typically develop arthritis between 11 and 14 days post-challenge with CFA. To control for the effects of vehicle and stress associated with handling, to establish baseline data, and to determine disease-related effects on test parameters, control groups received the same volume of (1) mineral oil alone, (2) *M. butyricum* suspended in sterile saline, (3) sterile saline or (4) no treatment. On day 12 post-challenge rats were

randomly assigned into appropriate groups (Control or AA) until sacrifice 126 days after immunization.

Preparation of Tissues.

At sacrifice, rats were deeply anesthetized with 1.0 ml of an 8% solution of chloral hydrate in sterile saline (overdose), and then perfused transcardially at room temperature with phosphate-buffered saline (PBS) containing 0.5% sodium nitrite (pH 7.2) followed by 250 ml of 4% paraformaldehyde in the same buffer (pH 7.2). The left ankles, with soft tissue intact, from each rat were imaged using micro-computed tomography (μCT; MicroCAT II, Siemans Medical Solutions USA, Inc., PA). The right ankles from each rat were stripped of their skin and decalcified.

The decalcification procedure consisted of putting 2 liters of deionized water in a 4-liter Erlenmeyer flask. Then dissolving 280 ml ammonium hydroxide into the water and adding 490 g of ethylenediaminetetraacetate (EDTA) free acid (pH=6). Ammonium hydroxide was added to bring the pH to 7.2, and then deionized water was added to bring the volume up to 5 liters. The ankles were then placed in this solution with a magnetic stir bar and left for 5 weeks. At this time, the ankles were rinsed in deionized water for 3 min. and cut grossly from the calcaneus to the interspace between the the 2nd and 3rd phalanx. They were embedded in paraffin as two halves with the cut side down. This would allow direct access to a parasagittal plane for sectioning. They were then sectioned at 5 μm for standard histology or 16 μm for immunocytochemistry (ICC). For all regular histology sections, the tissue was mounted on Fisher Superfrost Plus slides (Statlab, Louisville, Texas). For ICC, sections were mounted on subbed slides (Vectabond reagent, Vector

Laboratories Inc, Burlingame, Ca). Tissue sections were stained to reveal specific histological features, as follows: (1) hematoxylin & eosin (H&E) for general observations and to examine lymphocytic cellular infiltration; (2) tartrate-resistant acid phosphatase (TRAP) to visualize cells of the osteoclast lineage and assess bone area; (3) toluidine blue to characterize cartilage changes; (4) Masson's green trichrome to assess pannus formation; and (5) ICC to visualize tyrosine hydroxylase (TH)-positive, sympathetic nerves. After staining, tissue sections were dehydrated through series of graded ethanol solutions, cleared with xylene, and cover slipped with Cytoseal 28 (Stephens Scientific, div. of Richard Allan Scientific, Kalamazoo, MI) for sections stained using ICC, and Acrymount solution (Statlab, Louisville, Texas) for standard histology.

TRAP staining was performed on tissue sections using a post-coupling procedure. Sections were processed through two incubation steps, one with the substrate (naphthol AS-BI phosphate). The first incubation uses this as the substrate; the second reaction attaches the unstable dye to naphthol++ to create a colored reaction product. Since most acid phosphates are inhibited by tartrate, tartrate was added to each of the incubation solutions so that only TRAP will be active.

The substrate incubation procedure was performed by combining naphthol AS-BI phosphate solution (0.1 g naphthol AS-BI phosphate with 5 ml ethylene glycol monomethyl ether) with acetic buffer solution (4.6 g sodium acetate, 5.7 g L-(+) tartaric acid, 1.4 ml glacial acetic acid and 500 ml of water) in a ratio of 1:100, the pH was then adjusted to 4.7-5.0 using either 2N HCL solution or 5M NaOH solution and left at 37 °C for 1 hour. Next, 8 ml of sodium nitrate solution (1 g sodium nitrate with 25 ml of distilled water) was mixed with 8 ml a pararosaniline solution (1g pararosaniline chloride with 20

ml 2N HCl, which was filtered and then left to react for 2 min.). This dye stock solution was mixed with 400 ml of acetate buffer solution and left to incubate for 10 min., then rinsed with deionized water. Next, the slides were counterstained with methylgreen (21.5 ml 0.02M citrate buffer, 1 ml deionized water, and 0.2 ml of stock solution consisting of 10 g methyl green with deionized water brought up to 100 ml) for 1 min. Finally, they were dehydrated through series of graded ethanol solutions, cleared with xylene, and coverslipped with Acrymount solution.

To visualize the sympathetic nerves stained for TH, the rate-limiting enzyme for the synthesis of NE, a polyclonal rabbit anti-TH antibody (1:1000) was used.   Nickel sulfate intensification of the 3,3'diaminobenzidine (0.04%; DAB) chromagen reaction product (Hancock, 1986) was used to form a blue/black reaction product in TH+ nerves. All steps were carried out in 0.15 M phosphate buffer (pH 7.4) at 25 °C using gentle agitation, unless otherwise indicated. Sections were rinsed thoroughly in buffer and incubated for 30 min in 10% normal goat serum (NGS). The anti-TH primary antibody was diluted 1:500 in 0.15 M phosphate buffer containing 0.4% Triton X-100 and 0.25% bovine serum albumin. Incubation in the primary antibody was carried out at 4 °C for 24 h. Control sections were incubated in 0.15 M phosphate buffer in the absence of the primary antibody.

On day 2, sections were rinsed 6 x 10 min in PBS, and incubated for 30 min in 10% NGS, and then incubated in the secondary goat anti-rabbit antibody (Vector Elite kit) diluted in buffer (1:2,000 for 90 min. Sections then were rinsed 4 x 10 min in buffer and incubated in 2.5% methanol with 8% hydrogen peroxide for 30 min to remove endogenous peroxidase activity. Following 6 x 10 min rinses, sections were incubated in an avidin-biotin-peroxidase complex (ABC) (Vector Elite kit; 1:4,000 dilution in buffer) for 90 min.

Sections were rinsed 4 x 10 min in PBS buffer, followed by 2 x 10 min in 0.05 M acetate-imidazole buffer, pH 7.2, and then developed in acetate-imidazole buffer containing 0.25 g/100 ml nickel (II) sulfate, 0.04 g/100 ml DAB, and 0.005% hydrogen peroxide for 15 to 20 min. All sections then were rinsed 2 x 10 min in acetate-imidazole buffer, followed by 4 x 10 min rinses in phosphate buffer. Then the slides were coverslipped as described above.

<div align="center">3-D image analysis using μCT</div>

With 3-D imaging methods available in the μCT machine, the left ankles from each animal were used to determine tibial bone volume within a region of interest (ROI) using an Amira software program (Visage Imaging, Inc., Carlsbad, CA). The imaging equipment consisted of a 80keV X-ray source. The μCT's camera used a 2048^2 matrix, 4x4 binning with an exposure time of 200 ms. The x-ray parameters were 75 kVp at 100 μA with a 0.5 mm Al filter. The CT scan included 360 rotation steps for a total scan time of 10:45 min. The reconstructed image was 512^3 for a voxel size of 0.126^3 μm.

The distal tibias were evaluated for thickness by quantifying the number of slices from medial to lateral. From this measurement, the middle of the tibia was determined. By using the Point Probe function in the Amira program, it was possible to discern a difference between bone and soft tissue by setting its threshold to 2900. This was accomplished by selecting a spherical ROI with a radius of 1 mm just proximal to the apex of the distal articular cartilage in the middle slice.

Morphometric Analysis of Histologically-Stained Tissue

TH-stained sections were evaluated with Image-Pro Plus® software, version 5.0 (Media Cybernetics, Inc., Silver Spring, MD, USA). TH-stained nerves were identified by the presence of nickel-DAB chromagen and nerve density in the distal tibia and capsule. A percentage of TH stained pixels was obtained from the total pixels in the sample sites.

In H&E-stained tissue, the overall infiltration of lymphocytes throughout the whole ankle section was examined. An example of the overall infiltration is demonstrated in the distal tibia in figure 1B, in black. Cellular infiltration was evaluated using a grading scale of + (1 plus), ++ (2 plus), or +++ (3 plus), representing low cellular infiltration (<300 lymphocytes), moderate cellular infiltration (~300 to 600 lymphocytes), or high cellular infiltration (>900 lymphocytes).

Images from trichrome sections were captured by digital photography with an Olympus BH-2 microscope and analyzed with the Image-Pro Plus® software. Trichrome-stained images were used to determine the percentage of pannus in the bone compared with the total tissue. An example of the sites from which the anterior tibial joint capsule was sampled is demonstrated in figure 1A, in blue.

For the toluidine blue-stained tissue sections, the articular cartilage of the whole distal tibia and foot was analyzed for the percentage of cartilage present using the Image-Pro Plus program. An example of this area is demonstrated in figure 1B, in light blue.

The TRAP-stained sections were observed for bone area and analyzed with the semiautomated OsteoMeasure image analysis system (OsteoMetrics, Inc., Atlanta, GA) and digitizing pad. Three sample sites (zones 1 through 3), each consisting of a 350 x 350 μm^2 area, were examined from the distal tibia of each rat. Zone 1 (Figure 1A, in red),

encompassed tibial articular cartilage/cartilage remnants and the subchondral bone located proximally. Zone 2 (in red) encompassed any subchondral bone and trabecular bone. Zone 3 (in red), encompassed the trabecular bone located most superiorly in the sampling site. The bone that was present in each zone was outlined using the digitized pad and the area was then computed using the program. Osteoclasts were also counted in these zones. They were tagged and quantified with the digitized pad so they were not counted twice.

The examiner of all the histology was blinded to the treatment groups. Where appropriate, histological data were expressed as a mean $\pm$ SEM and treatment groups compared using one variable, one-way analysis of variance (ANOVA) with subsequent post-hoc comparison performed using the Tukey method for significant differences ($p<0.05$). Statistical analyses revealed there was no difference between any of control groups. So for the purposes of this study, all these groups have been collapsed into one group that will be designated as our control group.

Results

Sympathetic Nerves

The control animals showed a mean of 0.17% of the total pixels sampled ($\pm$ 0.022945%) were TH-stained nerves. The AA animals showed a mean of 0.0038% of the pixels sampled ($\pm$ 0.003083%, $p<0.0005$) were TH-stained nerves. The AA rats showed a significant decrease in sympathetic nerves compared with control rats (Figure 8). There were no corelations with any other variable.

Bone Volume

The mean bone volume of the control rats was 4,645.71 voxels per sphere ($\pm$ 21.33). The mean bone volume of the AA rats was 3,133.05 voxels per sphere ($\pm$ 181.19, $p<0.0001$). The 2 animals with increased activity displayed scores of 3,158.28 and 3,292.92. The AA rats showed a significant decrease in bone volume compared with control rats (Figure 9). There were no significant correlations between any other variables. AA rats showed a decrease of 32.56% bone volume compared with controls.

Lymphocyte Infiltration

The mean lymphocyte score for control rats was 1.0 ($\pm$ 0). The mean lymphocyte score for the AA rats was 1.6 ($\pm$ 0.42, $p<0.0007$). The AA rats showed a significant increase in lymphocytes compared with control rats (Figure 10). The majority of the lymphocytes were found in two of the six subjects where each animal scored a 3. The lymphocytes showed a significant ($p<0.05$) positive correlation with osteoclasts (0.81). AA rats also showed a 62.5% increase in lymphocyte score.
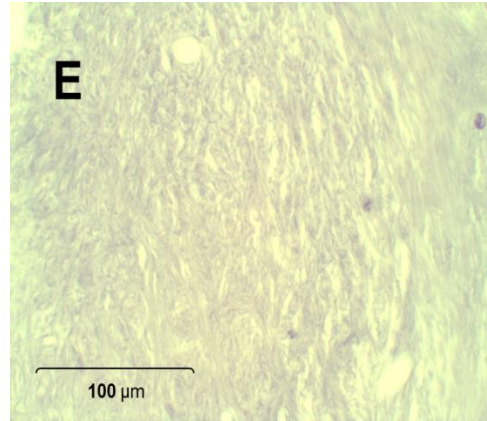
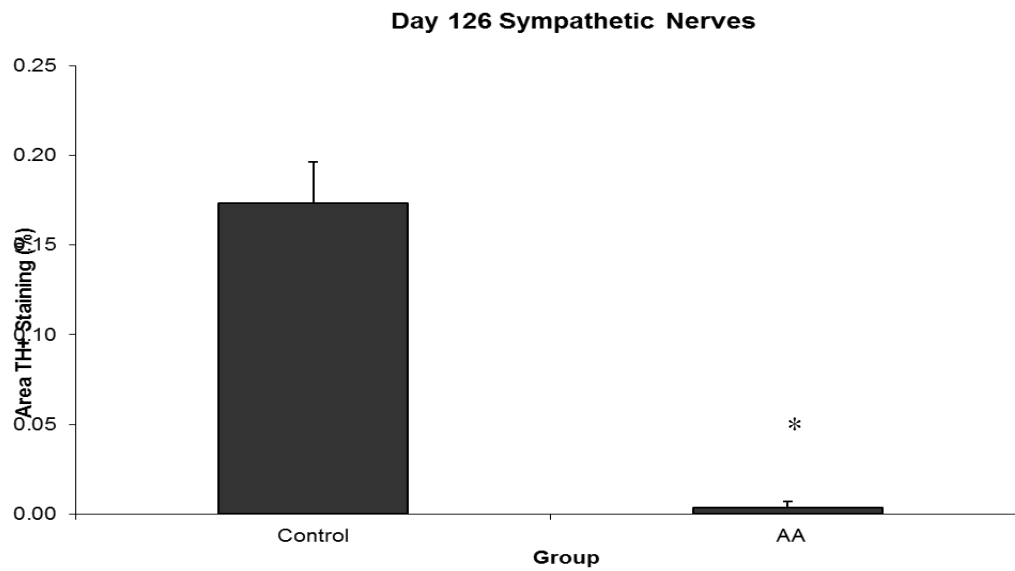Figure 8A. TH+ Nerve Density in the Distal Tibia at 126 Days. No TH+ staining in capsule.

Figure 8B. * AA rats showed a significant decrease ($p<0.05$, n=5) in nerves compared to the Control rats (n=10).
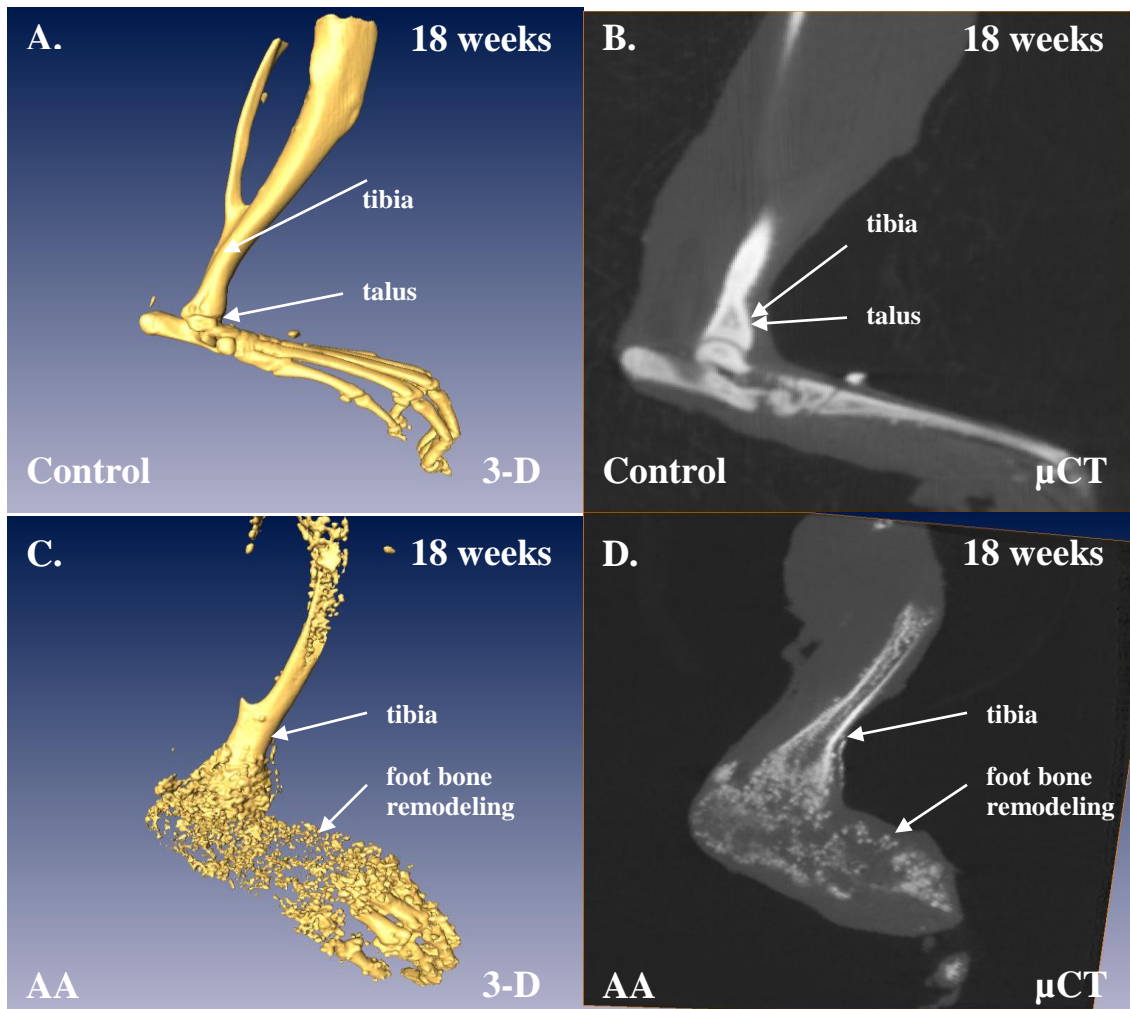
Figure 9. µCT imaging of the ankle at 126 Days A.-D.
A. An 18 week control rat 3-D reconstruction demonstrating the preservation of the tibia and foot bones.
B. An 18 week control rat µCT demonstrating the preservation of the tibia and foot bones
C. An 18 week AA rat 3-D reconstruction demonstrating the complete remodeling of the distal tibia and foot bones.
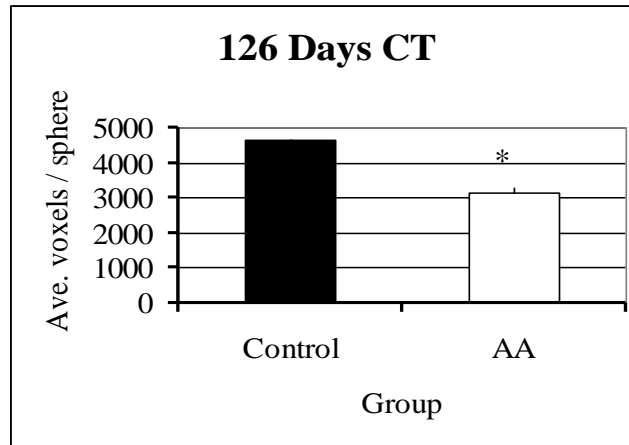D. An 18 week AA rat µCT demonstrating the complete remodeling of the distal tibia and foot bones.

Figure 9 E. *AA rats showed a significant decrease in bone volume (*p*<0.0001, n=7) compared with the control rats (n=30).
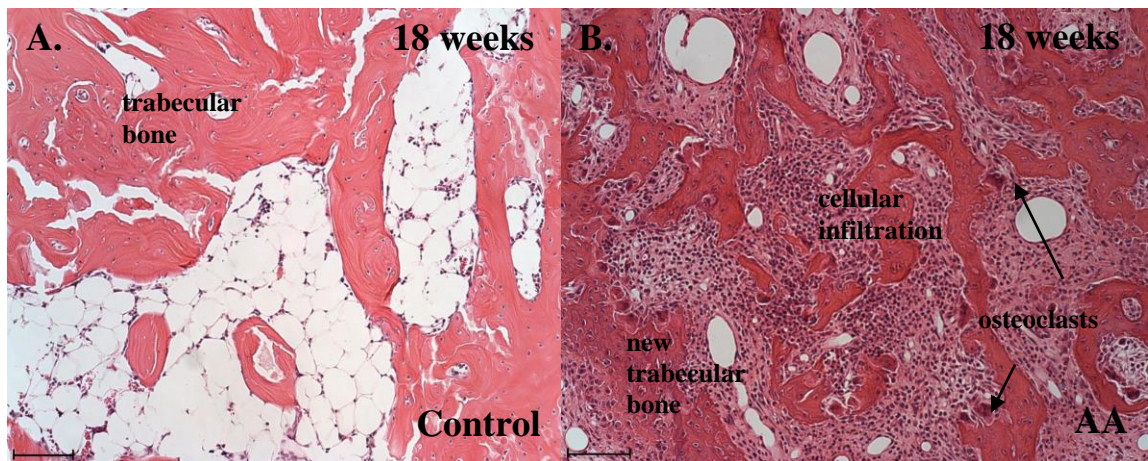

Figure 10. Inflammatory Cell Infiltration at 126 Days A. and B.
A. An 18 week control rat demonstrating the lack of inflammatory cells.
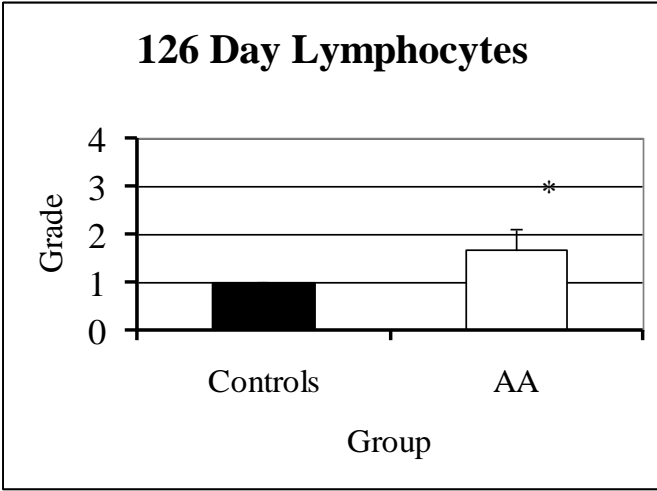B. An 18 week AA rat demonstrating the severe infiltration of inflammatory cells.

Figure 10 C. *AA rats showed a significant increase (*p*<0.0007, n=6) in lymphocytes compared with the Control rats (n=30).

Pannus Development

The mean percentage of pannus for control rats was 18.32 ($\pm$ 1.40). The mean percentage of pannus for AA rats was 48.53 ($\pm$ 3.76, $p<0.0001$). AA rats showed a significant increase in pannus formation (Figure 11). In the 2 animals that showed an increase in cellular activity there was no increase in pannus formation compared with the group that showed no increase in cellular activity. There were no significant correlations between any of the other variables. AA rats has a 265.0% increase in pannus development.

Articular Cartilage Area

Control rats had a mean articular cartilage percentage of 15.21% ($\pm$ 0.81). AA rats showed a mean articular cartilage percentage of 3.24% ($\pm$ 0.94, $p<0.0001$), and was significantly decreased compared with controls (Figure 12). One of the active animals showed an increased amount of cartilage compared to the the rest of the animals in this treatment group, with a percentage of 7.91. There were no significant correlations between any of the other variables. AA rats displayed a reduced percentage (78.7%) in articular cartilage compared with controls.

TRAP

The mean bone area for the control rats was 0.291 mm^2 ($\pm$ 0.028) (Figure 13). The mean bone area for the AA rats was 0.126 mm^2 ($\pm$ 0.105, $p<0.0001$), and was significant decreased compared with controls. The 2 animals showing the most activity displayed a bone area of 0.018 mm^2 and 0.101 mm^2. There was no correlation with any other variable. AA rats lost 57% of bone area compared with the controls.

The mean osteoclast count for control animals was 0.138 cells per three zones ($\pm$ 0.44). The mean osteoclast count for the AA animals was 11.16 cells per 3 zones ($\pm$ 20.54, $p<0.0004$). A significant increase in osteoclasts was found in AA rats compared with controls. Again, the same two animals that showed the most lymphocytic infiltration also had all the osteoclast activity with counts of 51 and 16. There was a strong correlation between osteoclast number and lymphocytic infiltration (0.81). There was a 98.77% increase in osteoclast activity in AA rats.
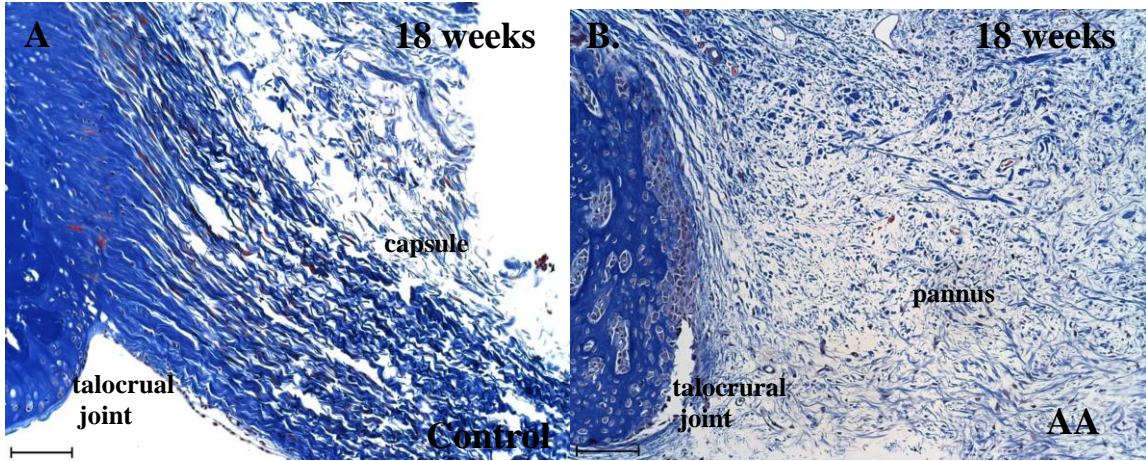
Figure 11. Pannus Formation at 126 Days A and B.
A. An 18 week control rat demonstrating the lack of pannus development.
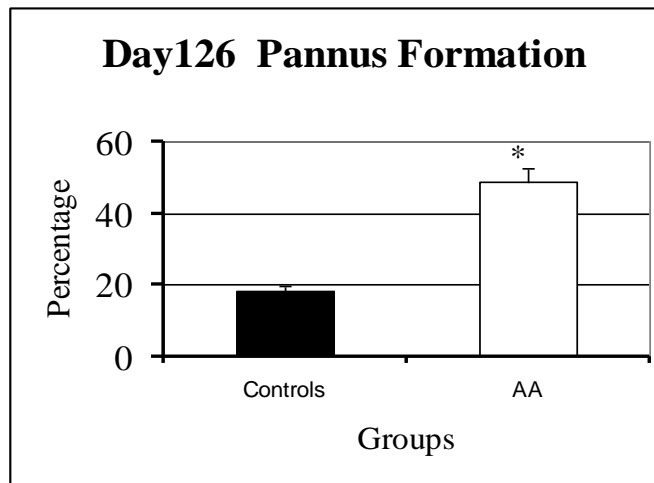B. An 18 week AA rat demonstrating capsular degradation and severe pannus development.

Figure 11 C. AA rats showed a significant increase ($p<0.0001$, n=6) in pannus formation compared to the Control rats (n=28).
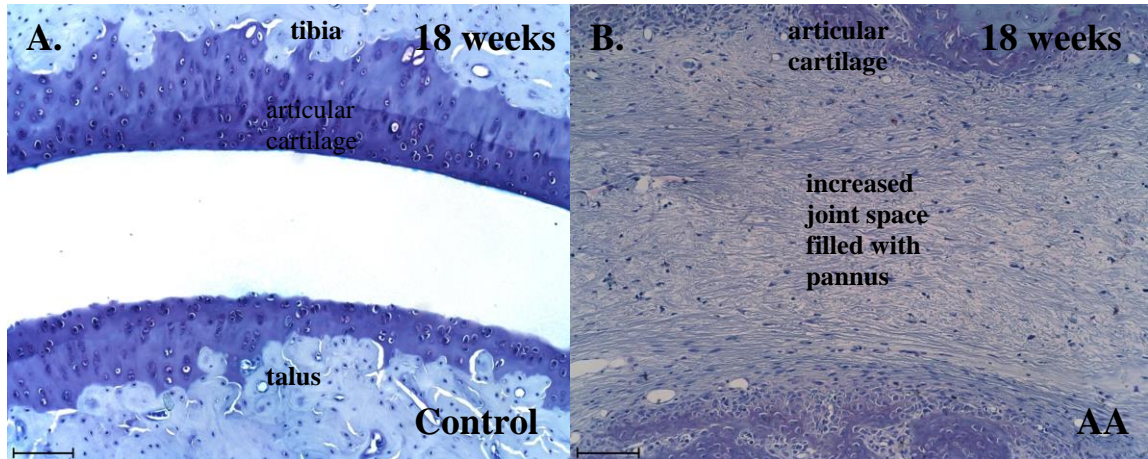
Figure 12. Talocrural Joint Articular Cartilage at 126 Days A. and B.
A. An 18 week control rat demonstrating the presence of articular cartilage on the tibia and talus.
B. An 18 week AA rat demonstrating articular cartilage degradation with an increased joint space.
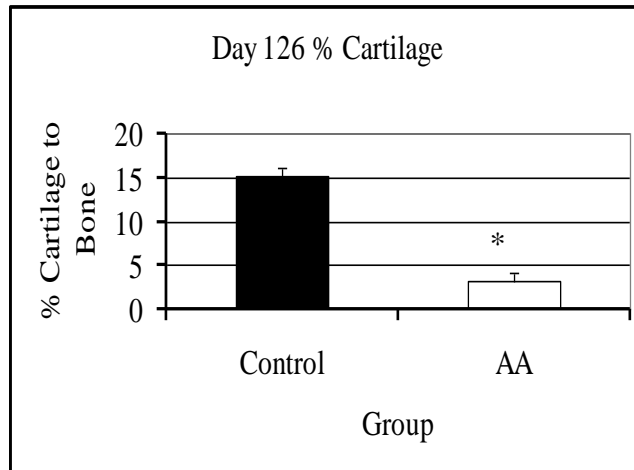

Figure 12 C. * AA rats showed a significant decrease in percentage of articular cartilage ($p<0.0001$, n=6) compared to the Control rats (n=26).
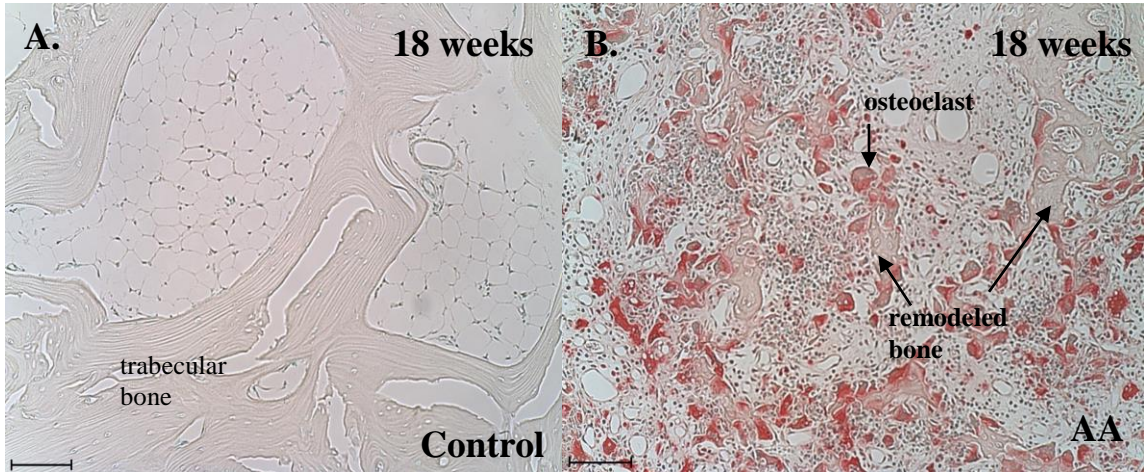
Figure 13. TRAP+ Staining for Osteoclasts in the Distal Tibia at 126 Days A. and B.
A. An 18 week control rat demonstrating intact trabecular bone and the lack of osteoclasts.
B. An 18 week AA rat demonstrating the severe bone resorption of remodeled bone and the increased presence of osteoclasts.

Figure 13 C. * The AA rats show a significant decrease ($p<0.0001$, n=6) in bone area compared to the Control rats (n=29).
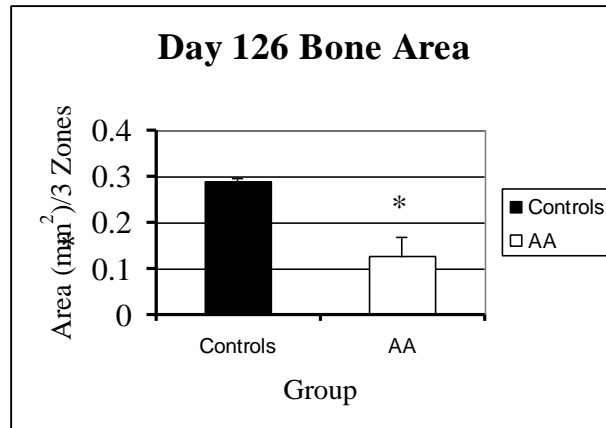
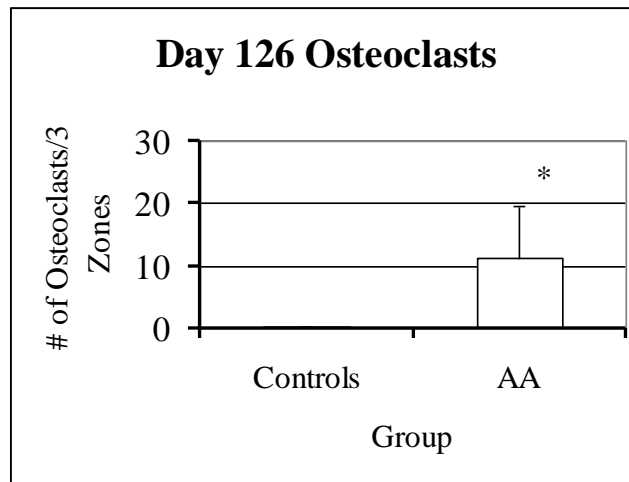Figure 13 D. * The AA rats showed a significant increase (*p*<0.0004, n=29) in osteoclast # compared with the control rats (n=6).

Discusion

Some AA animals showed increased inflammatory activity compared with other animals whose cellular infiltration was minimal. In the animals that demonstrated cellular activity, osteoclast activity/number, and lymphocyte activity were present together. However, the sampling sites for the nerve data acquisition did not demonstrate this remarkable change. The increased lymphocyte activity may be due to the sympathetic nerve density increase not captured in this particular method of assessment. As the concentration of NE increases, this neurotransmitter stimulates the lymphocytes to release more cytokines and activate more osteoclasts.

As the osteoclasts resorb bone, more bone is being laid down at the same time, even though osteoblasts are few at this time (Pearson and Wood 1963). Some of it is cartilage like, as evident on one of the animals with increased cell activity who demonstrated a 7.91% cartilage score, which was well above the average. In more than just this one animal, there were small clusters of cartilage, perhaps new bone that had not been calcified yet, scattered throughout the bone. This cartilage was not limited to the ends of the articular surface; it was dispersed though out the bone's length. This finding is consistent with Pearson and Wood's observations who demonstrated immature cartilage often surmounted the osteoid layer.

Even though the AA animals gross appearance of the ankle / foot complex looks larger, the number of bone voxels was less than the controls. Some of the size difference may be due to pannus formation. Our lab has previously investigated earlier time points at 14, 21 and 28 days and found that the intense osteoclast response occurs early on and osteoblast activity cannot keep up with the pace. However, at around 21 days, new bone is

144

formed. It looks as if this remodeling continues well into the 126th day, but now at a slower pace. Just as in the earlier time points, the bones at 126 days do not display cortical bone. It is made up of entirely what looks like trabecular bone. This differs from Pearson and Wood's (1963) observations of this new bone looking more like cortical bone. There is an attempt to repair the bone and articular complex in AA animals, but it does not return to the same morphology; instead it seems to form a fused, trabecular bone/ankle/foot complex. According to Pearson and Wood (1963) this is ankylosing is from the fibrous pannus.

There was no general trend, as we have seen in earlier time points, of proximal to distal resorption activity. The cellular activity here seems to be random in different areas / clusters in the bone. The presence of osteoclasts correlated with the lymphocytic infiltration as described above. There are also sympathetic nerves that are present in these areas of osteoclasts and lymphocytes, but they were unable to be detected by our sampling site.

Robust staining of the sympathetic nerves was present outside the sampling site, which was evident along the trabecular bone / cartilage interface of the tibia in the animals with high cellular activity in the AA group, which demonstrated the increased bone remodeling. There was a decrease in the robustness of the TH stain in the AA animals that did not show any cellular activity. The presence of this reinnervation in AA rats with high cellular activity strongly suggests an increase in NE concentration which may promote recruitment of lymphocyte into the joint. The presence of these nerves and cells causes an increased cytokine concentration and therefore osteoclast presence and bone resorption.

The sympathetic nerve signaling inhibits bone formation via β2-AR on osteoblasts (Elefteriou, 2008), it mediates the effects of hypothalamic leptin-induced inhibition of bone formation via a β2-AR-mediated mechanism (Elefteriou, 2008). Catecholamines affect regulatory proteins produced by osteoblasts and osteoclasts, including osteocalcin. Osteocalcin, an extracellular calcium-binding protein, is synthesized by osteoblasts and binds with high specificity to bone mineral crystals to promote bone formation. Absent sympathetic neural function following sympathetic ganglia blockade increased osteocalcin levels by 50%. NE helps regulate and release osteocalcin from bone (Takeuchi et al, 2000). The sympathetic nervous system also affects osteoclasts by impairing resorption, reducing the number of osteoclasts, impairing osteoclast access to the bone surface, and decreasing TRAP+ mononuclear preosteoclasts (Cherruau et al., 2003). These findings support a role for the SNS in regulating osteoclast differentiation and bone resorption.

The IL-1 and TNF-α strongly stimulate chemokine release by osteoblasts which could directly or indirectly effect bone remodeling mechanisms and cartilage destruction. This suggests that osteoblasts have a primary role capable of regulating autocrine / paracrine circuits that affect bone remodeling in RA (Lisignoli et al, 2003; Zini et al 2003). Indirect effects of bone resorption comes from of TNF-α and IL-1's effect on osteoblasts which compromise the cell-cell adhesion of osteoblasts which cover the bone surface which facilitates the direct adhesion of osteoclasts on the calcified bone matrix surface (Tsutsumimoto et al., 1999). This suggests that proinflammatory cytokines from inflammatory cells can modulate the signaling pathway of osteoblasts involved in bone remodeling and that the proinflammatory factors released in the bone marrow constantly

146

act on osteoblasts modulating gene expression and upregulates chemokine expression
resulting in an inflammatory response (Zini et al, 2003).

By studying the gross morphology of the rat ankle foot complex, it appears to be
quite larger than the controls and therefore have more bone. After observing the TRAP
bone area data, and the CT bone volume data, and the pannus data, the increased size of the
gross appearance looks to be due to pannus development and not bone formation alone.
This is substantiated by Pearson and Wood's observations (1963). Cartilage is not a factor
since it is nearly gone. The AA rats showed a decrease in bone volume per sample site.
One limitation of the study was that the whole bone was not measured, so it is possible that
there was circumferential growth that was not accounted for.

Conclusion

In conclusion, it is evident that there is still cellular activity into the chronic stages of
the disease when the disease is thought to be quiescent. Other authors have commented on
persistant active arthritis at levels of 25% in their samples. Our observations demonstrate a
similar 33.3% have continued flairs. These small or occasionally large foci can continue
up to the twelfth month (Pearson and Wood 1963). These flairs continue to give rise to
more bone remodeling and density changes. It seems the disease is episodic in nature and
does not cease its activity as previously thought. What is new in our study is that even
though these flairs do not correlate with the sampling site of where we obtained our
sympathetic nerve data, further investigation reveals that there are areas in the proximity
that demonstrate the regrowth of sympathetic nerves. This demonstrates the probability

that sympathetic nerves, bone cells and lymphocytes work together in order to remodel

bone in this chronic stage of the disease.

REFFERENCES

Adam C., Llorens A., Baroukh B., Cherruau M., and Saffar L. (2000) Effects of capsaicin induced sensory denervation on osteoclastic resorption in adult rats. Experimental Physiology ., 85.1, 61-66.

Adamopoulos I., Sabokbar A., Wordsworth B., Carr A., Ferguson D., Athanasou N. (2006) Synovial fluid macrophages are capable of osteoclast formation and resorption. Journal of Pathology, 208, 35-43.

Ahmed M., Bjurholm A., Schultzberg M., Theodorsson E., Kreicbergs A. (1995) Increased levels of substance P and calcitonin gene-related peptide in rat adjuvant arthritis. A combined immunohistochemical and radioimmunoassay analysis. Arthritis and Rheumatism ., 38, 699-709.

Aitken S., Landao-Bassonga E., Ralston S., Idris A. (2009) β2-Adrenorecptor ligands regulate osteoclast differentiation in vitro by direct and indirect mechanisms. Archives of Biochemistry, 482, 96-103.

Akiyama T., Mori S., Mashiba T., Miyamoto K., Komatsubara S., Cao Y., Manabe T., Norimatsu H., Dobashi H., Tokuda M. (2005) Incadronate disodium inhibits joint destruction and peri articular bone loss only in the early phase of rat adjuvant-induced arthritis. Jurnal of Bone Mineral Metabolism., 23, 295-301.

Akopian A., Demulder A., Ouriaghli F., Corazza F., Fondu P., Bergmann P. (2000) Effects of CGRP on human osteoclast like cell formation: a possible connection with the bone loss in neurological disorders. Peptides, 21, 559-564.

Arai M., Nagasawa T., Koshihara Y., Yammamoto S., Togari A. (2003) Effects of β adrenergic agonists on bone-resorbing activity in human osteoclast-like cells. Biochemica et Biophysica Acta., 1640, 137-142.

Badger A., Griswold D., Kapadia R., Blake S., Swift B., Hoffman S., Stroup G., Webb E., Reiman D., Gowen M., Boehm J., Adams J., Lee J. (2000) Disease-modifying activity of SB 242235, a selective inhibitor of p38 mitogen-activated protein kinase, in rat adjuvant-induced arthritis. Arthritis & Rheumatism., 1, 175-183.

Baldock P., Sainsbury A., Allison S., Lin E., Couzens M., Boey D., Enriquez R., During M., Herzog H., Gardiner E. (2005) Hypothalamic Control of Bone Formation: Distinct Actions of Leptin and Y2 Receptor Pathways. Journal of Bone and Mineral Research, 20 (10), 1851-1857.

Beckman N., Falk R., Zurbrugg S., Dawson J., Engelhardt P. (2003) Macrophage infiltration into the rat knee detected by MRI in a model of antigen-induced arthritis. Magnetic Resonance in Medicine., 49, 1047-1055.

Bekkelund SI, Jorde R, Husby G, Mellgren SI. (1996) Autonomic nervous system function in rheumatoid arthritis. A controlled study. Journal of Rheumatology., 23(10), 1710-4.

Bezerra M., Carvalho J., Prokopowitsch A., Pereira R. (2005) RANK, RANKL and osteoprotegerine in arthritic bone loss. Brazilian Journal of Medical and Biological Research, 38, 161-170.

Bezooijen R., van der Wee-Pals L., Papapoulos S., Lowik C. (2002) Interleukin 17 synergises with tumour necrosis factor α to induce cartilage destruction in vitro. Annals of the Rheumatic Diseases., 61, 870-876.

Biroc S., Gay S., Hummel K., Magill C., Palmer J., Spencer D., Sa S, Klaus J., Micheal B., Rasnick D., Gay R. (2001) Cysteine protease activity is up regulated in inflamed ankle joints of rats with adjuvant-induced arthritis and decreases with in vivo administration of a vinyl sulfon cysteine protease inhibitor. Arthritis and Rheumatism, 44(3), 703-711.

Boyle D., Moore J., Yang L., Sorkin L., Firestein G. (2002) Spinal adenosine receptor activation inhibits inflammation and joint destruction in rat adjuvant-induced arthritis. Arthritis and Rheumatism, 46 (11), 3076-3082.

Brown S., Meyers R., Brennan K., Rumble J., Narasimhachari N., Perozzi E., Ryan J., Stewart J., Fischer-Stenger K. (2003) Catecholamines in a macrophage cell line. Journal of Neuroimmunology., 135, 47-55.

Bulling D., Kelly D., Bond S., McQueen D., Sedkl J. (2001) Adjuvant-induced joint inflammation causes very rapid transcription of β-preprotachykinin and α-CGRP genes in innervating sensory ganglia. Journal of Neurochemistry, 77, 372-382.

Buma P., Elmans L., Van Den Berg WB., Schrama LH. (2000) Neurovascular Plasticity in the knee joint of an arthritic mouse model. The Anatomical Record, 260: 51-61.

Cherruau M., Morvan F., Schirar A., Saffar J. (2003) Chemical sympathectomy-induced changes in TH-, VIP-, and CGRP-immunoreactive fibers in the rat mandible periosteum: influence on bone resorption. Journal of Cellular Physiology, 194, 341-348.

Chillingworth, N., Donaldson L. (2003) Characteristics of Freund's complete adjuvant-induced model of chronic arthritis in mice. Journal of Neuroscience Methods, 128, 45-52.

Conway J., Wakefield J., Brown R., Marron B., Sekut L., Stimpson S., McElroy A., Menius A., Jeffery J., Clark R., McGeehan C. (1995) Inhibition of cartilage and bone destruction in adjuvant arthritis in the rat by a matrix metalloproteinase inhibitor. Journal of Experimental. Medicine, 182, 449-457.

Crosby LJ. (1988) Stress factors, emotional stress and rheumatoid arthritis disease activity. Journal of Advanced Nursing., 13(4), 452-61.

Cornish J., Callon K., Bava U., Kamona S., Cooper G., Reid I. (2001) Effects of calcitonin, amylin, and calcitonin gene related peptide on osteoclasts development. Bone, 29 (2), 162-168.

Cutolo M., Bijlsma J., Lahita R., Masi A., Straub R., Bradlow H. (2002) Altered neuroendocrine immune networks in rheumatology. Annals of the NewYork Acadamy of Sciences., 966: xiii-xviii.

Cutolo M., Straub RH. (2008) Circadian rhythms in arthritis: hormonal effects on the immune/inflammatory reaction. Autoimmunity Reviews. 7(3), 223-8.

Danks L., Sabokabar A., Gundle R., Athanasou N. (2002) Synovial macrophage-osteoclast differentiation in inflammatory arthritis. Annals of Rheumatic Diseases., 61, 916-921.

Di Comite G., Grazia Sabbadini M., Corti A., Rovere-Querini P., Manfredi AA. (2007) Conversation galante: how the immune and the neuroendocrine systems talk to each other. Autoimmunity Reviews., 7(1), 23-9.

Di Comite G., Rossi CM. (2007) Risk of diabetes in patients with rheumatoid arthritis taking hydroxychloroquine. The Journal of the American Medical Association., 298(20), 2368-9; author reply 2369-70.

DiPaola R., Cuzzocrea S. (2008) Predictivity and sensitivity of animal models of arthritis. Autoimmunity Reviews, 8, 73-75.

Edmonds ME., Saunders A., Sturrock RD. (1979) Rheumatoid arthritis associated with hypoparathyroidism and Sjögren's syndrome. Journal of the Royal Society of Medicine., 72(11), 856-8.

Elefteriou F. (2005) Neuronal signaling and the regulation of bone remodeling. Cellular and Molecular Life Sciences, 62, 2339-2349.

Elefteriou F. (2008) Regulation of bone remodeling by central and peripheral nervous sytem. Archieves of Biochemistry and Biophysics., 473, 231-236.

El-Sayed ZA., Mostafa GA., Aly GS., El-Shahed GS., El-Aziz MM., El-Emam SM. (2009) Cardiovascular autonomic function assessed by autonomic function tests and serum autonomic neuropeptides in Egyptian children and adolescents with rheumatic diseases. Rheumatology (Oxford). 48(7), 843-8.

Fassbender HG. 1975. Pathology of Rheumatic Diseases Heidelberg: Springer-Verlag.

Fassbender HG. (1983) Histomorphological basis of articular cartilage destruction in rheumatoid arthritis. Collagen and Related Research., 3, 141-155.

Frediani U., Becherini L., Lasagni L., Tanini A., Brandi M. (1996) Catecholamines modulate growth and differentiation of human preosteoclastic cells. Osteoporosis. International., 1, 14-21.

Goulet R., Goldstein S., Ciarelli M., Kuhn J., Brown M., Feldkamp L. (1994) The relationship between the structural and orthogonal compressive properties of trabecular bone. Journal of Biomechanics, 27 (4), 375-389.

Gradaigh D., Ireland D., Bord S., Compston J. (2004) Joint erosion in rheumatoid arthritis: interactions between tumour necrosis factor α, interleukin 1, and receptor activator of nuclear factor kB ligand (RANKL) regulate osteoclasts. Annals of Rheumatic Disease., 63, 354-359.

Greenfield E., Horowitz M., Lavish S. (1996) Stimulation by parathyroid hormone of interleukin-6 and leukemia inhibitory factor expression in osteoblasts is an immediate-early gene response induced by cAMP signal transduction. Journal of Biological Chemistry, 271 (18), 10984-10989.

Hadler N. (1976) A pathogenetic model for erosive synovitis. Arhritis and Rheumatism, 19 (2) 256-273.

Hanson N., Bagi C. (2004) Alternative approach to assesement of bone quality using micro-computed tomography. Bone, 35, 326-333.

Harle P., Straub R., Wiest R., Mayer A., Schölmerich J., Atzeni F., Carrabba M., Cutolo M., Sarzi-Puttini P. (2006) Increase of sympathetic outflow measured by neuropeptide Y and decrease of the hypothalamic‐pituitary‐adrenal axis tone in patients with systemic lupus erythematosus and rheumatoid arthritis: another example of uncoupling of response systems. Annals of Rheumatic Diseases, 65 (1), 51-56.

Heijnen C., van der Voort C., Wulffraat N., van der Net J., Kuis W., Kavelaars A. (1996) Journal of Neuroimmunology, 71, 223-226.

Hirayama T., Danks L., Sabokbar A., Athanasou N. (2002) Osteoclast formation and activity in the pathogenesis of osteoporosis in rheumatoid arthritis. Rheumatology, 41, 1232-1239.

Hogarth MB., Judd L., Mathias CJ., Ritchie J., Stephens D., Rees RG. (2002) Cardiovascular autonomic function in systemic lupus erythematosus. Lupus. 11(5), 308-12.

Hood V., Cruwys S., Urban L., Kidd B. (2001) The neurogenic contribution to synovial leucocyte infiltration and other outcome measures in a guinez pig model of arthritis. Neuroscience Letters, 299, 201-204.

Hopkins SJ., Rothwell NJ. (1995) Cytokines and the nervous system. I. Expression and recognition. Trends in Neurosciences., 18, 83-87.

Imai S., Matsusue Y. (2002) Neuronal regulation of bone metabolism and anabolism: calcitonin gene-related peptide-, substance P-, and tyrosine hydroxylase-containing nerves and the bone. Microscopy Research and Technique, 58, 61-69.

Imai S., Rauvala H., Konttinen Y., Tokunaga T., Maeda T., Hukuda S., Santavirta S. (1997) Efferent targets of osseous CGRP immunoreactive nerve fiber before and after bone destruction in adjuvant arthritic rat: an ultramorphological study on their terminal target relations. Journal of Bone Mineral Research., 12 (7), 1018-1027.

Imai S., Tokunaga Y., Maeda T., Kikkawa M., Hukuda S. (1997) Calcitonin gene related peptide, substance P, tyrosine hydroxylase immunoreactive innervation of rat bone marrows: an immunohistochemical and ultrastructural investigation on possible efferent and afferent mechanisms. Journal of Orthopedic. Research., 15, 133-140.

Imboden J., The Immunopathogenisis of Rheumatoid Arthritis. The Annual Review of Pathological Mechanisms of Disease, 4, 417-434.

Ishikawa T., Nishigaki F., Miyata S., Hirayama Y., Minoura K., Imanishi J., Neya M., Mizutani T., Imamura Y., Ohkubo Y., Mutoh A. (2005) Prevention of progressive joint destruction in adjuvant induced arthritis in rats by a novel matrix metalloproteinase inhibitor, FR217840. European Journal of Phamacology, 508, 239-247.

Itonaga I., Fujikawa Y., Sabokbar A., Murry D., Athanasou N. (2000) Rheumatoid arthritis synovial macrophage-osteoclast differentiation is osteoprotegerin ligand dependent. Journal of Pathology, 192, 97-104.

Iwanaga T., Schikichi M., Kitamura H., Yanase H., Nozawa-Inoue K. (2000) Morphology and functional roles of synoviocytes in the joint. Archives of Histolology and Cytology, 63 (1), 17-31.

Jimi E., Aoki K., Saito H., D'Acquisto F., May M., Nakamura I., Sudo T., Kojima T., Okamoto F., Fukushima H., Okabe K., Ohya K., Ghosh S. Selective inhibition of NF-kB blocks osteoclastogenesis and prevents inflammatory bone destruction in vivo. Nature Medicine, 10 (6), 617-624.

Kawahito Y., Kondo M., Tsubouchi Y., Hashiramoto A., Bishop-Bailey D., Inoue K., Kohno M., Yamada R., Hla T., Sano H. (2000) 15-deoxy-$\Delta^{12,14}$-PGJ$_2$ induces synoviocyte apoptosis and suppresses adjuvant-induced arthritis in rats. The Journal of Clinical Investigation, 106 (2), 189-197.

Kidd B., Mapp P., Gibson S. (1989) A neurogenic mechanism for symmetrical arthritis. Lancet, 11, 1128-1130.

Klippel J. 2001. Primer on the Rheumatic Diseases. 12 ed. Atlanta, Georgia.

Kondo A., Togari A. (2003) In vivo stimulation of sympathetic nervous system modulates osteoblastic activity in mouse calvaria. American Journal of Physiology: Endocrinology and Metabolism., 285, E661-E667.

Konttinen Y., Imai S., Suda A. (1996) Neuropeptides and the puzzle of bone remodeling. Acta Orthopaedica Scandinavica ., 67 (6), 632-639.

Kotake S., Udagawa N., Takahashi N., Matsuzaki K., Itoh K., Ishiyama S., Saito S., Inoue K., Kamatani N., Gillespie M., Martin T., Suda T. (1999) IL-17 in synovial fluids from patients with rheumatoid arthritis is a potent stimulator of osteoclastogenesis. The Journal of Clinical Investigation, 103 (9), 1345-1352.

Kuratani T., Nagata K., Kukita T., Hotokebuchi T., Nakasima A., Iijima T. (1998) Induction of abundant osteoclast-like multinucleated giant cells in adjuvant arthritic rats with accompanying disordered high bone turnover. Histology and Histopathology., 13 (3), 751-759.

Levine JD., Coderre JT., Helms C., Basbaum AI. (1988) β_2-Adrenergic mechanisms in experimental arthritis. Proceedings of the National Academy of Sciences . USA., 4553-4556.

Levine JD., Dardick SJ., Roizen MF., Helms C., Basbaum AI. (1986) Contribution of sensory afferents and sympathetic efferents to joint injury in experimental arthritis. Journal of Neuroscience., 6, 3423-3429.

Lisignoli G., Toneguzzi S., Pozzi C., Piacentini A., Riccio M., Ferruzzi A., Gualtieri G., Facchini A. (1999) Proinflammatory cytokines and chemokine production and expression by human osteoblasts isolated from patients with rheumatoid arthritis and osteoarthritis. Journal of Rheumatology., 26, 791-799.

Lisignoli G., Toneguzzi S., Grassi F., Piacentini A., Tschon M., Cristino S., Gualtieri G., Facchini A. (2003) Different chemokines are expressed in human arthritic bone

biopsies: IFN-γ and IL-6 differently modulate IL-8, MCP-1, and RANTES production by arthritic osteoblasts. Cytokine, 20, 231-238.

Lorton D., Lubahn CL., Bellinger DL. (2003) Potential use of drugs that target neural-immune pathways in the treatment of rheumatoid arthritis and other autoimmune diseases. Current Drug Targets Inflammation Allergy, 2, 1-30.

Lorton D., Lubahn C., Klein N., Schaller J., Bellinger D. (1999) Dual role for noradrenergic innervation of lymphoid tissue and arthritic joints in adjuvant-induced arthritis. Brain, Behavior, and Immunity, 13, 315-334.

Lorton D., Lubahn CL., Zautra AJ., Bellinger DL. (2008) Proinflammatory Cytokines and Sickness Behavior in Rheumatic Diseases. Current Pharmaceutical Design, 14, 1242-1260.

Lorusso L., Hart IK., Ferrari D., Ngonga GK., Gasparetto C., Ricevuti G. (2007) Autonomic paraneoplastic neurological syndromes. Autoimmunity Reviews. 6(3), 162-8.

Lubahn C., Shaller J., Bellinger D., Sweeney S., Lorton D. (2004) The importance of timing of adrenergic drug delivery in relation to the induction and onset of adjuvant induced arthritis. Brain Behavior Immunology, 18 (6), 563-571.

Lundberg P., Lie A., Bjurholm A., Lehenkari P., Horton M., Lerner U., Ransjo M. (2000) Vasoactive intestinal peptide regulates osteoclast activity via specific binding sites on both osteoclasts and osteoblasts. Bone, 27 (6), 803-810.

Malysheva O., Pierer M., Wagner U., Wahle M., Wagner U., Baerwald C., (2008) Association between β2 adrenergic receptor polymorphisms and rheumatoid arthritis in conjunction with human leukocyte antigen (HLA)-DRB1 shared epitope. Annals of the Rheumatic Diseases 67, 1759-1764.

Mapp P., Walsh D., Garrett N., Kidd B., Cruwys S., Polak J., Blake D. (1994) Effect of three animal models of inflammation on nerve fibres in the synovium. Annals of the Rheumatic Diseases, 53, 240-246.

McLaughlin F., Mackintosh J., Hayes B., Mclaren A., Uings I., Salamon P., Humphreys J., Meldrum E., Farrow S. (2002) Glucocorticoid-induced osteopenia in the mouse as assessed by histomorphometry, microcomputed tomography, and biochemical markers. Bone, 30 (6), 924-930.

Miller L., Joachim G., Scholmerich J., Straub R. (2002) Norepinepherine from synovial tyrosine hydroxylase positive cells is a strong indicator of synovial inflammation in rheumatoid arthritis. The Journal of Rhematology, 29 (3), 427-435.

Miller L., Justen H., Scholmerich J., Straub R. (2000) The loss of sympathetic nerve fibers in the synovial tissue of patients with rheumatoid arthritis is accompanied by increased norepinephrine release from synovial macrophages. FASEB Journal., 14, 2097-2107.

Mitrovic D. (1985) The mechanism of cartilage destruction in rheumatoid arthritis (letter). Arthritis and Rheumatism, 28, 1192-1193.

Mohr W., Wild A., Wolf H. (1978) Incorporation of 3H-proline into hyaline articular cartilage. Virchows Archiv : an international journal of pathology ., 28, 1-12.

Mori K., Iijima M., Koike H., Hattori N., Tanaka F., Watanabe H., Katsuno M., Fujita A., Aiba I., Ogata A., Saito T., Asakura K., Yoshida M., Hirayama M., Sobue G. (2005) The wide spectrum of clinical manifestations in Sjögren's syndrome-associated neuropathy. Brain, 128(Pt 11), 2518-34.

Mravec B. (2007) Autonomic dysfunction in autonomic disease: consequence of cause? Lupus., 16(9), 767-8.

Mundy G. (2007) Osteoporosis and Inflammation. Nutrition Reviews, 65 (12), S147-151.

Mundy G., Boyce B., Hughes D., Wright K., Bonewald L., Dallas S., Harris S., Ghosh-Choudhury N., Chen D., Dunstan C., Izbicka E., Yoneda T. (1995) The effects of cytokines and growth factors on osteoblastic cells. Bone, 17 (2), Suppl., S71-75.

Murase K., Ryu PD., Randic M. (1989) Excitatory and inhibitory amino acids and peptide-induced responses in acutely isolated rat spinal dorsal horn neurons. Neuroscience Letters., 103, 56-63.

Nagele E., Kuhn V., Vogt H., Link T., Muller R., Lochmuller E., Eckstein F (2004). Technical considerations for microstructural analysis of human trabecular bone from specimens excised from various skeletal sites. Calcified Tissue International, 75, 15-22.

Neugebauer V., Vanegas H., Nebe J., Rumenapp P., Schaible HG. (1996) Effects of N- and L-type calcium channel antagonists on the responses of nociceptive spinal cord neurons to mechanical stimulation of the normal and the inflamed knee joint. Journal of Neurophysiology, 76, 3740-9.

Nishida S., Tsurukami H., Sakai A., Sakata T., Ikeda S., Tanaka M., Ito M. (2002) Stage-dependent changes in trabecular bone turnover and osteogenic capacity of marrow cells during development of type II collagen-induced arthritis in mice. Bone, 30 (6), 872-879.

Niissalo S., Hukkanen M., Imai S., Tornwall J., Konttinen YT. (2002) Neuropeptides in experimental and degenerative arthritis. Annals of the New York Acadamy of Science., 966, 384-99.

Offley S., Guo T., Wei T., Clark D., Vogel H., Lindsey D., Jacobs C., Yao W., Lane N., Kingery W. (2005) Capsaicin sensitive sensory neurons contribute to the maintenance of trabecular bone integrity. Journal of Bone and Mineral Research., 20, 257-267.

Ogata Y., Kukita A., Kukita T., Komine M., Miyahara A., Miyazaki S., Kohashi O. (1999) A novel role of IL-15 in the development of osteoclasts: inability to replace its activity with IL-2. Journal of Immunology, 162, 2754-2760.

Ogawa Y., Ohtsuki M., Uzuki M., Sawai T., Onozawa Y., Nakayama J., Yonemura A., Kimura T., Matsuno H. (2003) Suppression of osteoclastogenesis in rheumatoid arthtitis by induction of apoptosis in activated CD4+ T cells. Arthritis and Rheumatism, 48 (12), 3350-3358.

Oku R., Satoh M., Takagi H. (1987) Release of substance P from the spinal dorsal horn is enhanced in polyarthritic rats. Neuroscience. Letters., 74, 315-9.

Otsuka M., Yoshioka K. (1993) Neurotransmitter functions of mammalian tachykinins. Physiological Reviews., 73, 229-308.

Owan I., Ibaraki K. (1994) The role of calcitonin gene related peptide in macrophages: the presence of functional receptors and effects on proliferation and differentiation into osteoclast like cells. Clinical Reviews in Bone and Mineral Metabolism., 2, 151-164.

Partsch G., Matucci-Cerinic M. (1992) Effect of substance P and somatostatin on migration of polymorphonuclear (PMN) cells in vitro. Inflammation, 16, 539-547.

Pearson CM. (1956) Development of arthritis, periarthritis and periostitis in rats given adjuvants. Proceedings of the Society for Experimental Biology and Medicine ., 91, 95-101.

Pearson C., Wood FD. (1959) Studies of polyarthritis and other lesions in rats by injection of mycobacterial adjuvant. I. General clinical and pathological characteristics and some modifying factors. Arthritis and Rheumatism, 2, 440-459.

Pearson C., Wood FD. (1963) Studies of arthritis and other lesions induced in rats by the injection of mycobacterial adjuvant. VII. Pathologic details of the arthritis and spondylytis. American Journal of Pathology, 42 (1), 73-95.

Polzer K., Joosten L., Gasser J., Distler J., Ruiz G., Redlich K., Bobacz K., Simolen J., van den Berg W., Schett G., Zwerina J. (2010) Interleukin-1 is essential for systemic inflammatory bone loss. Annals of the Rheumtic Diseases., 69, 284-290.

Pont-Kingdon G., Lyon E. (2005) Direct molecular haplotyping by melting curve analysis of hybridization probes: beta 2-adrenergic receptor haplotypes as an example. Nucleic Acids Research, 33 (10), e89.

Poole A. Arthritis and Allied Conditions, Baltimore: Lippincott, Williams and Wilkins, 2001.

Poole A, Alini M, Hollander A. Mechanisms and Models in Reumatoid Arthritis. New York: Academic Press, 1995

Raap T., Justen H., Miller L., Cutolo M., Scholmerich J., Straub R. (2000) Neurotransmitter modulation of interleukin 6 (IL-6) and IL-8 secrestion of synovial fibroblasts in patients with rheumatoid arthritis compared to osteoarthritis. The Journal of Rheumatology, 27 (11), 2558-2565.

Rainsford KD. (1982) Adjuvant polyarthritis in rats: is this a satisfactory model for screening anti-arthritic drugs. Agents Actions, 12, 452-458.

Randic M., Hecimovic H., Ryu PD. (1990) Substance P modulates glutamate-induced currents in acutely isolated rat spinal dorsal horn neurones. Neuroscience Letters., 117, 74-80.

Ransjo M., Lie A., Mukohyama H., Lundberg P., Lerner UH. (2000) Microisolated mouse osteoclasts express VIP-1 and PACAP receptors. Biochemical and Biophysical Research Communications ., 274, 400-404.

Redlich K., Hayer S., Ricci R., David J., Tohidast-Akrad M., Kollias G., Steiner G., Smolen J., Wagner E., Schett S. (2002) Osteoclasts are essential for TNF-α mediated joint destruction. The Journal of Clinical Investigation, 110 (10), 1419-1427.

Reines B. (2004) Is rheumatoid arthritis premature osteoarthritis with fetal-like healing? Autoimmunity Reviews, 3, 305-311.

Rhodes L., Tan A., Tanner S., Radjenovic A., Hensor E., Reece R., O'Conner P., Emery P., McGonagle D. (2004) Regional variation and differential response to therapy for knee synovitis adjacent to cartilage-pannus junction and suprapatellar pouch in inflammatory arthritis. Arthritis and Rheumatism, 50 (8), 2428-2432.

Riboldi P., Gerosa M., Luzzana C., Catelli L. (2002) Cardiac involvement in systemic autoimmune diseases. Clinical Reviews in Allergy and Immunology. 23(3), 247-61. Review.

Roos B., Fischer J., Pignat W., Alander C., Raisz L. (1986) Evaluation of the in vivo calcium regulation actions of noncalcitonin peptides produced by calcitonin gene expresion. Endocrinology, 18, 46-51.

Rothe L., Collin-Osdoby P., Chen Y., Sunyer T., Chaudhary L., Tsay A., Goldring S., Avioli L., Osdoby P. (1998) Human osteoclasts and osteoclast-like cells synthesize and release high basal and inflammatory stimulated levels of the potent chemokine interleukin-8. Endocrinology, 139 (10), 4353-4363.

Saidenberg-Kermanac'h N., Cohen-Solal M., Bessis N., De Vernejoul M., Boissier M. (2004) Role for osteoprotegerin in rheumatoid inflammation. Joint Bone Spine, 71, 9-13.

Sajti E., van Meeteren N., Kavelaars A., van der Net J., Gispen W., Heijnen C. (2004) Individual differences in behvior of inbred Lewis rats are associated with severity of joint destruction in adjuvant-induced arthritis. Brain, Behavior and Immunity, 18, 505-514.

Sandhu H., Herskovits M., Singh I. (1987) Effects of surgical sympathectomy on bone remodeling at rat incisor and molar root sockets. The Anatomical Record, 219, 32-38.

Sandhu H., Kwong-Hing A., Herskovits M., Singh I. (1990) The early effects of surgical sympathectomy on bone resorption in the rat incisor socket. Archives of Oral Biology., 35 (12) 1003-1007.

Schuerwegh A., Dombrecht E., Stevens W., Van Offel J., Bridts C., Cierck L. (2003) Influence of pro-inflammatory (IL-1α, IL-6, TNF-α, IFN-γ) and anti-inflammatory (IL-4) cytokines on chondrocyte function. Osteoarthritis and Cartilage, 11, 681-687.

Schwab W., Bilgicyildirim A., Funk R. (1997) Microtopography of the automomic nerves in the rat knee: a fluorescence microscopic study. Anatomical. Record., 247, 109-118.

Schett G. (2006) Rheumatoid arthritis: inflammation and bone loss. Wiener Medizinische Wochenschrift, 156, 34-51.

Segawa Y., Yamaura M., Aota S., Omata T., Tuzuike N., Itokazu Y., Oka H., Tamaki H., Nakamura T. (1997) Methotrexate maintains bone mass by preventing both a decrease in bone formation and increase in bone resorption in adjuvant-induced arthritic rats. Bone, 20 (5) 457-464.

Shinoda M., Honda T., Ozaki N., Hattori H., Mizunatani H., Ueda M., Sugiura Y. (2003) Nerve terminals extend into the temporomandibular joint of adjuvant arthritic rats. European Journal of Pain, 7, 493-505.

Shiozawa S. (1985) Reply to a letter by Dr. Mitrovic. Arthritis and Rheumatism, 28, 1193-1195.

Simjee S., Pleuvry B., Coulthard P. (2004) Modulation of the gait deficit in arthritic rats by infusion of muscimol and bicuculline. Pain, 109, 453-460.

Singh I., Klein R., Herskovitis. (1981) Autoradiographic assessment of 3H-proline uptake by osteoblasts following guanethidine-induced sympathectomy in the rat. Cell Tissue Research, 216, 215-220.

Sitia S., Atzeni F., Sarzi-Puttini P., Di Bello V., Tomasoni L., Delfino L., Antonini-Canterin F., Di Salvo G., De Gennaro Colonna V., La Carrubba S., Carerj S., Turiel M. (2009) Cardiovascular involvement in systemic autoimmune diseases. Autoimmunity Reviews., 8(4), 281-6.

Skerry T., Gowen M. Mechanisms and Models in Reumatoid Arthritis. New York: Academic Press, 1995.

Sluka KA., Milton MA., Willis WD., Westlund KN. (1997) Differential roles of neurokinin 1 and neurokinin 2 receptors in the development and maintenance of heat hyperalgesia induced by acute inflammation. British Journal of Pharmacology, 120, 1263-73.

Sorkin L., Maruyama K., Boyle D., Yang L., Marsala M., Firestein G. (2003) Spinal adenosine agonist reduces c-fos and astrocyte activation in dorsal horn of rats with adjuvant-induced arthritis. Neuroscience Letters, 340, 119-122.

Stojanovich L. (2009) Autonomic dysfunction in autoimmune rheumatic disease. Autoimmunity Reviews., 8(7), 569-72.

Stolina M., Adamu S., Ominsky M., Dwyer D., Asuncion F., Geng Z., Middleton S., Brown H., Pretorius J., Schett G., Bolon B., Feige U., Zack D., Kostenuik P. (2005) RANKL is a marker and mediator of local and systemic bone loss in two rat models in inflammatory arthritis. Journal of Bone and Mineral Research, 20 (10), 1756-1765.

Strand V., Kavanaugh A. (2004) The role of interleukin-1 in bone resorption in rheumatoid arthritis. Rheumatology, 43 (Suppl. 3) iii10-iii16.

Stronk J., Heinemann E., Neeck G., Schmidt K., Lang U. (2004) A new approach to studying angiogenesis in rheumatoid arthritis by means of power Doppler ultrasonography and measurement of serum vascular endothelial growth factors. Rheumatology, Concise Report; pg 1-4.

Suzuki Y., Tsutsumi Y., Nakagawa M., Suzuki H., Matsushita K., Beppu M., Aoki H., Ichikawa Y., Mizushima Y. (2001) Osteoclast-like cells in an in vitro model of bone destruction by rheumatoid synovium. Rheumatology, 40, 673-682.

Szekanecz Z., Koch A. (2007) Macrophages and their products in rheumatoid arthritis. Current Opinion in Rhematology, 19, 289-295.

Takayanagi H., Oda H., Yamamoto S., Kawaguchi H., Tanaka S., Nishikawa T., Koshihara Y. (1997) A new mechanism of bone destruction in rheumatoid arthritis: synovial fibroblasts induce ostoeclastogenesis. Biochemical and Biophysical Research Communications, 240, 279-286.

Takeuchi T., Tsuboi T., Arai M., Togari A. (2000) Adrenergic stimulation of osteoclastogenesis mediated by expression of osteoclast differentiation factor in MC3T3-E1 osteoblast-like cells. Biochemical. Pharmocology., 61, 579-586.

Tang Y., Shankar R., Gamelli R., Jones S. (1999) Dynamic norepinepherine alterations in bone marrow: evidence of functional innervation. Journal of Neuroimmunology, 96, 182-189.

Thomason BT., Brantley PJ., Jones GN., Dyer HR., Morris JL. (1992) The relation between stress and disease activity in rheumatoid arthritis. Journal of Behavioral Medicine., 15, 215-20.

Togari A. (2002) Adrenergic regulation of bone metabolism: possible involvement of sympathetic innervation of osteoblastic and osteoclastic cells. Microscopy Research and Technique, 58, 77-84.

Toh K., Kukita T., Wu Z., Kukita A., Sandra F., Tang Q., Nomiyama H., Iijima T. (2004) Possible involvement of MIP-1α in the recruitment of osteoclast progenitors to the distal tibia in rats with adjuvant-induced arthritis. Laboratory Investigation, 8, 1092-1102.

Toussirot E., Serratrice G., Valentin P. (1993) Autonomic nervous system involvement in rheumatoid arthritis. 50 cases. Journal of Rheumatology., 20(9), 1508-14

Toysaki-Maeda T., Takano H., Tomita T., Maeda-Tanimura Y., Shimaoka Y., Takahashi T., Itoh T., Ochi T. (2001) Differentiation of monocytes into multinucleated giant bone resorbing cells: two-step differentiation induced by nurse-like cells and cytokines. Arthritis Research, 3 (5), 306-310.

Tsutsumimoto, T., Kawasaki S., Ebara, S., Takaoka K. (1999) TNF-α and IL-1β suppress N-Cadhein expression in MC3T3-E1 cells. Journal of Bone and Mineral Research, 14 (10), 1751-1760.

Vaes G. (1981) Cartilage and bone tissue damage in arthritis: cellular co-operation and enzymatic mechanisms. Scandanavian Journal of Rheumatology, Suppl., 40: 65-71.

Wahle M., Krause A., Pierer M., Hantzschel H., Baerwald C. (2002) Immunopathogenesis of rheumatic diseases in the context of neuroendocrine interactions, Annals of the New York Acadamey of Sciences., 966, 355-364.

West M., Huang W. (1994) Spinal cord excitatory amino acids and cardiovascular autonomic responses. American Journal of Physiolology. 267(3 Pt 2), H865-73.

Wlodarski K., Wlodarski P. (2009) Leptin as a modulator of osteogenesis. Ortopedia, Tramotologia, Rehabilitacja., 11(1), 1-6.

Wooley D. Mechanisms and Models in Reumatoid Arthritis. New York: Academic Press, 1995.

Wu Z., Toh, K., Nagata K., Kukita T., Iijima T. (2004) Effect of the resection of the sciatic nerve on the Th1/Th2 balance in the synovial of the ankle joint of adjuvant arthritic rats, Histochemistry and Cell Biology., 121, 141-147.

Wu Z., Nagata K., Iijima T. (2002) Involvement of sensory nerves and immune cells in osteophyte formation in the ankle joint of adjuvant arthritic rats. Histochemistry and Cell Biology, 118, 213-220.

Xu B., Arlehag L., Rantapaa-Dahlquist S., Lefvert A. (2005) β2 Adrenoceptor gene single nucleotide polymorphisms are associated with rheumatoid arthritis in northern Sweden. Annals of the Rheumatic Diseases., 64,773-776.

Yamashita A., Yonemitsu Y., Okano S., Nakagawa K., Nakashima Y., Irisa T., Iwamoto Y., Nagai Y., Hasegawa M., Sueishi K. (2002) Fibrobalst growth factor-2 determines severe joint disease in adjuvant-induced arthritis in rats. The Journal of Immunology, 168, 450-457.

Zaidi M., Fuller K., Bevis P., Gainesdas R., Chambers T., MacIntyre I. (1987) Calcitonin gene related peptide inhibits osteoclastic bone resorption: a comparative study. Calcified Tissue International, 40, 149-154.

Zaidi M., Chambers T., Gainesdas R., Morris H., MacIntyre I. (1987) A direct action of human calcitonin gene related peptide on isolated osteoclasts. Journal of Endocrinology, 115, 511-518.

Zini N., Lisignoli G., Solimando L., Bavelloni A., Grassi F., Guidotti L., Trimarchi C., Facchini A., Maraldi N. (2003) IL1β and TNF-α induce changes in the nuclear polyphosphoinositide signaling system in osteoblasts similar to that occurring in patients with rheumatoid arthritis: an immunochemical and immunocytochemical study. Histochemistry and Cell Biology., 120, 243-250